MASARYK UNIVERSITY
FACULTY OF SCIENCE
DEPARTMENT OF GEOGRAPHY

SROVNÁNÍ VÝVOJE SEVERU A JIHU – HOLOCENNÍ ABIOTICKÁ PALEOLIMNOLOGIE VYSOKÉ ARKTIDY A PŘÍMOŘSKÉ ANTARKTIDY

COMPARING THE EVOLUTION OF NORTH AND SOUTH – HOLOCENE ABIOTIC PALAEOLIMNOLOGY OF HIGH ARCTIC AND MARITIME ANTARCTICA

Master's diploma thesis

Tomáš Čejka

SUPERVISOR: Assoc Prof. Daniel Nývlt, PhD.

BRNO 2018

Bibliografický záznam

Autor:	Bc. Tomáš Čejka
	Přírodovědecká fakulta, Masarykova univerzita
	Geografický ústav

Název práce:	Srovnání vývoje severu a jihu – holocenní abiotická paleolimnologie Vysoké Arktidy a Přímořské Antarktidy
Studijní program:	Geografie a kartografie
Studijní obor:	Fyzická geografie
Vedoucí práce:	doc. Mgr. Daniel Nývlt, Ph.D.
Akademický rok:	2017/2018
Počet stran:	88+6
Klíčová slova:	jezerní sedimenty, Neoglaciace, klimatické optimum, Malá doba ledová, ostrov Vega, Západní Špicberk, paleolimnologie, magnetická susceptibilita, rentgenová fluorescence, uhlík, síra, proxy záznam, rozsivky, ^{14}C, ^{210}Pb, ^{137}Cs, časově-hloubkový model

Bibliographic Entry

Author:	Tomáš Čejka, BSc
	Faculty of Science, Masaryk University
	Department of Geography
Title of Thesis:	Comparing the evolution of North and South – Holocene abiotic palaeolimnology of High Arctic and Maritime Antarctica
Degree Programme:	Geography and Cartography
Field of Study:	Physical geography
Supervisor:	Assoc Prof. Daniel Nývlt, PhD.
Academic Year:	2017/2018
Number of Pages:	88+6
Keywords:	lake sediments, Neoglaciation, climate optimum, Little Ice Age, Vega Island, Spitsbergen, palaeolimnology, magnetic susceptibility, X-ray fluorescence, carbon, sulphur, proxy record, diatoms, ^{14}C, ^{210}Pb, ^{137}Cs, age-depth model

Abstract

The lake systems in the Polar regions have experienced pronounced environmental changes during the Late Holocene, and most of these were appropriately reflected in the lake sedimentary records. For this thesis, two cores from the Vega Island (Lake Anonima, Antarctic Peninsula) and the Spitsbergen (Lake Mathiesondalen 3, Svalbard) were analysed using multi-proxy approach to obtain more-detailed view on the palaeoenvironmental evolution. Geochemical (carbon and sulphur content, X-ray fluorescence spectroscopy), petrophysical (magnetic susceptibility, grain-size composition) and biological (diatom biostratigraphy) analyses were performed, and supplemented by a robust sedimentation chronology based on radiocarbon (^{14}C) and short-lived (^{210}Pb, ^{137}Cs) isotope dating. Principal component analysis (PCA) and cluster analyses were applied to access the dominating patterns in the sediment composition. Lake Anonima covers the last 2400 cal. yrs b2k and provides a record of the climate history in the James Ross Archipelago, North-east Antarctic Peninsula. The Lake Anonima records the Late Holocene Hypsithermal and the Neoglacial Period. The Lake Mathiesondalen 3 covers the last 700 cal. yrs b2k and presents a record of changes in the Mathiesondalen lake and catchment, as well as unique perception of the Little Ice Age mild course.

Abstrakt

Jezerní systémy v polárních oblastech prodělaly během pozdního holocénu řadu výrazných environmentálních změn, které lze vhodně rekonstruovat z jezerních sedimentárních záznamů. Pro tuto práci byly analyzovány dvě jádra z ostrova Vega (jezero Anonima, Antarktický poloostrov) a Západního Špicberku (jezero Mathiesondalen 3, Svalbard) a to s využitím multi-proxy přístupu za účelem získání detailnější informace o paleoenvironmentálním vývoji. Byly aplikovány geochemické (podíl uhlíku a síry, rentgenová fluorescence), petrofyzikální (magnetická susceptibilita, laserová granulometrie) a biologické (biostratigrafie rozsivek) analýzy, jež byly posléze doplněny o robustní chronologii sedimentace založenou na radiouhlíkovém (^{14}C) datování a datování izotopů s krátkým poločasem rozpadu (^{210}Pb, ^{137}Cs). Za účelem zjištění dominantních trendů v sedimentárním složení byla provedena, společně se shlukovou analýzou, analýza hlavních komponent. Sedimentární záznam z jezera Anonima zahrnuje posledních 2400 kal. let b2k a poskytuje záznam klimatické historie souostroví Jamese Rosse. Jezero Anonima zaznamenává pozdně holocenní klimatické optimum a období neoglaciace. Záznam z jezera Mathiesondalen 3 zahrnuje posledních 700 cal. let b2k a zahrnuje změny v jezeře a jeho povodí, stejně tak jako unikátní záznam mírnějšího průběhu Malé doby ledové.

Masarykova univerzita

Přírodovědecká fakulta

ZADÁNÍ DIPLOMOVÉ PRÁCE

Student: **Tomáš Čejka**
Studijní program: **Geografie a kartografie**
Studijní obor: **Fyzická geografie**

Ředitel Geografického ústavu PřF MU Vám ve smyslu Studijního a zkušebního řádu MU určuje diplomovou práci s tématem:

Srovnání vývoje severu a jihu – holocenní abiotická paleolimnologie Vysoké Arktidy a Přímořské Antarktidy

Comparing the evolution of North and South – Holocene abiotic palaeolimnology of High Arctic and Maritime Antarctica

Zásady pro vypracování:

Deglaciace níže položených částí Vysoké Arktidy a Přímořské Antarktidy na přechodu pleistocénu a holocénu vedla ke vzniku množství jezer, která v krajině přetrvala až do současnosti. Vhodnými příklady z obou polárních oblastí jsou jezera v Mathiesondalen ve střední části ostrova Západní Špicberk, souostroví Svalbard a v předpolí Glaciar Bahía del Diablo na ostrově Vega při východním pobřeží Antarktického poloostrova. Obě tato jezera poskytují poměrně kontinuální sedimentární záznamy posledních několika tisíciletí.
Práce vhodně naváže na bakalářskou práci studenta a bude založená na kombinaci použití analytických metod, jejich interpretace a diskuze ve vztahu k přírodním podmínkám během sedimentace v těchto jezerech. Analytické práce budou zahrnovat stanovení magnetických vlastností, podílů hlavní litofilních prvků, zrnitostního složení a vytvoření časového modelu depozice na základě aplikace vhodných datovacích metod. Získané výsledky interpretované pro každou z oblastí budou pro lepší pochopení průběhu přírodních změn v obou polárních oblastech během mladší části holocénu srovnány s okolními záznamy v dané oblasti a vzájemně. Předpokládá se publikování výsledků v mezinárodním recenzovaném periodiku.

Rozsah grafických prací: podle potřeby

Rozsah průvodní zprávy: cca 60 až 80 stran

Seznam odborné literatury:

Björck, S. et al. (1991); Björck, S. et al. (1996); Blaauw, M. (2010); Chaparro, M.A.E. et al. (2014); Cohen, A.S. (2003); D'Andrea, W.J.D. et al. (2012); Evans, J. et al. (2005); Hjort, C. et al. (1997); Ingólfsson, Ó. et al. (1992); Johnson, J.S. et al. (2011); Lecomte, K.L. et al. (2016); Miller, G.H. et al. (2010); Mulvaney, R. et al. (2012); Nedbalová, L. et al. (2013); Nývlt, D. et al. (2014); Pudsey, C.J. et al. (2006); Rachlewicz, G. et al. (2007); Reimer, P.J. et al. (2013); Roman, M. (2014); Roman, M. et al. (2015); Sterken, M. et al. (2012); Svendsen, J.I. a Mangerud, J. (1997); Velle, G. et al. (2011); Vincent, W.F. a Laybourn-Parry, J. (2008).

Jazyk závěrečné práce: čeština

Vedoucí diplomové práce: doc. Mgr. Daniel Nývlt, Ph.D.

Podpis vedoucího práce: .....

Datum zadání diplomové práce: listopad 2016
Datum odevzdání diplomové práce: do 3. května 2018

prof. RNDr. Petr Dobrovolný, CSc.
ředitel Geografického ústavu

Zadání práce převzal(a): ..... *dne* .....

Acknowledgements

Here, I want to express my sincere gratitude to thesis supervisor Daniel Nývlt for his inspiring, encouraging and professional attitude. His valuable commentary contributed to a significant improvement in the whole work, as well as did his supporting spirit. I must acknowledge a foundation of my scientific interest has been, definitely, set by him.

The work on this thesis has been supported by the projects of the Ministry of Education, Youth and Sports of the Czech Republic no. LM2015078 and CZ.02.1.01/0.0/0.0/16_013/0001708.

I would also like to show gratitude to many other colleagues, namely Lenka Lisá (*Institute of Geology, Czech Academy of Sciences*) for providing the laser granulometry analysis and for her cooperation during the measurement, Kateřina Kopalová and Marie Bulínová (*Department of Ecology, Charles University*) together with Bart Van de Vijver (*Antwerp University*) for diatom biostratigraphy analysis and discussions, Viktor Goliáš (*Institute of Geochemistry, Mineralogy and Mineral Resources, Charles University*) for short-lived radioisotope dating, Eva Geršlová (*Department of Geological Sciences, Masaryk University*) for providing X-ray fluorescence method and Matěj Roman (*Department of Geography, Masaryk University*) for his assistance and help. I am also grateful to Jan Kavan (*Department of Geography, Masaryk University*), Silvia H. Coria, Marcos A. E. Chaparro and Juan M. Lirio (*Instituto Antártico Argentino*) for core retrieval during the field campaigns.

I also gratefully acknowledge the support from my family, and most importantly, Míša.

Thank you for showing me the right direction.

Declaration

I hereby certify that this master's diploma thesis is entirely the result of my own work and that I have conducted this paper under supervising of Assoc Prof. Daniel Nývlt, PhD. I have faithfully and properly cited all sources used in this thesis.

Brno, 3rd May 2018 ...……

Tomáš Čejka

TABLE OF CONTENT

1 INTRODUCTION, RATIONALE AND AIMS

Polar Regions have experienced significant environmental alternations associated predominantly with hydrometeorological and thus long-term climatic fluctuations in the Late Holocene (4250 years b2k – modern era). These changes led to a formation of differently-parameterized terrestrial ecosystems, glacier zones, catchment areas, and most importantly for this study, lake systems. In the chapter 2 of this thesis, author presents a comprehensive literature review focused on a physical-geographical setting of selected polar areas with a particular emphasis on the Late Holocene types of paleoenvironmental records supplemented by actual researches. This brief summary will enable the reader to understand later-presented (chapter 5 and 6) research results in their larger complexity and coherence.

Based on a composite and traditionally used modern multi-proxy analyses, two lacustrine sedimentary archives from Antarctica (Lake Anonima) and Svalbard Archipelago (Lake Mathiesondalen 3), are going to be subjected to a high-resolution, using both biotic and abiotic, techniques, to extract information about the short- as well as long-term reactions of these systems to driving environmental changes. The main points of this thesis aim to provide answers to the following questions. “How have evolved the studied polar areas over the time? Have there been recognizable shifts in particular proxy parameters? How have been the biodiversity spectra changing? How are the glacier behaviour and hydrological regime changes marked in the records?” And many others…

Due to the wide relationship complexity within the physical-geographical sphere, this thesis does not aim to explain all causes and consequences in their best detail and the closest look. In such a situation, the reader is referred to an appropriate literature discussing selected phenomena in a wider scope.

2 LITERATURE REVIEW – PALAEOENVIRONMENTAL RECORDS

2.1 North-eastern Antarctic Peninsula

2.1.1 Physical setting and geographical description

The Antarctic Peninsula (AP) comprises a narrow (<250 km wide) chain of mountains, rising to a maximum of 3500 m (but mostly much lower) along its ~1250 km length. It constitutes an averagely continuous plateau with few disruptions below 2000 m and it projects substantially further north than the rest of Antarctica. In many respects the AP is geologically similar to the South American cordillera. It comprises a pre-Jurassic basement overlain and intruded by Jurassic–Neogene magmatic arc rocks related to eastwards-directed subduction of oceanic lithosphere along the western (Pacific) margin of the AP. A comprehensive description of the setting of the AP is given by Domack et al. (2003b).

The AP is heavily glaciated with outlet glaciers terminating in the ocean along both its western and eastern margins. There is a clear boundary, south of which glacier termini feed into ice shelves, and north of which there are no ice shelves (Morris and Vaughan, 2003). This boundary is further south (67–70°S) on the western side of the AP than on the east (64–68°S), although during the last decades there have been recorded several ice shelves disintegrations around the AP (Cook and Vaughan, 2010). There are only few larger ice-free areas, where terrestrial palaeoenvironmental records from the Holocene have been preserved (see 2.1.2), with perhaps the most important being in the north-eastern part the AP (James Ross Archipelago), South Shetland Islands, eastern Alexander Island (Ablation Point Massif) and the coastal area around Marguerite Bay. There are numerous small ice-free areas on ridges between outlet glaciers, and on nunataks of the central plateau, but most of these are rocky with few surface deposits or lakes (Bentley et al., 2009).

In many aspects, the AP is climatically different to the Antarctic continent (Fig. 1). It is narrow piece of land thus it experiences a strong marine influence, particularly on its western side, which is exposed to the southern westerly winds. The AP is the most northerly part of Antarctica and as such is the most subjected to the influence from mid-latitudes. In particular, the western side of the AP receives relatively warm, moist air masses derived from mid-latitudes (Bentley et al., 2009). Moreover, the western AP is the only part of Antarctica where there is a demonstrated negative correlation between winter temperatures (at Faraday/Vernadsky Station) and the extent of sea-ice (in the Bellingshausen Sea to the

west of the station; King, 1994). It has been suggested that sea-ice may play an important role in environmental change around the AP (Vaughan et al., 2003) and affects also surface air temperatures. The eastern side of the AP is less influenced by the westerlies and experiences a substantially colder and drier climate because of the northwards extension of cold continental air masses from the Antarctic interior into the Weddell Sea embayment (Reynolds, 1981). Specifically, cold barrier winds (or low-level jets; Schwerdtfeger, 1975; Stensrud, 1996) flowing along the eastern coast of the AP bring cold and dry air towards the northern part of the AP.

Towards marine environment, the Antarctic Circumpolar Current (ACC) flows clockwise in a broad zone around Antarctica, carrying Circumpolar Deep Water (CDW), and is separated from the coast by the katabatic-driven west-flowing Antarctic Coastal Current. The north–south landmass of the AP acts as a barrier to this flow and so the southern boundary of the ACC runs NE along the edge of the AP shelf as the ACC is deflected to the north and through the constriction of the Drake Passage (Fig. 1). Thus, the Pacific margin continental shelf of the AP is likely to be affected by any variations in the flow of the ACC. This is particularly important because the ACC propagates changes in oceanic conditions between the Pacific, Atlantic and Indian Oceans (Simmonds, 2003), including the effects of the El Niño Southern Oscillation (ENSO; Bentley et al., 2009).

Some areas of the continental shelf on the western side of the AP experience intrusions of CDW. This is a relatively warm (>1.5 °C), salty (34.65–34.7‰) intermediate depth water mass (Klinck et al., 2004) that is derived from modified North Atlantic Deep Water. The top of the CDW is at 200 m depth and so only areas of continental shelves deeper than this are affected. These intrusions bring heat and salt onto the continental shelf. CDW is substantially warmer than typical Antarctic surface waters and so where mixing occurs then intrusions of CDW along the western AP shelf are characterized by surface waters that are above the freezing point in winter. The inner AP shelf has significant topography and this roughness may contribute to mixing (Bentley et al., 2009). At places, it is the onshore flow of the ACC that provides the impetus to pump CDW onto the shelf, particularly along the troughs that formed the paths of palaeo ice streams (Smith et al., 1999; Smith and Klinck, 2002; Klinck et al., 2004).

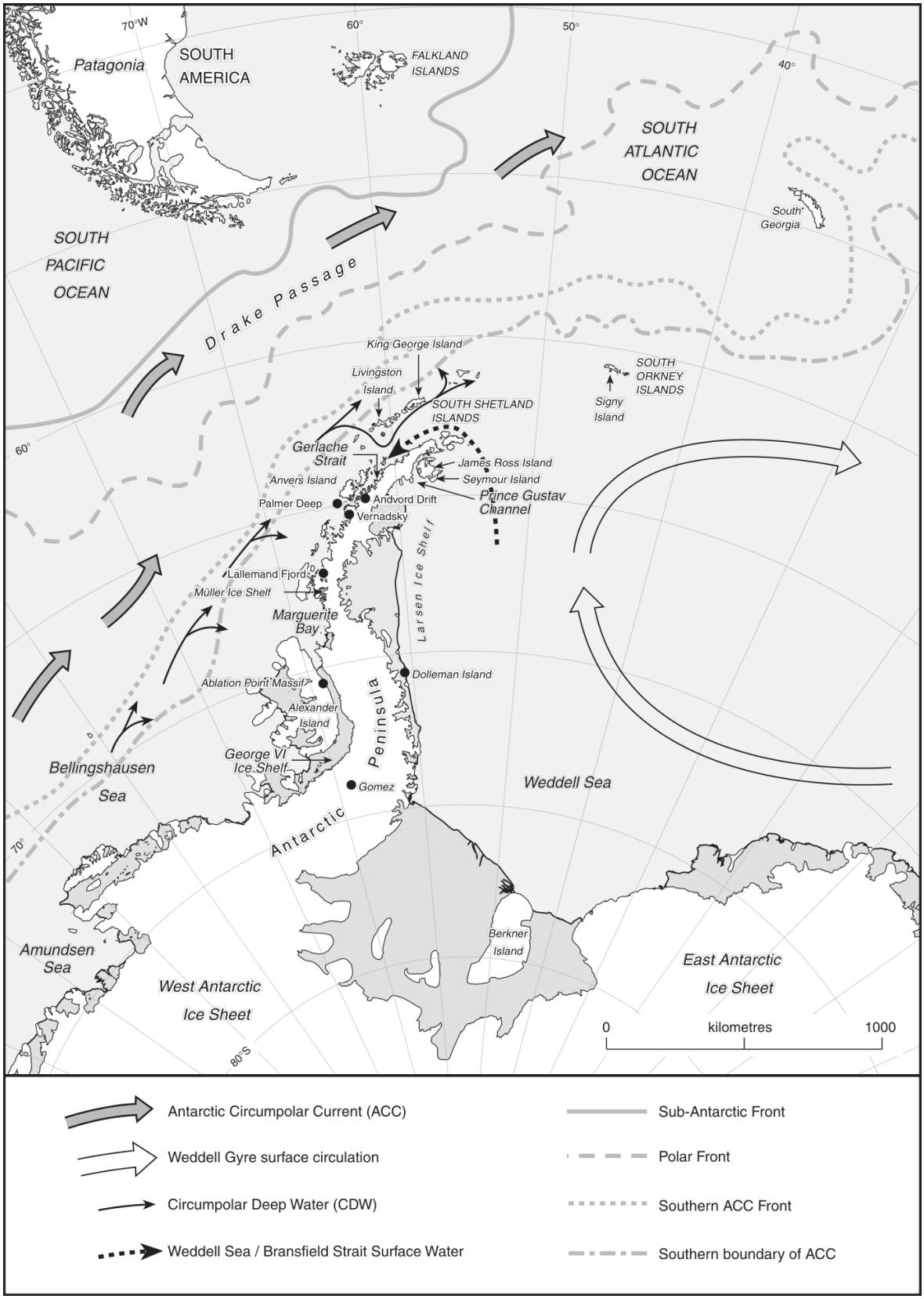

Figure 1 Setting of the AP and southernmost South America showing sites discussed in text. Ocean circulation and frontal boundaries are from Hernández-Molina et al. (2006), Orsi et al. (1995) and Naveira Garabatoa et al. (2002) – adopted from Bentley et al. (2009).

2.1.2 Palaeoenvironmental records

In comparison to other Antarctic regions, the AP provides largest amount of palaeoenvironmental records predominantly due to the large ice-free areas, each of which present different information on the patterns, processes and mechanisms of the (Late) Holocene climate and environmental evolution.

Ice cores, considered as one of the most solid and long-term type of record, provide an information on environmental change in the interior from which it is possible to obtain past atmospheric temperatures, average regional sea-ice extent, precipitation and changes in atmospheric composition (Bentley et al., 2009). Aristarain et al. (1986) were among the firsts who has carried out an analysis of deuterium isotope (δD) content of Dallinger Dome (James Ross Island – JRI, AP) within a period AD 1850–1980. This has been followed by Peel and Mulvaney (1992), who analysed δD, $\delta^{18}O$ and Cl^- content in Dolleman Island ice core (AD 1795–1986), to infer changes in weather and air mass patterns within the Weddell Sea zone. Furthermore, Thompson et al. (1994) examined ice samples (oxygen isotope ratios, dust content, chemical species, net accumulation) from Dyer Plateau, covering the period AD 1510–1989. The most recent study, performed in previous years by Mulvaney et al. (2012), reveals nowadays the most accurate and comprehensive dataset of climate conditions of the entire Holocene above the JRI and north-eastern AP, respectively.

Marine sediments represent another valuable environmental archive, although extracting such records requires rather expensive and more sophisticated apparatus. Marine sediment from various environments, such as abyssal plains, offshore continental shelfs and fjords provide information about variation in sedimentation rate during previously triggered processes, such as deglaciation (e.g.; Heroy and Anderson, 2005; Evans et al., 2005). Furthermore, it is also possible to obtain information about palaeoceanographic changes – specifically surface water productivity (Sjunneskog and Taylor, 2002), the proximity and stability of ice shelves and glaciers (Pudsey and Evans, 2001; Brachfeld et al., 2003), extent of sea-ice (Gersonde et al., 2003), the influx of meltwater and terrigenous sediments (Domack et al., 1994), and clues to the behaviour of ocean currents such as the ACC (Howe and Pudsey, 1999).

Another type of archive – lake sediments, are also frequently used for palaeo reconstructions (onto the AP). This sort of sediment provides not only a record of deglaciation, but also a record of changing biological productivity (linked to temperature),

changes in ecology and species assemblages, and lake ice cover (Hodgson and Smol, 2008). Near-coastal lakes or lagoons can also be used as isolation basins to determine relative sea-level change (Bentley et al., 2005a). Epishelf lakes can provide proxy records of ice shelf presence and absence (Roberts et al., 2008).

Glaciomorphological records from land surface and continental shelf provide supplementary information on past glacier extent and thickness (land-terminating glaciers), and the timing of glaciation and/or deglaciation in individual areas (Sugden et al., 2006). A variety of onshore geomorphological features have been used to determine AP ice sheet extent, including till stratigraphy, moraines, striations, trimlines and erratics analyses (e.g. Clapperton and Sugden, 1982; Rabassa, 1983; Bentley et al., 2006). Marine glacial geomorphology, as an offshore-focused discipline, uses widespread technique of titled swath bathymetry (i.e. sonar mapping) to obtain closer look onto the character of landforms on the continental shelf seabed (Wellner et al., 2006).

2.2 Svalbard Archipelago

2.2.1 Physical setting and geographical description

Svalbard is an Arctic archipelago located north of the Norway between Greenland and Franz Josef Land in the Arctic ocean. The archipelago is composed of nine main islands (Spitsbergen – formerly West Spitsbergen, North East Land, Edge Island, Barents Island, Prins Karls Foreland, Kvit Island/Gilles Land, Kong Karls Land/Wiche Islands, Bjørn/Bear Island, Hopen), located between 10°–35° E and 74°–81° N, while the Spitsbergen is the largest one and the only one with permanent settlements (Moholdt et al., 2010).

The Central Svalbard, including Billefjorden region consist mainly of Carboniferous and Permian sedimentary rocks, which are divided into three groups. The Billefjorden Group consisted largely of terrestrial deposits, which formed under the humid sub-tropical climate during the Early Carboniferous. The Gipsdalen Group represents a mixture of siliciclastic and calcareous sediments, and followingly Tempelfjorden Group (Kapp Starostin Formation) is represented by sediments, which were deposited during a transgression (Harland et al., 1997).

From a climate perspective, the general large-scale air currents are determined by the low-pressure area near Iceland and the relatively high-pressure area over Greenland and the

Arctic Ocean. This resulted in transport of mild air from lower latitudes towards Svalbard. Further north, the circulation is mostly anticyclonic with prevailing easterly or northeasterly winds. Large temperature differences occur between the two air masses originating from the southwest and northeast, causing extreme fluctuations in weather and temperature. The greatest variations occur in winter when the contrasts between the two air masses are most marked. When snow accumulation is measured on the glaciers in spring, traces of mild periods can be often seen as ice layers in the snow pits. However, snow may fall at any time during the summer months. On the western coast of Spitsbergen, the average annual temperature is about –6 °C, and it is slightly and more continental further inland. The average temperature on the western coast in the warmest month, July, is about 5–6 °C, while in the coldest period, January – March, it is about –15 °C. Precipitation is about 400 mm annually on the western coast of Svalbard and half of it in central inland areas. Ocean currents and general air circulation explain the relatively mild climate. Part of the warm Norwegian Current, a branch of the Gulf Stream, flows into the Barents Sea and part along the western coast of Spitsbergen (West Spitsbergen Current – WSC), where it creates the northernmost area of open water in the Arctic in winter (Førland et al., 2011).

The total glaciated area of Svalbard is 34,560 km^2, representing about 6 % of the worldwide glacier cover outside of Greenland and Antarctica. Spitsbergen is the most alpine island, having small cirque glaciers as well as extensive ice fields and valley glaciers. The eastern islands, facing the Barents Sea, have less relief and are dominated by low-elevation ice caps. Most glaciers and ice caps are considered to be polythermal (e.g., Bjornsson et al., 1996), and 60 % of the glaciated areas drain into tidewater glaciers (Blaszczyk et al., 2009). Glacier dynamics are typically slow with velocities < 10 $m.yr^{-1}$ (Hagen et al., 2003a), but surge events has been observed over most of Svalbard (Hamilton and Dowdeswell, 1996), also in recent years (Sund et al., 2009).

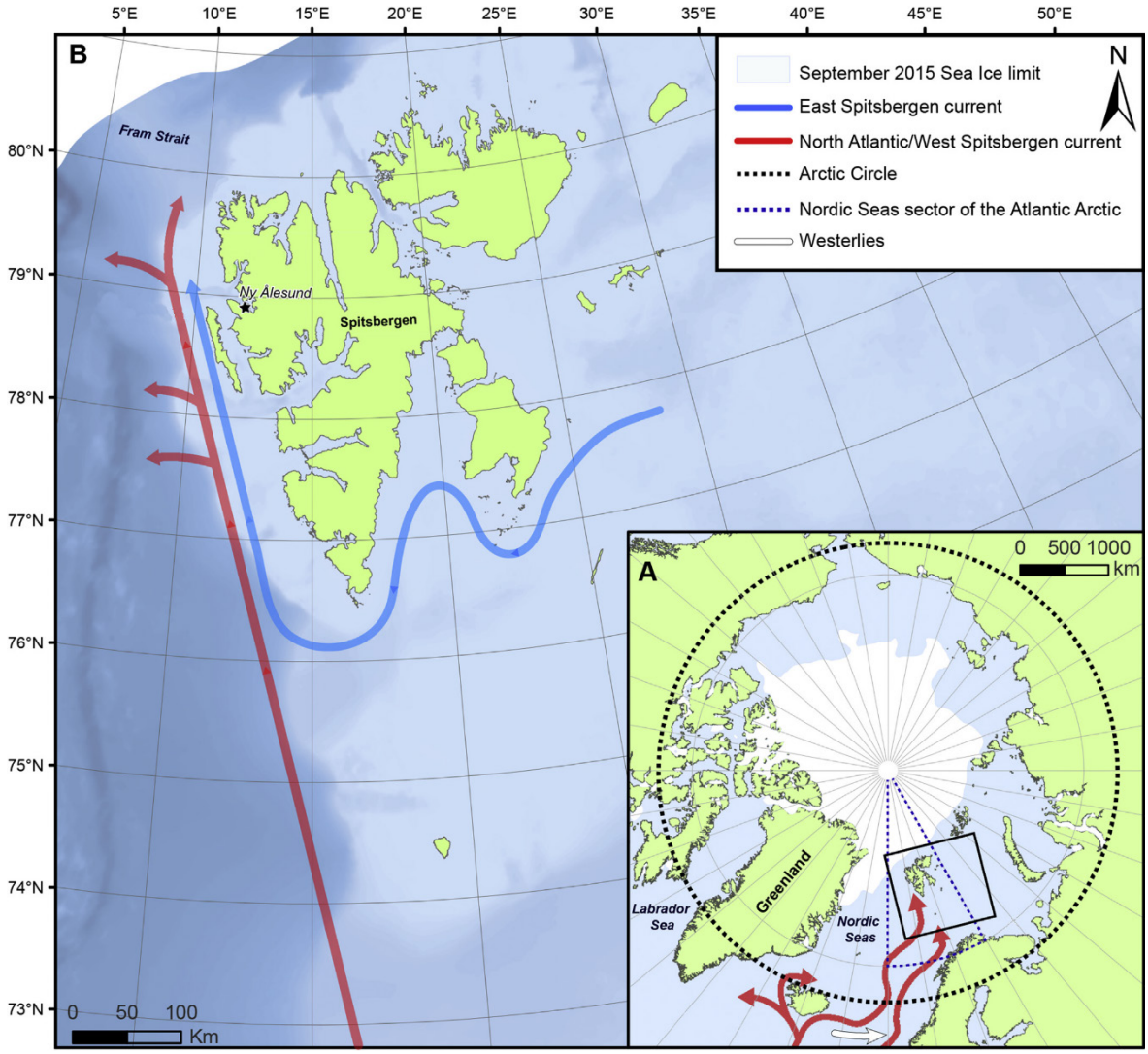

Figure 2 A: Overview map of the Arctic, highlighting the polar (Arctic) Circle, the Nordic seas sector of the Arctic Atlantic as modelled by Zhang et al. (2016), poleward circulation patterns, modified after Larsen et al. (2013) and September 2015 sea-ice coverage. B: High Arctic Svalbard Archipelago, indicating East and West Spitsbergen currents after Winkelmann and Knies (2005). Modified from van der Bilt et al. (2018).

2.2.2 Palaeoenvironmental records

In the Svalbard Archipelago, there are numerous extensive palaeoenvironmental records, which provide environmental observations within the context of the last millennium. Unlike the Antarctic Peninsula, a lot more paleo-research comes from Svalbard Archipelago, which entails more-detailed view on the palaeoenvironmental evolution. This is associated with the fact, that author will only present a review of a limited number of published studies, considered as the most relevant to this thesis.

Major part of the previously published studies are the reconstructions focused on the ocean-atmosphere interactions based on marine sedimentary cores. Specifically, Müller et

al. (2012) infer changes in the sea-ice conditions through a IP_{25} proxy in the Fram Strait for the last 8550 yrs b2k (sea-ice cover during the last 650 yrs b2k). Spielhagen et al. (2011) presents a multidecadal-scale record of ocean temperature variations during the past 2050 yrs b2k, derived from marine sediments off western Svalbard (79 °N). Sarnthein et al. (2003) shows a sea surface temperature reconstruction based on a planktonic foraminifera biostratigraphy for the last 10,750 yrs b2k in the eastern Svalbard. Dylmer et al. (2013) reveal composite record based on three marine sedimentary deposits, in order to investigate changes in the poleward flow of Atlantic waters (mostly within a Barents Sea region) over the last 3050 yrs b2k, using a coccolith proxies.

Furthermore, some of the researches focus as well on the ice core records. Isaksson et al. (2001) retrieved 121-metre-long ice core from the highest point of Lomonosovfonna (1250 m a.s.l.), one of the largest ice cap of the Svalbard Archipelago. This record provided climate record for the period AD 1920–1997 using numerous parameters, such as $\delta^{18}O$ or melt index. Followingly, this was supplemented by Isaksson et al. (2005), who presented two ice core records from Austfonna and Lomonosovfonna for the period since 600 yrs b2k. However, ice cores particularly have been studied also by several other researches (not only in the presented regions), especially since the early 1980's (e.g.; Matsuoka et al., 1997).

Palaeolimnological research on Svalbard is also comparatively plentiful. Kaufman et al. (2009) synthesize 2000 years of proxy data from lakes above 60 °N latitude with complementary ice core and tree ring records, in order to create a palaeoclimate reconstruction for the Arctic with a 10-year resolution. D'Andrea et al. (2012) present a sub-decadal- to multidecadal-scale record of summer temperature for the past 1850 yrs b2k from lake sediments of Kongressvatnet in the western Svalbard. Van der Bilt et al. (2015) study sediment from glacier-fed lake in the north-western Svalbard, in order to reconstruct glacier and local climate variability. Not only temperature, but also hydroclimate (precipitation) alters have been widely studied, e.g., Balascio et al. (2018) analyse δD composition of leaf wax compounds (*n*-alkanes; C_{25}-C_{31}) in the lake sediment from north-western Svalbard to carry out precipitation chronology for the last 12,950 yrs b2k. Another lake sediment from north-western Svalbard, which covers the entire Holocene environmental history, is analysed by De Wet et al. (2018) using multi-proxy approach. History of the last circa 5050 yrs b2k within the same region is also delivered by Gjerde et al. (2018).

Another approach for reconstruction – the study of glacial landforms on Svalbard is also widely applied. Specifically, Rachlewicz et al. (2007) focus on a "post" Little Ice Age (LIA) glacier retreat rates in the Billefjorden region, Central Svalbard. Subsequently, Phillips et al. (2017) use ^{10}Be dating of two glacier moraines in south Svalbard. However, there are also some less often methods, such as lichenometry of stabilized moraines (Werner et al., 1993). To sum up, it is essential to mention, that presented studies are only a small fraction of what has been studied overall in Svalbard.

3 SETTINGS

To investigate palaeoenvironmental evolution in polar areas two coring sites, far apart from each other, were chosen to accomplish this task. First core retrieval was performed in Lake Anonima (*Lago Anónima*) on Vega Island along the north-eastern coast of the AP. Second core was retrieved from Lake Mathiesondalen 3, situated in Mathiesondalen valley, Billefjorden region of Central Svalbard. Both sites withstand different physical-geographical conditions (see 2.1.1, 2.2.1) as well as they have been subjected to different Holocene development (see 2.1.2, 2.2.2).

3.1 Lake Anonima, Vega Island, north-eastern Antarctic Peninsula

Lake Anonima (63°49'20.34"S, 57°19'29.61"W; 24 m a.s.l.) is located in the northern part of Vega Island, ~9 km east of the Ulu Peninsula and ~3 km north of the Terrapin Hill on JRI. The lake is ~60 m long and ~40 m wide, with surface area ~2000 m^2. Bathymetric measurements proved to be a shallow lake with two subbasins of maximum depth 4.1 m (NE) and 4.6 m (SW), separated by shallow ridge. Lake is situated in an outwash plain (proglacial zone) of the local glacier Bahía del Diablo (Marinsek and Ermolin, 2015), whereas water depth at a core retrieval place was 3.8 m with a lake floor being slightly sloped.

Local bedrock is formed by Cretaceous sediments of the Marambio Group, while surrounding area of elevated volcanic mesas by Neogene back-arc volcanic rocks (basalts, hyaloclastite breccias) of the James Ross Island Volcanic Group (JRIVG; Smellie et al., 2008, 2013). Cretaceous strata consist of a set of fossiliferous marine shales, sandstones and conglomerates of Santa Marta, Snow Hill Island and López de Bertodano formations (Roberts et al., 2014). Proglacial valley floor is filled mainly with Holocene till with predominant local volcanic rocks and in a smaller proportion by Cretaceous sediments (Zale and Karlén, 1989). Along the northern coast of Bahía del Diablo, deltaic and marine deposits produced by marine transgressions after the early Holocene deglaciation are interbedded with till deposits. In the southern part of the valley, tills were partially reworked and are covered by glaciofluvial sediment (Ermolin et al., 2002).

Figure 3 (a) and (c): Proglacial zone (outwash plain) of Bahía del Diablo; (b): Lake Anonima in the northern part of Vega Island (AP) with Neogene volcanic mesas of Cape Well-met (right) and Sandwich Bluff (left) formation in the background; (d): Core retrieval using flap gouge auger (all photographed by Jan Kavan).

The climate in the James Ross Archipelago is semi-arid with annual snowfall 200–500 mm.yr^{-1} w.e. (Hrbáček et al., 2017). Summer season is relatively short (December–February) with mean annual temperature –7.0 °C (J.G. Mendel Station, period 2005–2010; Ambrožová and Láska, 2016). Lake collects surface runoff and simultaneously is connected to a water input from streams and snowmelt water with a sediment load that has formed a small delta on the southwest coast of the lake (Chaparro et al., 2017). Despite the fact that the lake basin is by Chaparro et al. (2017) considered as endorheic, the ice in till plain damming the lake seasonally melts, causing fluctuations in a water level (~1 m), as well as in underground drainage into surface streams and nearby lake systems (Jan Kavan, personal communication). On account of that, lake is classified as through-flow here. During winter, the lake surface is frozen and snow accumulates on the surface. With increasing temperatures in late spring, the snow starts to melt first, followed by thawing of the ice layer. When the summer temperature is high enough, active layer develops on the permafrost, putting the complete water cycle into operation (Chaparro et al., 2017).

Local flora is represented only by bryophytes and lichens and its distribution is usually limited due to the deficiency in liquid water (Robinson et al., 2003). They are located mainly in close neighbourhood of the lakes or streams. On the other hand, the micro-flora, mostly composed of cyanobacteria, green algae and diatoms is well developed in freshwater ecosystems such as seepages, lakes and streams that are usually supplied by melting water from retreating glaciers and snowfields (Engel et al., 2012). In lakes *Boeckella poppei* (Mrazek) and *Branchinecta gainii* (Daday) are present (Nedbalová et al., 2017), however the invertebrate fauna has been so far poorly studied. There is no penguin colony in the study area, but several seabirds frequently visit the island. The nearest Adélie penguin colony is located on Devil Island, ~3.5 km north-east of Lake Anonima. The human presence is very limited, only summer campaigns have been regularly present.

Table 1 Physical-chemical properties of the water in Lake Anonima registered on 16 Jan. 2013.

Temp (°C)	pH field	conductivity field ($\mu S.cm^{-1}$)	Acid neutralization capacity 4.5 (mmol/l)	Na^+ (mg/l)	K^+ (mg/l)	Ca^{2+} (mg/l)	SO_4^{2-} (mg/l)
11.40	8.9	156	0.6	15.1	0.86	5.13	4.06
Cl^-	TN	TP	DOC	F^-	NH_4–N	NO_3–N	NO_2–N
24.3	0.32	0.0162	1.65	0.028	0.037	0.0107	0.001

3.2 Lake Mathiesondalen 3, Mathiesondalen, Central Svalbard

Lake Mathiesondalen 3 (78°33'42.60"N, 16°35'28.90"E; 34 m a.s.l.) is situated in the Mathieson Valley on the eastern coast of the Billefjorden in Central Svalbard. Studied site lies in the western part of the Sassen–Bünsow Land nasjonalpark. Lithostratigraphically, sequences in the valley (surrounding slopes) are correlated with Minkinfjellet, Wordiekammen and Gipshuken formations (Carboniferous–Permian), all of them belonging to Campbellryggen Subgroup, Gipsdalen Group and Dickson Land Subgroup (Dallmann et al., 2004). Formations consist predominantly of carbonate and evaporate rocks – dolomite, limestone and gypsum. Late Permian high-elevated peaks belong to Kapp Starostin Formation (Tempelfjorden Group), dominated by chert, siliceous shale, sandstone and limestone (Dallmann et al., 2004). The outer part of the valley, where the Lake Mathiesondalen 3 is located, is covered by Holocene raised beach (uplifted marine terrace) sediments in the form of terraces and beach ridges (Feyling-Hanssen, 1955). The valley floor itself is occupied by a braided river system, and small tributary streams which have eroded gullies in unconsolidated sediments (Salvigsen et al., 1983).

Figure 4 (a): Search for the core's retrieval point in the Lake Mathiesondalen 3; (b): Field coring preparation (surrounding/background slopes formed mainly by dolomite, limestone and gypsum); (c): Gravity corer used for extraction (all photographed on 21/08/2015 by Matěj Roman and Jan Kavan).

The lake is ~115 m long and ~55 m wide, with surface area ~5700 m^2. Geomorphologically is this water body placed on the surface of uplifted marine terrace (34 m a.s.l.), while the lake catchment is supplied mostly by meltwater from Fairweatherbreen and other land-terminating glaciers. The local climate in the fjord head of Billefjorden is more continental, meaning mean annual temperature oscillates around –6 °C, while the winter season is distinctive by temperatures around –15 °C (Gibas et al., 2005; Láska et al., 2012). Mean annual precipitations do not exceed 500 mm, though in central Svalbard the total sum is around 200 mm. In general, climate is highly influenced by West Spitsbergen Current (WSC), making the Fram Strait (west of Svalbard) absent of sea-ice (Aagaard et al., 1987), although in inner fjords (Billefjorden) the sea-ice is rather present during the winter (December – May) season (Láska et al., 2012).

Terrestrial biota of Billefjorden is represented mainly by some megafauna species, such as *Ursus maritimus*, *Rangifer tarandus platyrhynchus* as well as by some birds –

Plectrophenax nivalis, or *Lagopus muta hyperborea*. The lake water fauna consists mainly of zoobenthos *Chironomidae* larvas, however particularly in this lake none of the diatom, nor *Cladocera* species are present (Daniel Vondrák, personal communication). The nearest permanent human settlement is ~11.7 km (north-west) far old mining Russian town Pyramiden.

4 MATERIALS AND METHODS

4.1 Cores retrieval, sediment sampling and description

The drilling of the Lake Anonima sedimentary core was undertaken during the Antarctic summer season 2012/13 (11/02/2013) by Marcos A. E. Chaparro (CONICET, Argentina), Jan Kavan (Masaryk University, Czechia) and other expedition members. The 69-cm long sediment core was extracted from Lake Anonima (referred to as AN13) using the flap gouge auger. Subsequently the core was enwrapped (to prevent moisture contamination and microbial overgrowth) in a plastic tube and after transport was stored at a room temperature for two and half years. Prior to analyses, sediment was photographed at high-resolution, sliced in one-centimetre steps and stored. The order of the implemented analyses, was determined primarily by their destructiveness. Due to non-freeze storage of the sediment samples, nitrogen content measurement was not possible.

Core from the Lake Mathiesondalen 3 (referred to as M3-15) was retrieved during the 2015 (21/08/2015) summer campaign by Matěj Roman and other members of the Polar Ecology Course 2015, organized by University of South Bohemia (Czechia). After a retrieval using a flap gouger auger, the 23.5-cm long sediment core was sliced in half-centimetre steps and stored. In both cases, compaction effect was not considered due to uncertainty associated with degree of compaction (auger type, mass densification etc.).

4.2 Radiocarbon dating

Radiocarbon (^{14}C) dating of nine selected samples (Tab. 2, 3; terrestrial macrofossil remains or, in the absence thereof, bulk sediment) was performed at Poznan Radiocarbon Laboratory (Poznańskie Laboratorium Radiowęglowe) in Poland by means of Accelerated Mass Spectrometry (AMS). In general, obtained ^{14}C ages are related to BP scale ("before present"), conventionally referring to AD 1950. It is due to major anthropogenic influence notable during the 2nd half of the 20th century (burning fossil fuels – affecting the so called "Suess effect"; Suess, 1955 and nuclear explosions and testing; Nydal and Lövseth, 1983), causing significant changes of radiocarbon reservoir in the atmosphere and the oceans (Bradley, 2015). Nevertheless, all results (proxy data) in this thesis related to "age data" are presented on a b2k (before AD 2000) time-scale with established present AD 2000.

Conventional radiocarbon (^{14}C) ages had to be calibrated so that they can be placed onto a calendar year timescale and to eliminate differencies associated with rather inhomogeneous spatial and temporal radiocarbon activity in the troposphere. However, using more accurate tropical years instead of calendar ones would be more appropriate, because one tropical year consists of 365,242192129 days, which in general results in less accurate calibration. However, this makes not an important difference for the last few millennia of the sedimentary records present here. Also, due to a different geographical position of sampling sites, different calibration data sets were chosen. SHCal13 (Southern Hemisphere; Hogg et al., 2013) curve based on dendrochronological records of terrestrial material together with marine sediments, was applied to sedimentary core from Antarctica, whereas for a lacustrine record from Svalbard a "global" IntCal13 data set (Reimer et al., 2013), based on a global calibration curve, was applied. The latter is composed of dendrochronological record, and for a period >13.9 ka cal. yrs b2k of marine (Cariaco Basin in Central Atlantic) and lacustrine (varve chronology from Lake Suigetsu in Japan) sediments, which in addition are compared with coral samples dated by uranium-series disequilibrium dating. Negative ^{14}C ages (post-bomb dates) are calibrated with the post-bomb curve (Hua et al., 2013) available for northern, as well as for southern hemisphere. In case of Lake Anonima (Vega Island, Antarctica) lacustrine samples, SH Zone 1–2 region data set was applied for the post-bomb age calculation.

The age-depth modeling of calibrated ages was processed in the R-code package Clam ver. 2.2 (Blaauw et al., 2010), using linear interpolation (Anonima) and smooth spline (Mathiesondalen 3) method with 10,000 iterations. Calibrated best-age was processed using weighted averages (Anonima), or mid-points (Mathiesondalen 3) of the age-depth model derived ages. To obtain valid chronostratigraphic sequence a smoothing (0.54) was applied in case of Mathiesondalen 3 record. Since ^{14}C ages are related to the appropriate depth interval (e.g., sample AN13_5-6 equals to the sediment depth between 5–6 cm), a half-centimetre (Anonima) and quarter-centimetre (Mathiesondalen 3) correction had to be made, so each (^{14}C) age corresponds to mid-point values, not interval ones. This step was done directly in R code (for best-age as well as for 95 % – Anonima and 99 % – Mathiesondalen 3 confidence ranges). Subsequently, a sedimentation rate for each centimetre (yr.1 cm^{-1}; age equals to mid-centimetre value) and year ($mm.yr^{-1}$) was calculated, and due to linear time scale usage, some depth values of corresponding ages were recalculated to obtain more realistic age-depth model.

4.3 ^{210}Pb and ^{137}Cs (short-lived radionuclide) dating

For a recent chronology and sedimentation trend changes, the upmost 9 (Anonima) and 3.5 (Mathiesondalen 3) centimetres of the core were analysed by gamma spectroscopy for the specific activity of isotopes ^{210}Pb ($t_{1/2}$ = 22.3 years), ^{137}Cs ($t_{1/2}$ = 30.1 years) and ^{226}Ra ($t_{1/2}$ = 1600 years). The measurements were performed in the Radiometric laboratory of the Institute of Geochemistry, Mineralogy and Mineral Resources, Charles University in Prague by Viktor Goliáš on SILAR gamma-ray spectrometry analyser. Assumption of non-uniform sedimentation led to application of CRS (constant rate of ^{210}Pb supply) model (Appleby et al., 1979), while chronology was supplemented and supported by comparison of ^{137}Cs specific activity with ^{137}Cs fallout curve (decline since 1963; Last and Smol, 2001).

4.4 Signal of magnetic susceptibility

Generally, low field or initial magnetic susceptibility (κ) is a measure of how easily a material can be magnetized (Thompson and Oldfield, 1986). κ measurement was performed at the Institute of Geophysics of the Czech Academy of Sciences in Prague on MFK1-FB Kappabridge instrument in three measuring frequencies (976 Hz, 3 904 Hz and 15 616 Hz) with induced magnetic field 200 mA.m^{-1}. To obtain mass-specific magnetic susceptibility (χ) data, the weight of each sample together with predefined volume (~10 cm^3) was determined to three decimal values. Thus, calculation of χ could have been then expressed as follows:

$$\chi = \frac{(M \div H)}{\rho}, \text{ where}$$

M stands for acquired magnetization per unit volume, and *H* represents (uniform) magnetic field. In SI units, both *M* and *H* are measured in A/m, so κ is dimensionless. Hence, to obtain the χ, κ (or equivalent *M/H*) should be divided by sample density *ρ* (Evans and Heller, 2003).

Due to a H_2O being classified in terms of magnetism and on the basis of its physical properties as a diamagnetic matter (one of the strongest; Evans and Heller, 2003), it slightly influences magnetic signal of remaining (paramagnetic and ferromagnetic) matter and therefore causes final data distortion. Nonetheless, all Anonima samples were measured in their original wet conditions with a limited amount of water content (only apparent moisture). However, by preserving the assumption of the same remaining water content across the entire core after three years of storage, the water content may be neglected. On

the other side samples from Mathiesondalen 3 were measured in their natural "soaking wet" conditions as well as in their dried form. Presented χ data are related to appropriate frequencies, unless stated otherwise.

In order to get information of superparamagnetic (SP) grains shares in studied cores, frequency-dependent χ (χ_{FD}), introduced by Dearing et al. (1996), was calculated according to the following relationship:

$$\chi_{FD} = 100 \times \frac{K_{LF} - K_{HF}}{K_{LF}}, \text{ where}$$

K_{LF} stands for 1st frequency (976 Hz) and K_{HF} represents 3rd frequency (15,616 Hz). In other words, χ_{FD} values basically equal to percentage loss of χ and indirectly refer to ultrafine grain content (with diameter 0–0.03 μm) in the sample.

4.5 Grain-size distribution

This method was applied to determine grain-size distribution of all samples from Anonima core, and of selected ones from Mathiesondalen 3 core. The measurements were performed at the Institute of Geology of the Czech Academy of Sciences in Prague on CILAS Particle Size Analyser 1190L. Prior analysis, all samples were pre-treated in various steps to separate foreign matter affecting the grain-size spectrum of siliciclastic constituent. Foreign matter is in general composed of authigenic minerals such as carbonates and diatom valves (biogenic silica) with diameter range 5–200 μm (Round et al., 1990) and their fragments. The proportion of diatoms may vary largely, being even up to 50 % of the bulk sediment, which would be the source material for diatomite (Kadey, 1983). All samples (2–3 g) were thus mixed with 10% KOH solution in 120 ml acid-proof plastic tubes and then placed in an 80 °C water bath for 10 minutes. Subsequently, samples were centrifuged in Rotofix 32A instrument for 6 minutes at 3500 rpm to separate the dissolved matter (suspension).

Nevertheless, grain-size distribution is also influenced by present organic matter. To avoid damaging grains during pretreatment, wet oxidation was here preferred instead of combustion organic matter removal. In general, widely used oxidants are potassium dichromate (Walkley and Black, 1934) and hydrogen peroxide (H_2O_2; Schumacher, 2002; Allen and Thornley, 2004). In this research, 30% H_2O_2 was used for organic matter oxidization. Hydrogen peroxide was continually added to the sample until sample frothing ceased. As in the previous case, the samples were heated to 80 °C during hydrogen peroxide

addition to increase the speed and completeness of hydrogen peroxide digestion. After the active reaction ended, the samples were washed with distilled water by centrifugation at 3500 rpm for six minutes and the solution was decanted. As before, all chemical procedures were carried out in high-temperature-proof (> 100 °C) and acid proof 120 ml centrifuge tubes. On the other hand, previous carbon and sulphur content analyses revealed the presence of carbonates below the level of detection, thus no carbonated matter removal in Anonima sediment (grain-size in Lake Mathiesondalen 3 not assured) by 10% HCl (Vaasma, 2008) was required.

The measurement itself proceeded along with the ultrasound particle dispersion on the aforementioned apparatus, with a measurable range of 0.04–2500 μm. The measurement time was set to 35 seconds, which did not include rinsing and ultrasound triggering. Volumetric grain-size parameters (mean grain-size, clay, silt and sand content, sand/silt ratio, mode, sorting, skewness, kurtosis, polymodality) were calculated from the raw grain-size data in the GRADISTAT software, v 8.0 (Blott and Pye, 2001), and are presented with graphical method (in μm) of Folk and Ward (1957).

4.6 Geochemical composition

4.6.1 Lithophile elements determination by means of X-ray fluorescence (XRF)

XRF is a nondestructive method and produces (in case of scanning approach) high-resolution records of elemental variations (Rothwell et al., 2006; Böning et al., 2007). The elemental data are measured as peak areas, i.e. the area under the peak of XRF spectrum, and are then transformed to counts per unit time per unit area. This provides a relative measure of concentration changes in the sediment. Notably also changes in sediment density, water content, organic matter and porosity can affect XRF core measurements. According to Moseley's law, heavier elements emit relatively high fluorescence intensities with more scatter and are therefore more sensitive to sample heterogeneities and mineralogical effects such as X-ray penetration depth (Weltje and Tjallingii, 2008). The sediment pore water also absorbs X-ray radiation, which leads to weaker fluorescence energies (Hennekam and Lange, 2012).

Main lithophile element content through the cores was determined using the Innov-X DELTA PREMIUM hand analyser at the Department of Geological Sciences, Masaryk University in Brno. As for grain-size distribution, samples were measured with remaining

water content (Anonima, Mathiesondalen 3), or without it after drying (Mathiesondalen 3). Every sample was measured three times in Geochem/Vanad mode, whereas final data were arithmetically averaged. It should be noted, that during XRF measurement all samples were stored in zip locks of the same batch meaning possible influence of storing material elemental composition during an analysis. However, by preserving the assumption of the same elemental composition of each plastic bag, such influence may be neglected. Besides, the measurement of empty plastic bags confirmed that selected elements contents are several orders lower than for sediment matter itself. Furthermore, to avoid heterogeneity and variable water influence, ratios over content (ppm) values were preferred in results and interpretation.

4.6.2 Carbon and sulphur content

Determination of total organic (TOC), inorganic (TIC) and total carbon (TC), together with total sulphur (TS) was performed by a professional laboratory analyst at the Czech Geological Survey (Brno branch) with ELTRA Metalyt-CS-1000S analyser equipped with infrared detection. All laboratory measurements were conducted under the strict accredited procedure (SOP-HC). To achieve highest accuracy and representativeness of the results, all samples had been homogenized before measurement. They were dried and mill grounded, so only bulk (homogenized) material could be extracted. After calibration and "blank test", when steadiness of the analyser is examined, TC and TS content of all primary sample weights were measured, using thermal combustion (1350 °C). The exact amount of material loss was measured via infrared detection. Secondary weight samples were measured to determine the amount of TIC using H_3PO_4 (1:1). Exhibited CO_2, attributed to TIC was then detected by detector, whereas TOC component was calculated by subtracting TIC from TC.

4.7 Diatom biostratigraphy

Diatom samples were oven-dried for 24 hours at 50 °C and only 1 g of dry sediment was used for further sample preparation. Samples were later prepared following the method described in van der Werff (1955). Small parts of the samples were cleaned by adding 37% H_2O_2 and heating to 80 °C for about one hour, followed by addition of $KMnO_4$. After digestion and centrifugation (3 × 10 minutes at 3700 × g), the material was diluted with distilled water to avoid excessive concentrations of diatom valves and to unify the sample

volumes. Then 50 µl of every sample was mixed with 50 µl of sonicated (10 min) microsphere solution (6792.4 MS/µl) and 400 µl distilled water and mounted in Naphrax®. Samples and slides are stored at the Department of Ecology, Charles University in Prague, Czech Republic.

In the Anonima core, approximately in every second sampled layer 400 valves (due to low abundance only 50 valves in layers 33–51) were enumerated on random transects at 1,000 x magnification under oil immersion using an Olympus BX43 microscope, equipped with Nomarski Contrast and Olympus DP27 camera using the cellSence Entry Imaging Software. Terminology is based mainly on Hendey (1964), Ross et al. (1979) and Round et al. (1990). For taxonomical identification of Antarctic species, Iconographia Diatomologica vol. 24 written by Zidarova et al. (2016) was used as a main source of information. For several species, identification up to species level was not possible due to their unclear taxonomic situation and further morphological and taxonomical research will be necessary.

4.8 Statistical data analyses

Principal component analysis (PCA) was applied to summarise graphically the major variation patterns of geochemical, petrophysical and selected biological data. Prior to PCA the suitability of correlation matrix was tested by Kaiser-Meyer-Olkin (KMO) test, while minimum data contribution in each variable was designated to 80 % except biostratigraphy data, where diatom abundance was analysed in every second sample. Delivered correlations (Pearson *r*) are significant at the 0.01 level unless stated otherwise. Biological data (diatom species) are expressed as relative abundances (% of total diatom valves per sample). Diatom characteristics – number of valves per gram of sediment, species richness, Shannon diversity (Shannon and Weaver, 1949) and Evenness (Pielou, 1966) – were calculated according to cited publications. Significant diatom clusters were identified and divided using stratigraphically constrained cluster analysis (CONISS) with significant division based on comparing a CONISS distance matrix with a random model based on broken stick model (Bennett, 1996) using the *rioja* package in R (Juggins, 2009). All presented graphs were produced in Grapher v. 11.

5 RESULTS

5.1 Lake Anonima

5.1.1 Lithology and age-depth model

Lithological profile is comparatively undifferentiated with undeveloped annual lamination or visible stratification (Fig. 5). For an age-depth model of deposition in Lake Anonima (Fig. 5) five radiocarbon ages were obtained from the core and are presented in Tab. 2., although the fifth and concurrently nethermost sample (66–67 cm) revealed significantly underestimated radiocarbon age. Due to reversal age of the lowermost sample, only the topmost four radiocarbon ages, revealing suitable chronostratigraphic sequence (goodness-of-fit value 4.96), were included into the calculation of age-depth model with a base onset at 2440 cal. yrs b2k (54–55 cm). Tab. 2 shows that the topmost part (5.5–0 cm) accumulated after 1950 AD, therefore post-bomb radiocarbon age, where the amount of nuclide is conventionally expressed as pMC entailing "percentage of modern carbon" – normalized to 100 % (Reimer et al., 2004). Short-lived isotopes (^{137}Cs, ^{210}Pb) dating proved very low specific activities (Bq/g) in the samples, thus relationship purification between age and depth within recent decades was not possible.

Table 2 Radiocarbon ages of dated samples from the Lake Anonima.

Sample	Laboratory code	Depth (cm)	Material	mg C[a]	^{14}C years BP	Min.–Max. age cal. yrs b2k (± 2σ)
AN13_5-6	Poz-85803	5–6	lacustrine moss	0.09	100.99 ± 0.39 pMC	43–44
AN13_16-17	Poz-89401	16–17	lacustrine mud	–	555 ± 30	554–604
AN13_28-29	Poz-89403	28–29	lacustrine mud	–	1650 ± 30	1468–1615
AN13_54-55	Poz-89402	54–55	lacustrine mud	–	2130 ± 30	1991–2204
AN13_66-67	Poz-85804	66–67	lacustrine mud	0.06	1260 ± 80	–

[a] milligrams of carbon in the analysed sample, where the amount of carbon was < 0.1 mg

Sedimentation rate along the profile varies in range 0.13–0.97 mm.yr^{-1} suggesting variable clastic input within time. Interval 2440–1560 cal. yrs b2k shows comparatively higher sedimentation rate (0.45 mm.yr^{-1}) followed by long sediment input reduction between 1560–90 cal. yrs b2k (0.13–0.21 mm.yr^{-1}). Near the core's top the sedimentation rises steeply to 0.97 mm.yr^{-1}, which might correspond with smaller compaction of topmost part of the core.

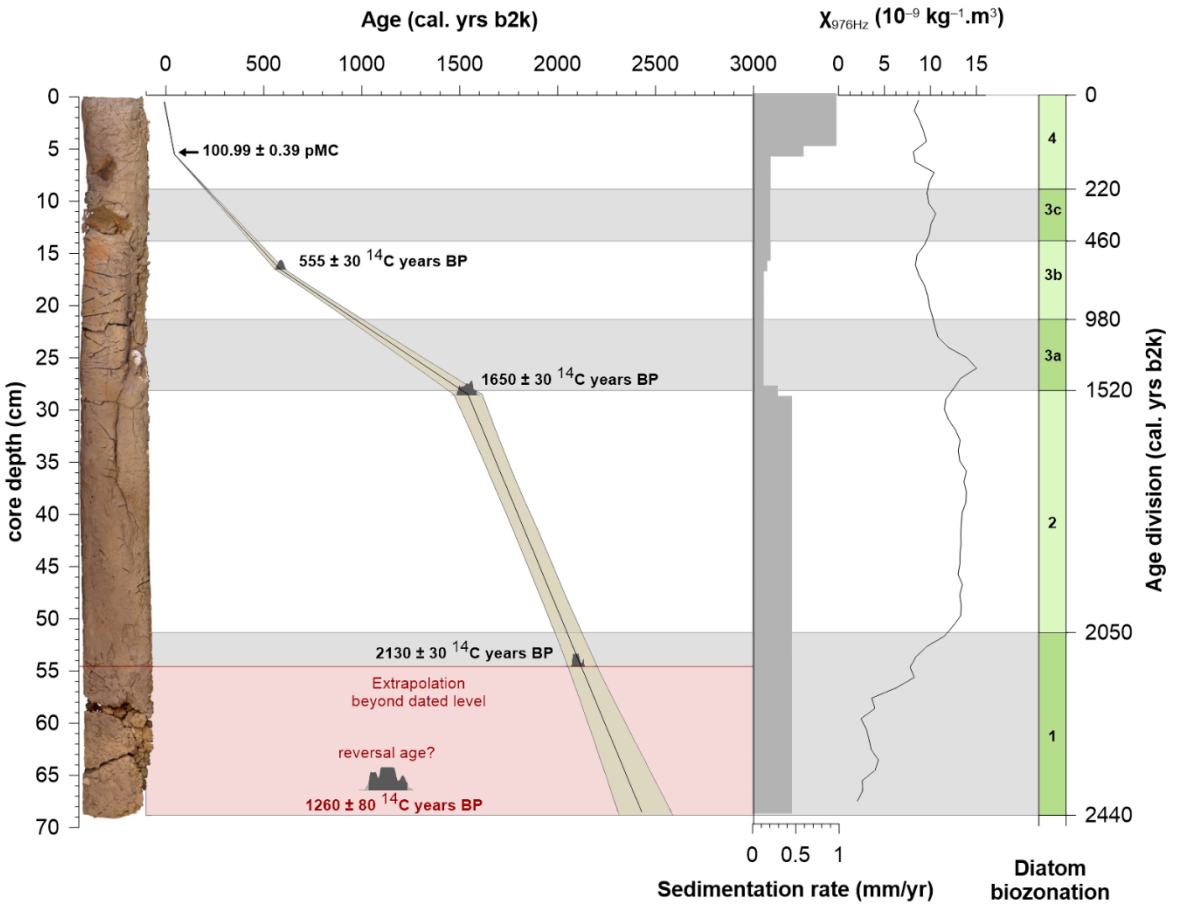

Figure 5 Best estimate age-depth model (black line) with 2σ uncertainty envelope (95 % confidence interval) based on four ^{14}C ages derived from the Lake Anonima. The lowermost reversal ^{14}C age is not included in age-depth model calculation. Supplemented by probability distribution curves of calibrated ages, sedimentation rate (mm.yr^{-1}), mass magnetic susceptibility (χ_{976Hz}) and diatom biozonation (Bennett, 1996 model).

5.1.2 Physical proxies

Measurements of χ and χ_{FD} were performed with samples in original wet conditions with a limited quantity of water content (merely apparent moisture). Still, by preserving the assumption of the same remaining water content across the entire core after three years of storage, paramagnetism and diamagnetism of the water might be neglected. The values of χ obtained throughout the core are rather low (generally in the range of 10^{-9} m^3.kg^{-1}) showing a limited influence of ferri- and ferromagnetic particles and dominance diamagnetic and paramagnetic material.

Lowest part (2440–2200 cal. yrs b2k) of the core section is distinctive by comparatively low χ vacillating around ~3 × 10^{-9} m^3.kg^{-1}, followed by emergent shift (2200–2000 cal. yrs b2k) to increased values (~13 × 10^{-9} m^3.kg^{-1}) towards the middle section of the core (2000–1400 cal. yrs b2k). Abrupt apex at 1400 cal. yrs b2k initiated continuously decreasing drift

ceasing at 550 cal. yrs b2k (~8 × 10^{-9} $m^3.kg^{-1}$). Time interval 550–0 cal. yrs b2k exhibited χ variation in the range ~8–10 × 10^{-9} $m^3.kg^{-1}$. Calculated proxy parameter χ_{FD} revealed apparent variability throughout the profile. Nonetheless, lowest part shows relatively higher χ_{FD} (~5 %) with a rapid decrease at 2100 cal. yrs b2k (to ~3.5 %), corresponding to opposite shift in χ. Time interval 2000–0 cal. yrs b2k reports continuously increasing course (~3.5 to 5 %) towards the core top.

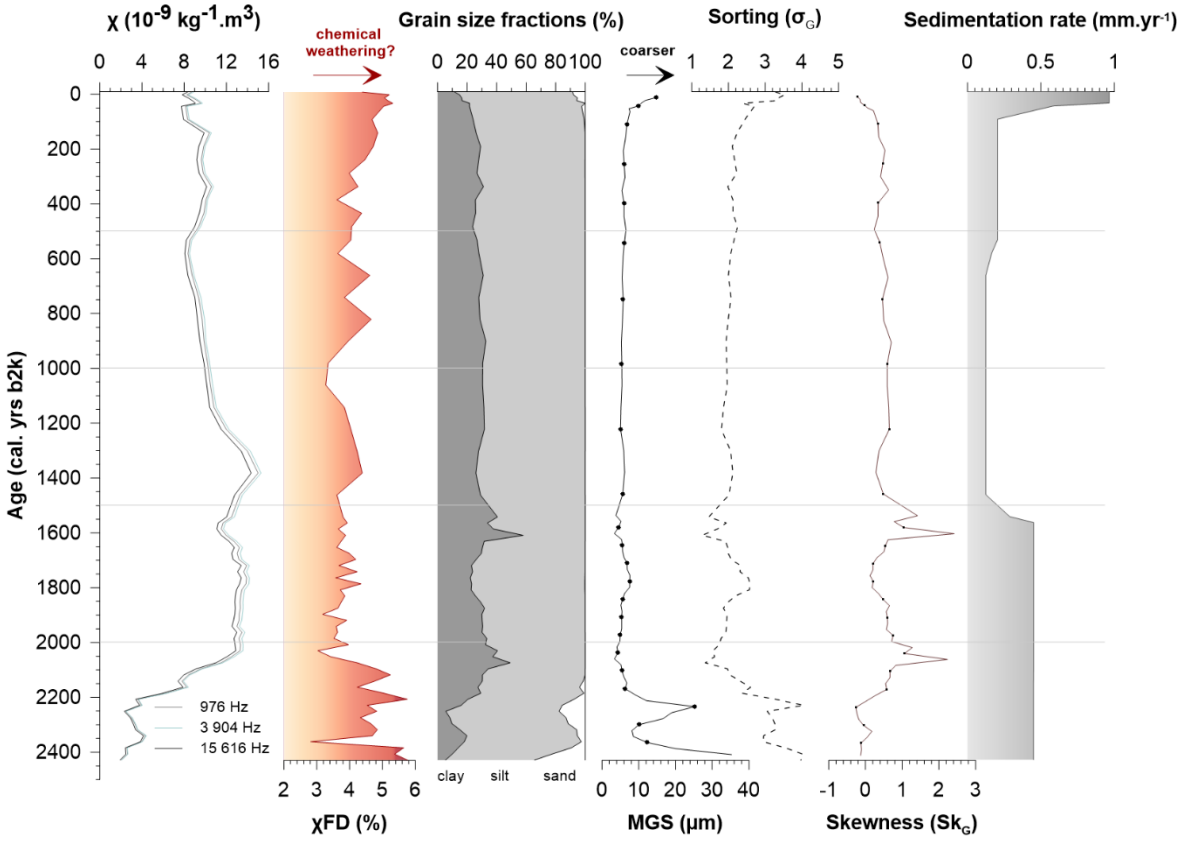

Figure 6 Physical proxies (left to right): mass magnetic susceptibility χ (10^{-9} $kg^{-1}.m^3$), frequency-dependent magnetic susceptibility χFD (%), grain-size fractions (%), mean grain-size MGS (μm), sorting degree, skewness and sedimentation rate ($mm.yr^{-1}$) plotted against b2k time-scale.

Sediment has predominantly unimodal distribution with lowermost 15 cm (2440–2110 cal. yrs b2k) and topmost 19 cm (780–0 cal. yrs b2k) being poorly sorted. Middle section (2110–780 cal. yrs b2k) comprises changes of sorting in each 5–7 cm interval from moderately sorted to poorly sorted and conversely, respectively. Degree of sorting is appositely reflected in grain-size distribution, where sections with higher shares of sand fractions tends to be less sorted. Anyhow last 50 cal. yrs b2k are characterised by increasing sand (~5 %) and decreased clay (~17 %) content correlating with higher mean grain-size (MGS; ~10 %).

Period 50–1500 cal. yrs b2k shows relatively static clastic input with clay fraction oscillating around 28 % (silt ~72 %) whereas sand fraction is not present. Lower part of the core has more inferior the same fraction proportion, although at 1610 and 2070 cal. yrs b2k two steep peaks of clay fraction (up to 58 and 49 %) are apparent. The oldest part of the profile demonstrates diminishing curve in clay fraction down to 12 % with sand fraction increase up to 13 %. MGS parameter variation correlates well with fine sand fraction (r = 0.93).

5.1.3 Geochemistry

Whilst none inorganic carbon was detected in the entire core, TOC and TS courses correspond to each other with their highest relative content (maximum TOC 5.1 % and TS 0.2 %) in the bottom section (2440–2130 cal. yrs b2k). Organic carbon and sulphur then rapidly reduces almost to zero, which is compensated in upper section (1420–260 cal. yrs b2k), where TOC oscillates around 1 %. Fluctuations linkage with subsequent inorganic proxies is best expressed with light elements (LE) content (r = 0.90) and Rb/Sr (r = 0.87) plus Fe/Mn (r = 0.86) ratios. Direct relationship between the latter two is also apparent (r = 0.89), whereas biogenic silica (BSi) presence expressed circuitously by Si/Ti ratio as well corresponds with TOC (r = 0.81) very fitly. Grain-size Zr/Ti and Al/Si proxies also bear cognation (r = –0.86) establishing these two ratios as a solid proxy for grain-size distribution. To distinguish main processes, material sources in the catchment area and heterogeneity and variable water influence in the core, the author relies on ratios over ppm content of individual elements.

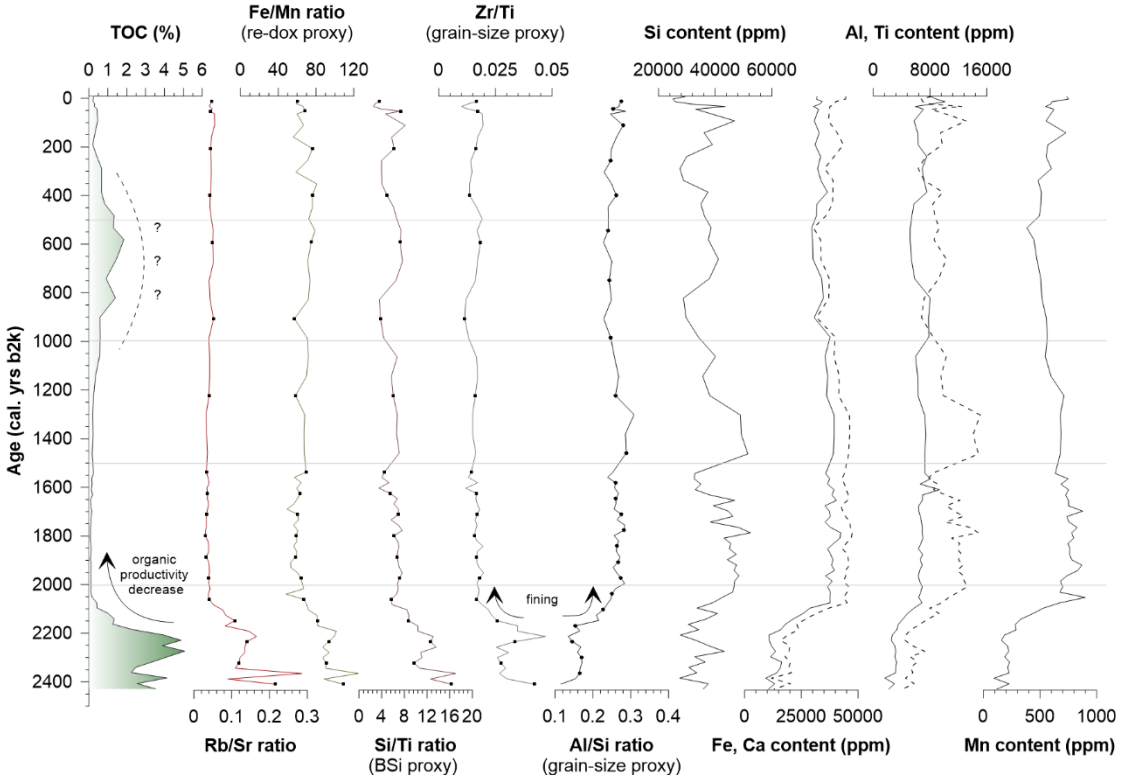

Figure 7 Geochemical proxies (left to right): total organic carbon TOC (%), Rb/Sr, Fe/Mn, Si/Ti, Zr/Ti and Al/Si ratios, Si, Fe, Ca, Al, Ti and Mn contents (ppm).

5.1.4 Diatom biostratigraphy (by Kateřina Kopalová and Marie Bulínová)

The complete diatom flora of the Lake Anonima core reveal 80 species in total, belonging to 26 genera. Based on the CONISS cluster analysis the Lake Anonima core is being divided into six diatom zones (from now on a "biozone" term is used), four of which are statistically significant based on the broken stick model (biozones 1–4). Subdivisions within the biozone 3 are not statistically significant, but they are retained due to their correspondence with changeable TOC content within the biozone 3 (Fig. 8). Diatom productivity mirrors patterns in TOC, which is the highest in biozone 1, where the diatom species reach their highest abundance 604 × 10^4 valves per gram of dry sediment. The lowest productivity subsists in the biozone 2 where the observed maximum is only 10 × 10^4. More intermediate and variable is in the biozones 3 and 4 (ranging 20 × 10^4–210 × 10^4 valves per gram of dry sediment).

Richness increases overall from the biozone 1 to the biozone 4 with the peak in the recent material in the biozone 4, and being lowest in biozones 1 and 2. Shannon diversity is more stable, but has the lowest values in biozone 1 ranging between 1.36 and 2.49 and the greatest values in biozone 4, where the maximum value of 2.89 is remarked. Evenness shows a more

fluctuating pattern with the greatest value in biozone 2 reaching its maximum 0.93. The diatom community as a whole is dominated by the genus *Nitzschia* (average share of the genus in the core is almost 41 %) and the abundances are relatively uniform within the core. The next most abundant taxon is *Planothidium rostrolanceolatum*, which occurs in share up to ~ 41 % in the biozone 3. All other taxa contribute by smaller proportions and are more variable within the core. Specific patterns in diatom community in individual biozone follow.

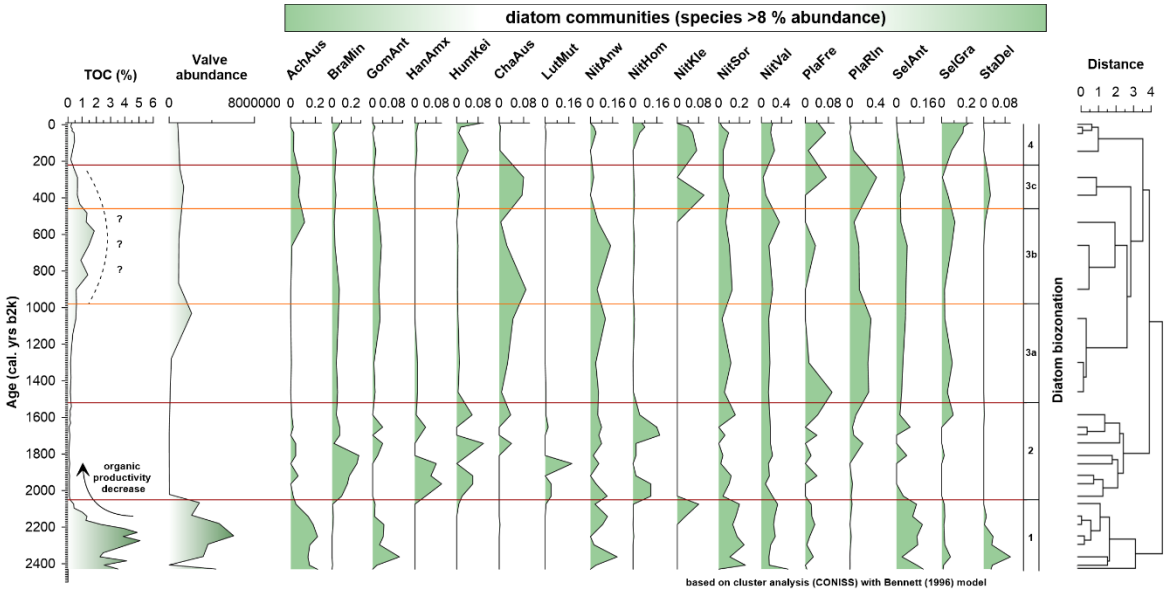

Figure 8 Diatom stratigraphy of the Lake Anonima sedimentary core plotted against b2k time-scale. Zonation is based on a CONISS analysis of the diatom species composition. Only diatom species with a relative abundance >8 % are depicted. Significant group divisions are marked with red lines. Photomicrographs of presented species are to be found in Zidarova et al. (2016). Supplemented by TOC (%) and valve abundance/productivity (both left).

Biozone 1 (2440–2050 cal. yrs b2k) is dominated by the genus *Nitzschia* (46–67 %), followed by *Achnanthidium australexiguum* (4–22 %), S*ellaphora antarctica* (4–16 %), *Stauroneis delicata* (0.2–10 %, being mostly present only in the biozone 1 and subzone 3c), and *Gomphonema maritimo-antarcticum* (0.7–11 %). *Brachisira minor*, the most abundant species in the biozone 2, shows almost no presence in biozone 1. Diatom biozone 2 (2050–1520 cal. yrs b2k) is different, than all other biozones characterized by very low total diatom valve concentration (Fig. 8). In the biozone 2, only 50 valves per sample were counted in comparison to 400 in other biozones due to extremely low valve concentration, which may have artificially reduced the calculated species richness and increased Evenness. The diatom

communities present mostly (semi-)terrestrial diatom species such as *Brachisira minor* showing the highest abundance in the biozone 2 (2–28 %), *Hantzschia amphioxys* (0.5–10 %), *Luticola muticopsis* (0.5–18 % appearing only in the biozone 2), and also genera *Humidophila* is present. In much of biozone 2, *Sellaphora gracillim*a is absent. The community is still dominated by genus *Nitzschia*, but within this genus *Nitzschia homburgiensis* comprises up to 18 % of the community in contrast to the rest of the core, where it appears in very low abundances.

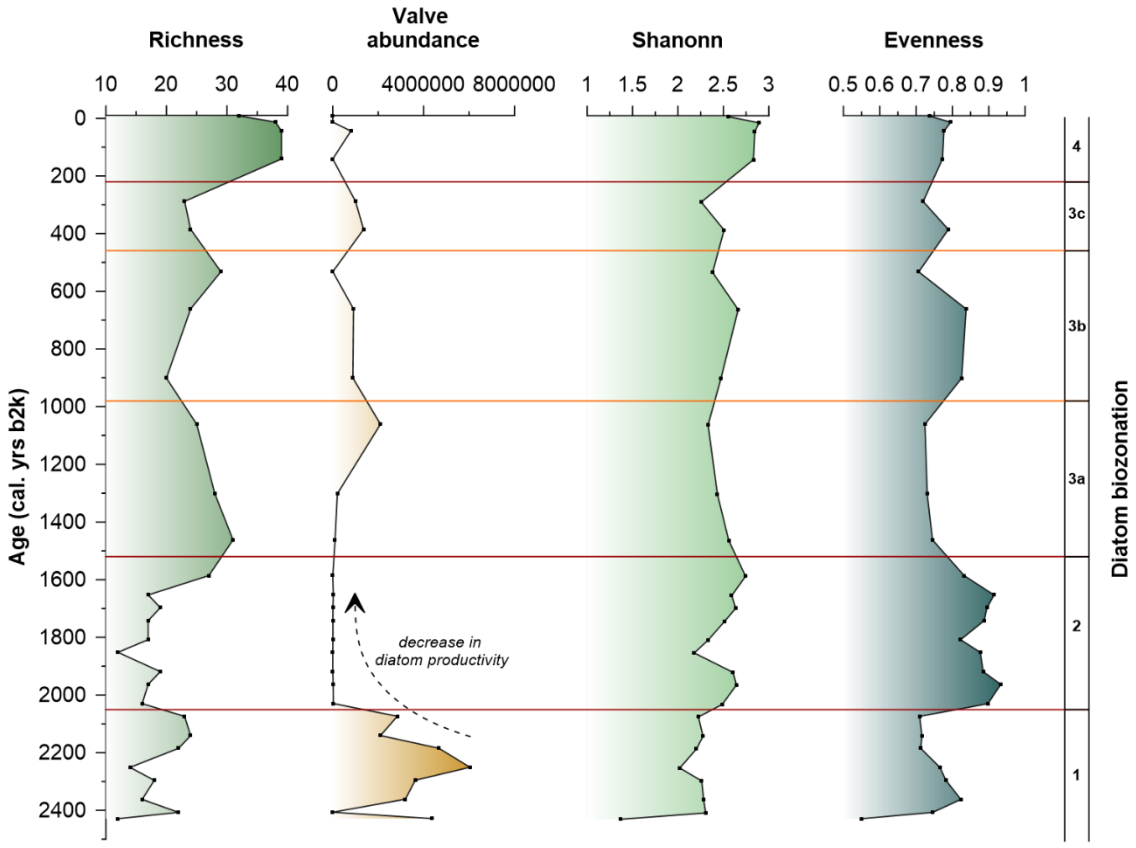

Figure 9 Diatom characteristics: (Diatom species) richness is the number of taxa in the sample, Valve abundance presents diatom valves per one gram of dry matter (sediment), Shannon diversity summarises the diversity of a population in which each member belongs to a unique group (species), and species Evenness refers to homogeneity of the species. The zonation is based on the CONISS analysis of the diatom species composition (Fig. 8).

Diatom biozone 3 (1520–220 cal. yrs b2k) is subdivided into three sub-zones (3a: 1520–980 cal. yrs b2k, 3b: 980–460 cal. yrs b2k and 3c: 460–220 cal. yrs b2k). Biozone 3 is characterised by co-dominance of *Planothidium rostrolanceolatum* and the genus *Nitzschia*. *Planothidium rostrolanceolatum* has the highest abundance in the sub-zone 3c (14–32 %). *Achnanthidium australeexiguum*, which is present in sizable amount throughout the core is

almost absent in biozone 3a. The characteristic feature of biozone 4 (220 cal. yrs b2k – current age) is the reduction of the abundance of *Planothidium rostrolanceolatum* and increase of abundance of *Sellaphora gracillima*. *Humidophila keiliorum* is present again after being almost absent in biozone 3.

5.1.5 PCA

First PCA (total explained variance 84.10%; KMO value 0.83 – "meritorious" sample adequacy; Fig. 13) showed that major variability of non-biotic data together with diatom indexes within a core is driven mainly by PC1 with 61.73 % of explained variance. PC2 (9.84 %) together with PC3 (6.75 %) and PC4 (5.78 %) are not considered as substantial due to their low explained variance and thus low interpretable clarity. PC1 bears a strong positive correlation with LE (r = 0.97), TOC (r = 0.94), Rb/Sr (r = 0.92), Fe/Mn (r = 0.91), Zr/Ti (r = 0.84), Rb (r = 0.81), Si/Ti (r = 0.80), sand fraction (r = 0.78), TS (r = 0.76) and also strong negative correlation with Fe, Sr, Ca (r = −0.98), Zn (r = −0.97), Cu (r = −0.96), χ_{976Hz} (r = −0.95), Mn, Al/Si (r = −0.94). PC2 has an appropriate reflection with Shannon and Evenness (r = 0.96), richness (r = 0.92), but only fair correlation with productivity (r = 0.50).

Second PCA (KMO value 0.79 – "middling" sample adequacy; Fig. 14) suggested lower degree of total explained variance (72.42 %) due to probable influence of increased data heterogeneity (several diatom species) in the analysis. PC1 however explains 53.28 % of total variance within sediment, and unlike in the previous PCA (Fig. 13), a PC2 explains slightly more input data variability (12.64 %). Nevertheless, due to a low explained variance (6.50 %) a PC3 is not considered to explain a substantial process role during sedimentation, thus it is not included in interpretation. Most significant loadings (correlations) in the PC1 correspond to PC1 of the previous analysis – i.e. organic matter represented by TOC (r = 0.93) and LE (r = 0.97) majorly correlates positively with PC1. As well Rb/Sr (r = 0.91), Fe/Mn (r = 0.90), Zr/Ti (r = 0.84) and Si/Ti (BSi r = 0.80) elemental ratios do have a significant positive relationship, while binding between petrophysical proxies and PC1 is still significant, but less intense (sand r = 0.79, χ_{FD} r = 0.58). Indirect link of PC1 is visible with a few elements (Fe, Ca, Sr, Zn r = –0.97; Ti r = −0.86; Al r = −0.79), as well as with elemental ratio Al/Si (r = −0.94) and petrophysical proxies (clay r = −0.65, χ_{976Hz} r = −0.95). Diatom assemblages are associated more with PC2 (*Sellaphora Antarctica* r = 0.63, *Sellaphora gracillima* r = 0.56, *Brachysira minor* r = 0.54), while diatom characteristics

relate to PC2 as well (Shannon, Evenness $r = 0.95$; richness $r = 0.89$), except productivity, which has littler same correlation coefficient with both components (PC1 $r = 0.54$, PC2 $r = 0.49$).

5.2 Lake Mathiesondalen 3

5.2.1 Lithology and age-depth model

Due to direct field sub-sampling of the core, lithostratigraphic description was not taken into consideration, meaning that lithological units throughout the sediment were not later identified and described. In addition, prevailing absence of terrestrial macrofossils led to the analyses of bulk sediment samples. However, four radiocarbon ages supplemented by uppermost seven samples measured for short-lived (^{210}Pb, ^{137}Cs) isotopes, revealed comparatively robust chronological sequence (goodness-of-fit value 9.85), which covers the last ~700 years of natural history.

Table 3 Radiocarbon ages of dated samples from Lake Mathiesondalen 3.

Sample	Lab code	Depth (cm)	Material[a]	mg C	^{14}C years BP	Min.–Max. age cal. yrs b2k (± 3σ)	Min. – Max. (including reservoir 4380 ± 40 ^{14}C BP)
M3-15_1.5-2	Poz-96535	1.5–2	lac. mud	0.35	4330 ± 40	4837–5031	–
M3-15_8.5-9	Poz-96536	8.5–9	lac. mud	0.6	5500 ± 40	6214–6398	935–1174
M3-15_16.5-17	Poz-96537	16.5–17	lac. mud	–	5080 ± 40	5739–5913	556–728
M3-15_23-23.5	Poz-96538	23–23.5	lac. mud	–	4840 ± 40	5476–5652	330–625

[a] ”lac. mud” = lacustrine mud

Table 4 Short-lived isotope activity and associated ages of the core top from Lake Mathiesondalen 3.

Sample/depth (cm)	specific activity [Bq/g]			Calculated yrs b2k
	^{210}Pb (± 1σ)	^{137}Cs (± 1σ)	^{226}Ra (± 1σ)	(± 1σ)
0–0.5	0.330 ± 0.024	0.027 ± 0.008	0.141 ± 0.013	−14 ± 4.0
0.5–1	0.316 ± 0.013	0.031 ± 0.004	0.130 ± 0.007	−12 ± 3.8
1–1.5	0.300 ± 0.015	0.023 ± 0.005	0.156 ± 0.009	−5 ± 3.8
1.5–2	0.269 ± 0.007	0.028 ± 0.002	0.135 ± 0.004	−1 ± 3.5
2–2.5	0.250 ± 0.007	0.040 ± 0.003	0.133 ± 0.004	10 ± 3.7
2.5–3	0.257 ± 0.009	0.043 ± 0.003	0.138 ± 0.005	22 ± 3.9
3–3.5	0.194 ± 0.007	0.047 ± 0.003	0.126 ± 0.004	44 ± 3.6

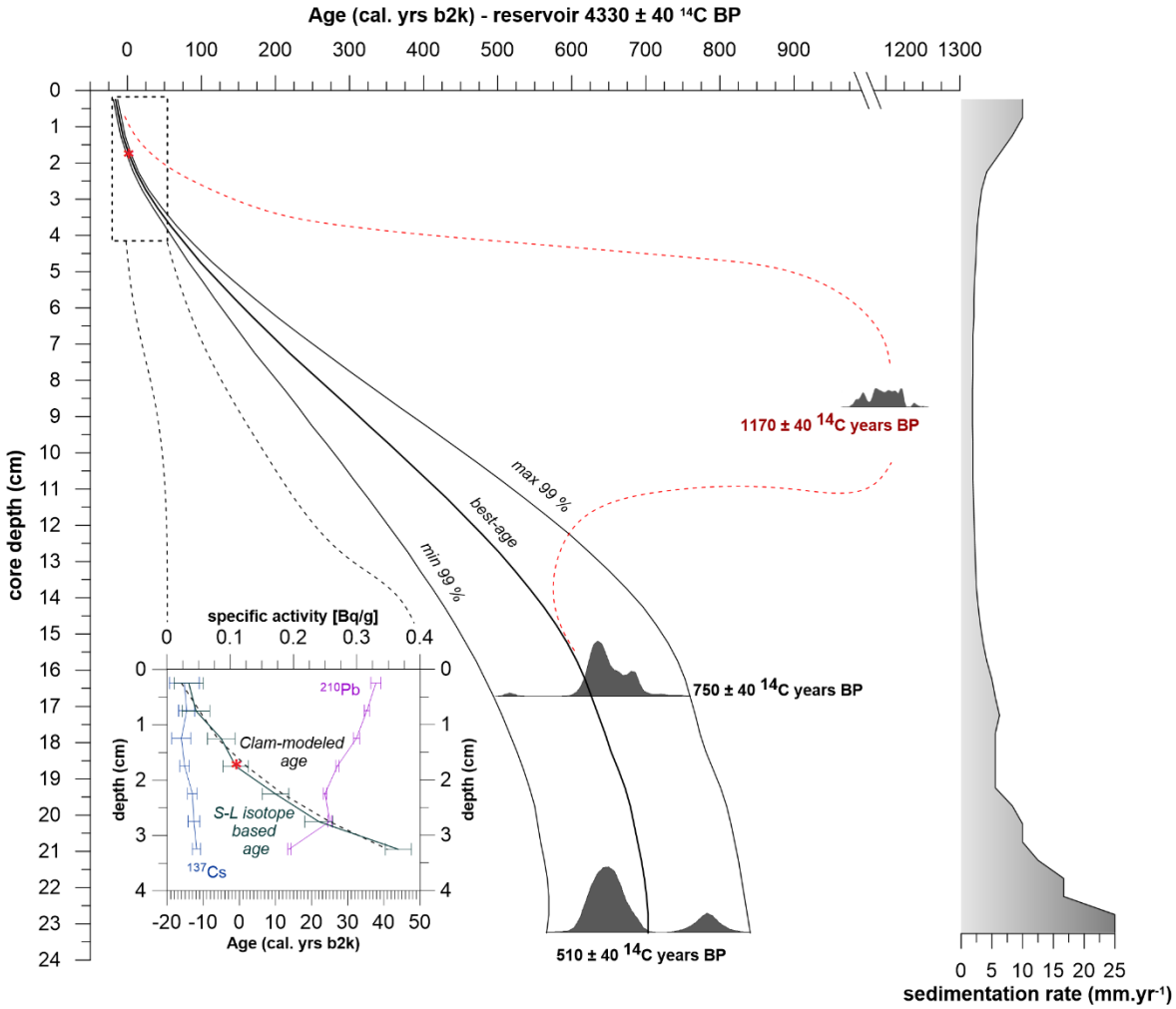

Figure 10 Best estimate age-depth model (middle bold black line) with 3σ uncertainty envelope (99 % confidence interval) based on three ^{14}C and seven short-lived (^{137}Cs, ^{210}Pb) isotope (inset) based ages. Combination of such methods enabled establishment of upmost ^{14}C age (red star marks) being equal to -1 yrs b2k. The 8.5–9 cm reversal ^{14}C age is not included in age-depth model calculation. Supplemented by probability distribution curves of calibrated ages (3σ) and sedimentation rate (mm.yr^{-1}).

Based on the comparison of two independent methods (^{14}C vs. ^{210}Pb and ^{137}Cs) for the material form 1–1.5 cm depth, a radiocarbon reservoir was determined at 4380 ± 40 ^{14}C yrs BP, whereas significantly overestimated radiocarbon age (5500 ± 40 ^{14}C yrs BP) at 8.5–9 cm depth was not taken into account for the age-depth model build-up. Since a smooth spline method was applied for an age modelling, sedimentation rate does not change abruptly, but rather continuously with less pronounced shifts. Rate of material input alters within a range of 1.85–25 mm.yr^{-1}, with its highest sedimentation rate (25 mm.yr^{-1}) being distinctive for the lowest section (~23 cm; ~700 cal. yrs b2k). It is followed by a continual decrease (25 mm.yr^{-1} → 1.85 mm.yr^{-1}) to 300 cal. yrs b2k (8.75 cm), and in the upper part of the succession, the sedimentation rate steadily rises to 10 mm.yr^{-1} at the core's top, which might

be an artefact of uneven distribution of dated samples. Handed-down uncertainty associated with the compaction effect is, also here, on point.

5.2.2 Geochemical and physical proxies

The carbon and sulphur content proved significant changes over time. Continual increase in TC (8.91 % → 10.59 %) towards the present is apparent, while opposite course is marked by TS (0.13 % → 0.07 %). TOC content shows comparatively increased variability, although between 700–380 cal. yrs b2k a recorded decrease (~5.98 % → 4.50 %), with following (since 380 cal. yrs b2k till present; ~4.50 % → 6.23 %) opposite (and more variable) increase, is evident. Unlike TOC, TIC shows in the time range 700–380 cal. yrs b2k a continuous increase (2.93 % → 4.50 %) with succeeding, however more variable trend towards the present.

Inorganic geochemistry results (ppm content and ratios) are presented in dried (*d*) as well as in original wet conditions (*w* – in Figs. 11 and 12 titled as "+H_2O samples"). However, only few of the presented elemental contents (Fig. 11) do bear a considerable course and/or variability. Generally, the moist samples show significantly lower contents of chemical elements (Fig. 11) due to variable water absorption of X-ray radiation. From this perspective, the XRF data obtained from dried samples should be preferred. For instance, Si and Al (both *d*) contents decrease since ~380 cal. yrs b2k, while Fe and Ca (*w*+*d*) show rather long-term decrease and increase, respectively. Selected elemental ratios (Fig. 11) reveal permanent increase (e.g., Si/Ti, Zr/Ti), while other ratios reveal decrease (e.g., Rb/Sr, Fe/Mn). However, notably, values of all ratios (with an exception of Rb/Sr) do fluctuate quite sensitively, resulting in more wavering and less indicating trends. Al/Si ratio does not suggest any long-term course.

Due to logistic issues, the magnetic susceptibility (χ) of the upmost 5 cm of dried samples were not analysed, thus they are not presented in the results. However, as in the Lake Anonima χ values obtained throughout a core are rather low (both *d* and *w* – generally in the range of 10^{-8} $m^3.kg^{-1}$) showing a limited influence of ferri- and ferromagnetic particles and concurrently dominance of diamagnetic and paramagnetic matter. Also, all three frequencies of χ show persistent decreasing trend since 700 cal. yrs b2k. Nevertheless, magnitude of decrease is more intense for dried samples between the period 700–500 cal. yrs b2k. Due to

the overlapping χ of different frequencies (*w* and *d*), the χ_{FD} parameter displays negative values (*w* and *d*).

Relationships between variables of interest have been revealed using correlation counts, however for some tight connections, the independence of both variables was violated (i.e. *r* = 0.97 between Rb/Sr and Rb), which have resulted in exclusion from the analysis. Separate measurements of dry samples revealed that strongest positive coherence is present between Rb and Zn (*r* = 0.98), Si and Al (*r* = 0.94), and Rb/Sr and Zn (*r* = 0.92). There is also strong positive correlation of Rb/Sr with Fe/Mn (*r* = 0.81), χ_{3904Hz} (*r* = 0.88) as well as with $\chi_{15616Hz}$ (*r* = 0.86), however very weak with χ_{976Hz} (*r* = 0.46). Separate Rb content is linked well with χ_{3904Hz} (*r* = 0.81) and Fe content (*r* = 0.86). Fe correlates quite fitly with Zn (*r* = 0.87), χ_{3904Hz} (*r* = 0.86) and $\chi_{15616Hz}$ (*r* = 0.85). Also, Si and K relationship corresponds rather well (*r* = 0.85). On the other side, the strongest indirect correlation is mostly associated with TC behaviour. Specifically, strongest negative correspondence of TC is with Rb (*r* = –0.94), Rb/Sr and Zn (both *r* = – 0.91), Fe/Mn (*r* = –0.87), Ni (*r* = –0.84), Cu (*r* = –0.79), K (*r* = –0.77), Zr (*r* = –0.75), Cr and χ_{3904Hz} (both *r* = –0.74). This is supplemented by Ca and K (*r* = –0.87), and indirect connection of Sr with Fe/Mn (*r* = –0.75).

Analyses of moist samples also revealed certain substantial linkages among variables. Particularly, positive coherence is tightest between Zn content and K and Rb (both *r* = 0.95), respectively. As in the context of dried samples, Rb content behaviour is linked quite tightly with K (*r* = 0.94), Zr (*r* = 0.90) and Fe (*r* = 0.89). Furthermore, Al corresponds highly with Ti (*r* = 0.93), while Si/Ti is linked with Zr/Ti (*r* = 0.88). Strong positive relationship is also between Rb content and χ_{976Hz}, χ_{3904Hz} (both *r* = 0.91) and $\chi_{15616Hz}$ (*r* =0.90). On the other hand, some of the strong indirect correlations are related to TC variability throughout a profile. TC corresponds negatively mostly with Rb (*r* = –0.94), Rb/Sr (*r* = –0.88), Zr (*r* = –0.85), K (*r* = –0.84), Zn (*r* = –0.83), Fe (*r* = –0.80) as well as with all three χ frequencies – χ_{976Hz} (*r* = –0.84), χ_{3904Hz} (*r* = –0.84), $\chi_{15616Hz}$ (*r* = –0.83). LE content behaviour within dried samples is in line with Ca (*r* = –0.81) and Sr (*r* = –0.76), while sufficient negative relationship is also between Al content and Zr/Ti (*r* = –0.67), and Ca and Rb/Sr (*r* = –0.79). Further correlations and linkages among variables are provided by PCA results, presented in 5.2.3.

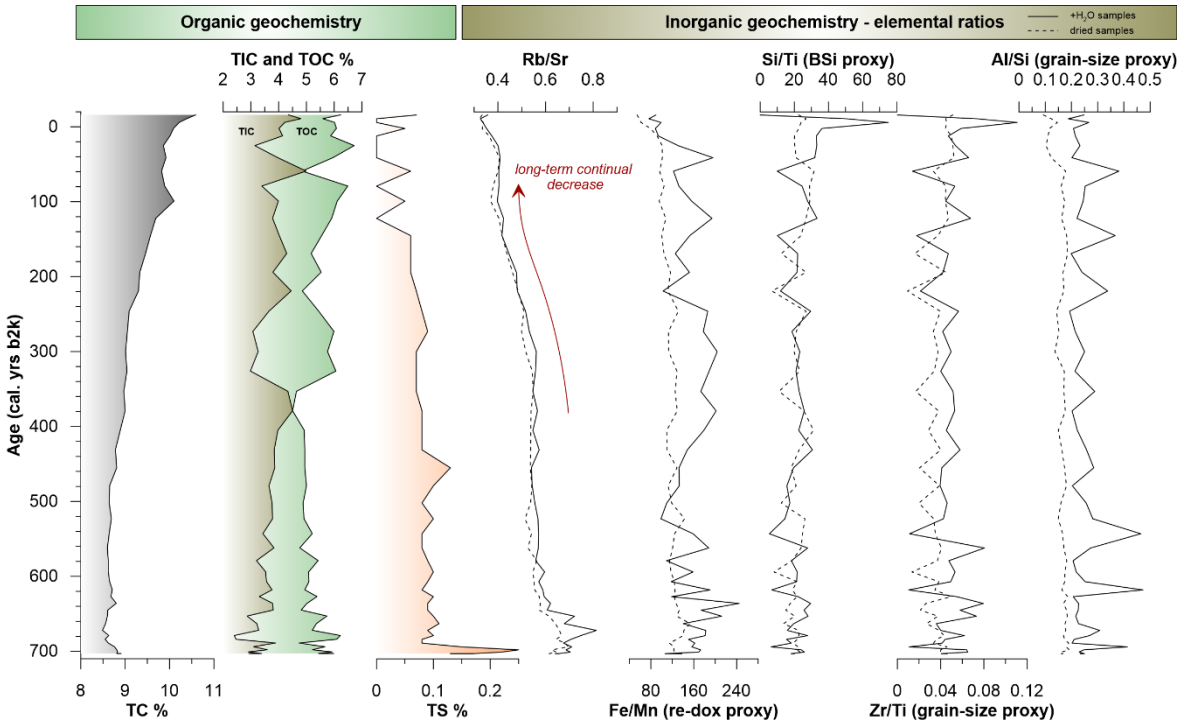

Figure 11 Geochemical organic proxies (TC, TIC and TOC, TS – all %) together with selected elemental ratios (Rb/Sr, Fe/Mn, Si/Ti, Zr/Ti and Al/Si) plotted against b2k time-scale.

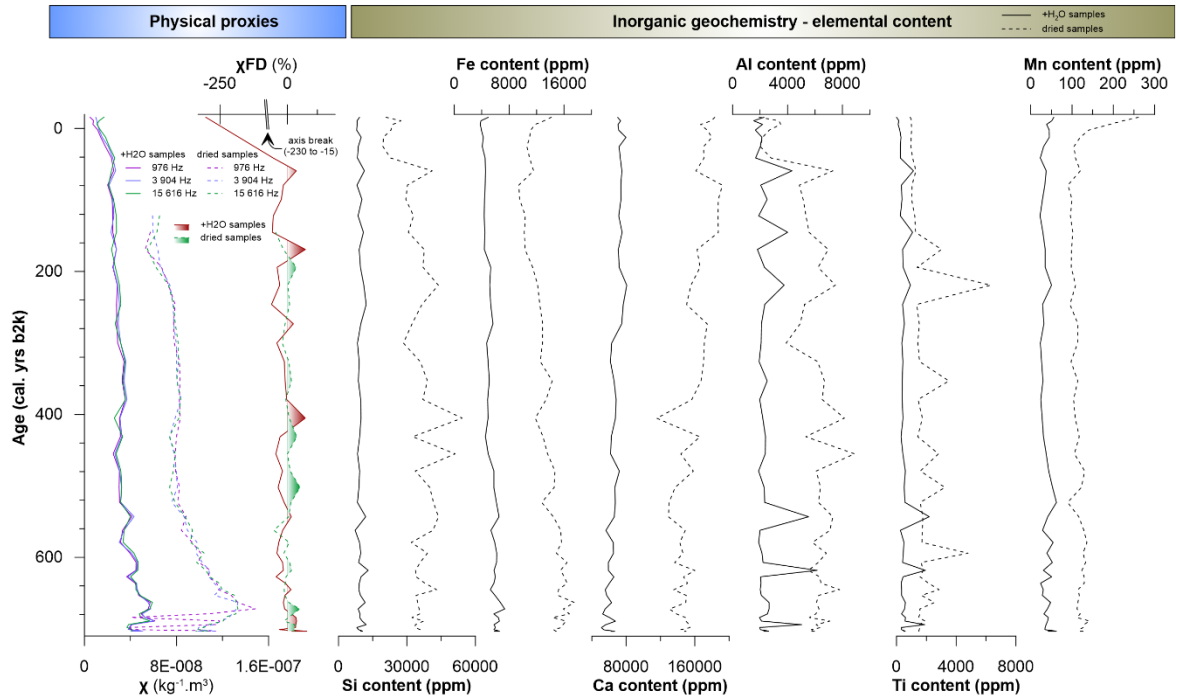

Figure 12 Physical proxies (left) together with elemental content (centre to right) plotted against b2k time-scale.

5.2.3 PCA

PCA was performed on all geochemical and physical data to obtain information about the dominating patterns within a core composition. However, for more-detailed interpretation PCA was performed on both moist and dried samples, meaning this has enabled taking a separate H_2O influence into the consideration.

Analysis of moist samples (Fig. 15) revealed, that core's geochemical and physical composition consists of six components in total, whereas only PC1 (40.40 %) and PC2 (17.81 %) could be considered as substantial due to their relatively high level of explained variance. First component bears strong positive correlation with some alkali metal elements, i.e. Rb ($r = 0.96$), and K ($r = 0.90$), as well as with transition metal elements – Zn ($r = 0.90$), Zr ($r = 0.87$) and Fe ($r = 0.91$). This is supplemented by strong positive correlation with χ_{976Hz} ($r = 0.93$), χ_{3904Hz} ($r = 0.93$), $\chi_{15616Hz}$ ($r = 0.91$), Rb/Sr ratio ($r = 0.93$) and comparatively strong relationship with TS ($r = 0.69$). In contrast, reduction of these variables results conditionally in forcing of TC and Ca, which are in negative correlation ($r = –0.93, –0.62$) with PC1. Second component positively correlates rather with Si ($r = 0.63$), Ti ($r = 0.64$), Ca ($r = 0.59$), Al/Si ($r = 0.56$), but negatively with LE ($r = –0.77$).

The statistical procedure within dried samples (Fig. 16) showed, that core's composition consists of five components in total, however only the first two are conceived as fundamental. PC1 explains 53.07 % of total variability, while PC2 explains only 12.20 %. Positive PC1 agrees with increased TC ($r = 0.97$) and Ca ($r = 0.79$), as well as with Sr content ($r = 0.72$). TIC ($r = 0.47$) and TOC ($r = 0.56$) positions fit appropriately within a two-dimensional PC1. On the contrary, negative feedback of PC1 is associated with increase of variables group consisted of χ_{976Hz} ($r = –0.88$), χ_{3904Hz} ($r = –0.94$), $\chi_{15616Hz}$ ($r = –0.94$), Rb ($r = –0.95$), Rb/Sr ($r = –0.94$), TS ($r = –0.71$), Fe ($r = –0.75$), Zr ($r = –0.76$), Zn ($r = –0.92$), Fe/Mn ($r = –0.86$), Ni ($r = –0.86$), K ($r = –0.81$) and Al/Si ($r = –0.73$). Al, Si and Ti contents reveal comparatively substantial negative bound to PC1 ($r = –0.79, –0.70, –0.40$) as well as considerable positive one to PC2 ($r = 0.46, 0.51, 0.70$). LE and χ_{FD} seem to be probably significantly unrelated to either the PC1 ($r = –0.31, 0.19$) or PC2 ($r = –0.52, 0.39$).

Based on the abiotic variables changes a main phases (sections) were identified. The earlier phase is defined between 700–380 cal. yrs b2k, while the latter one comprises period since 380 cal. yrs b2k till present times.

6 DISCUSSION

6.1 Lake Anonima evolution in the Late Holocene

6.1.1 2440–2050 cal. yrs b2k: Productive warmer period

According to the age-depth model's best estimate age (Fig. 5), Lake Anonima sedimentary record spans the last ~2450 years (sediment base 2440 cal. yrs b2k) attaining thus environmental and climatic history over the major part of the Late Holocene. Data variability of individual proxies showed significant alternations in environmental, climatic and lake conditions of the north-eastern AP region.

First period 2440–2050 cal. yrs b2k is distinctive by comparatively low χ (~3 × 10^{-9} $m^3.kg^{-1}$) relating to low content of (iron-bearing) paramagnetic and ferromagnetic minerals (Evans and Heller, 2003), as well as to potentially warmer climatic phase (Maher and Thompson, 1999). Increased χ_{FD} (~4.72 %) in the core links to higher share of SP grains with diameter <0.3 μm (Dearing et al., 1996), however its literal origin is yet unresolved, since necessary specifies for chemical weathering (good aeration, mild precipitation, near neutral pH and warm climate) does not tally with the Antarctic environments (Worm, 1998). Based on the outcomes of elemental and chemical composition of soils, Navas et al. (2008) conclude that the (outcropping) bedrock type has the strongest influence, and thus physical weathering is the main driving force of pedogenesis in Antarctica. However, Haus et al. (2016) prove that driving element of chemical weathering within the studied region are enhanced by tephra depositions from Deception Island. Due to these issues, χ_{FD} parameter, or SP grains origin hence demands further and more-detailed investigations in the context of extreme (Polar) environment.

Association of magnetic parameters is regardlessly conveyed with grain-size variation of the sedimentary material deposited in the lake. Higher sand fraction (~13 %) and coarser MGS (~11.8 μm) in the given time interval are in comparison to the following period (since 2050 cal. yrs b2k) associated with higher siliciclastic input into the lake basin, induced by thawing of local glaciers and permafrost active layer. Increased input coincides well with higher sedimentation rate (~0.45 $mm.yr^{-1}$) and appropriately with elemental ratios data, utilized as grain-size (Zr/Ti, Al/Si; Kylander et al., 2013), or chemical proxies (Rb/Sr; Xu et al., 2010). For explanation, Zr is associated with coarse silt, whereas Ti is bound to clay

fraction (Taboada et al., 2006), and similarly, clay is represented by Al, while sandy grains by Si (Lopez et al., 2006).

This period almost precisely equals to biozone 1 (2440–2050 cal. yrs b2k) and is characterized by higher abundance of diatom aquatic species – *Achnathidium australexigum* (4–22 %), *Stauroneis delicate* (0.2–10 %) and *Sellaphora antarctica* (4–16 %). To define most accurate ecological niche of the species from Lake Anonima, data were compared with adjacent lakes on the JRI (Bart van de Vijver, personal communication). *Achnathidium australexigum* and *Stauroneis delicata* are being mostly present in stable shallow lakes (pH 7.2–7.5) with low nutrient content and thus low conductivity, however *Sellaphora antarctica* is oppositely distinctive for lakes with silt drapes and algal mats developed on the lake floor. Species abundance is supplemented by highest productivity (~299 × 10^4 valves per gram of dry sediment) within this period, but comparatively also by low species richness (~19) and Shannon index (~2.2) suggesting a productive, but uniform (low biodiversity) environment in the lake. Uniformity is supported by relatively low values of Evenness (~0.74) proposing appropriately developed inequality within a relative abundance, meaning probable dominance of certain group among all the species. TOC and TS show comparatively highest content (max. 5.07 % and 0.91 %) in this period, which corresponds to highest diatom productivity as well as to Fe/Mn redox proxy (O'Sullivan and Reynolds, 2008) values. PCA 1 (Fig. 13) however prove, that productivity parameter is explained almost equally by both (PC1 61.73 %, PC2 9.84 %) components, meaning correlation between organic matter and productivity, nor with indexes (Shannon, richness, Evenness), is not strictly clear. Due to that, productivity could not be considered as a single-dependent parameter in this study.

PC1 mostly correlates with those variables, which are linked to climate fluctuations processes, intending specifically that latent variable (PC1) change is indisputably associated with alternation of climate variables (temperature, moisture). On top of that, increase of PC1 has positive feedback on organic matter content (LE, TOC, TS, Fe/Mn), as well as on Si/Ti ratio, representing proxy for biogenic silica content (BSi). Tight correlations between Si/Ti (BSi), sand fraction and (more less) productivity suggest a substantial proportion of biogenic origin of siliceous material within a core. Above that, this is endorsed by negative (opposite) relationship between these variables and Si, suggesting Si does not clearly have only inorganic (lithogenic) origin. Linkage between χ_{FD} together with sand fraction and positive PC1 suggests, that SP grains are climate dependent, and even though χ_{FD} is associated with

sand fraction, its origin is more probable due to a chemical, rather than physical weathering. Rb/Sr close relationship with PC1 increase also establishes Rb/Sr as a proxy for chemical weathering, rather than for chemistry changes conditioned by different lithology. Usage of Rb/Sr proxy as a provenance indicator is quite debatable; therefore, it demands further investigations in the context of Antarctic environment. On the other side, negative PC1 influence results in positive feedback of clay fraction, meaning the presence of colder conditions, which is in correspondence with sediment fining. This is supported by close correlation of this variable with Al/Si (grain-size) proxy, and opposite correlation with Zr/Ti (grain-size) proxy. Tight link of these variables with χ_{976Hz} suggests that susceptibility signal is bounded to clay fraction (magnetite, maghemite).

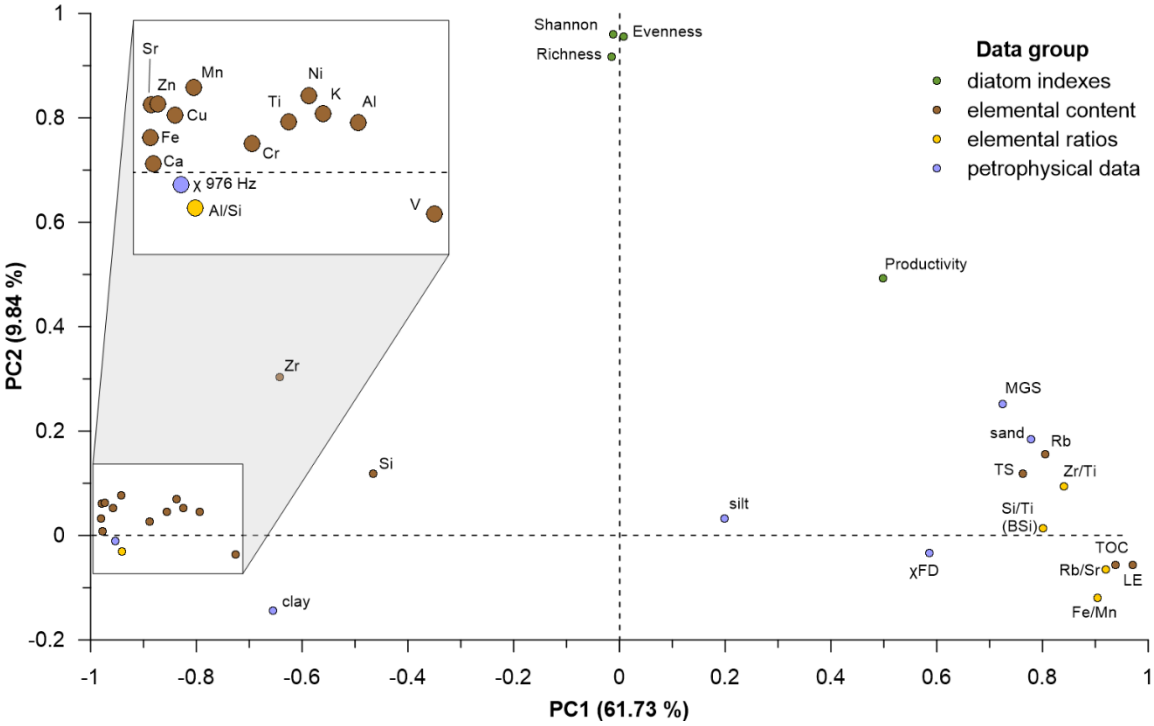

Figure 13 Lake Anonima: PCA 1 (two-dimensional) biplot plotting PC1 (61.73 %) against PC2 (9.84 %) along with all abiotic and selected biotic variables being colourised by data type. Note space distortion (variable positions) due to PC2 axis adjusted range.

PC2 probably explains changes, which do not feature linkage to climate fluctuations, entailing latent component as chemically conditioned by different lithology. Position of diatom species close to the PC2 axis suggests, that assemblages are chemically, rather than climate-dependent. This is especially true for diatom species typical for biozones 2 (*Brachysira minor, Nitzschia homburgensiensis*) and 3 (*Planothidium rostrolanceolatum, Sellaphora gracillima*). However, some of the species (mostly biozone 1 – *Sellaphora*

antarctica, *Stauroneis delicata*, *Achnanthidium australexiguum*) do have noticeable positive relationship with PC1 as well, meaning those assemblages are also linked with climate factor.

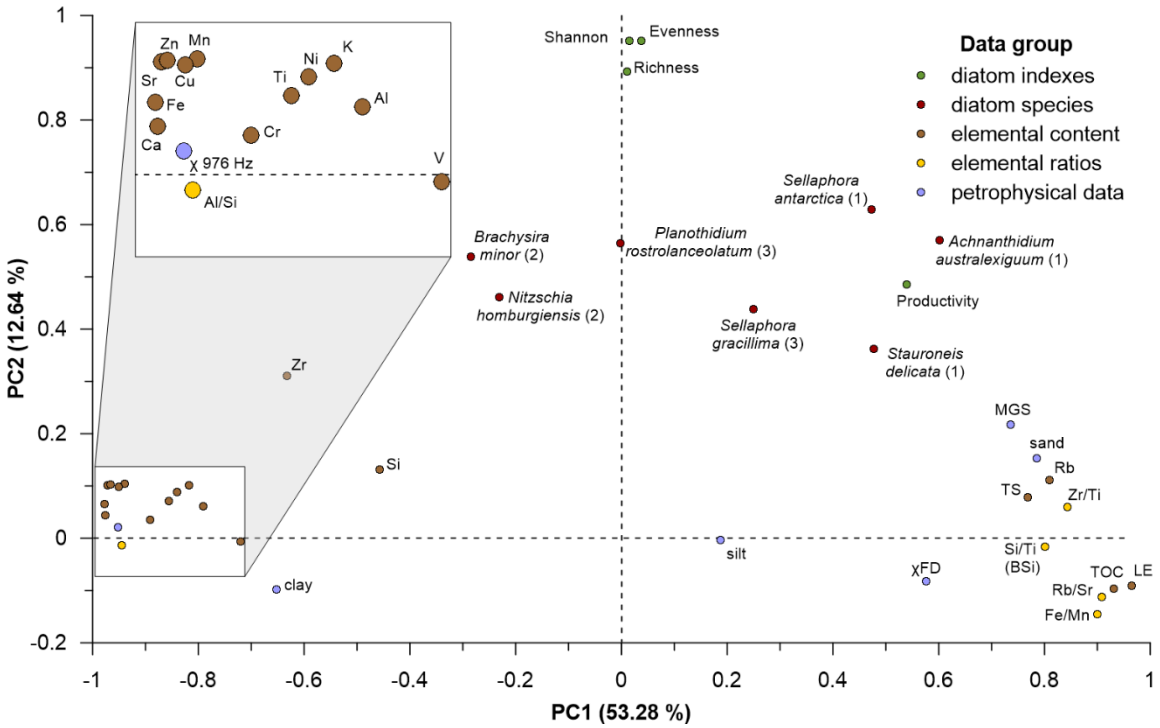

Figure 14 Lake Anonima: PCA 2 (two-dimensional) biplot plotting PC1 (53.28 %) against PC2 (12.64 %) along with all abiotic and selected biotic variables being colourised by data type. Numbers in brackets over the diatom name constitutes for which biozone the diatom species is representative. Note space distortion due to PC2 axis adjusted range.

6.1.2 2050–1520 cal. yrs b2k: Colder phase → decline in primary productivity

Subsequent zone time interval is expressed by biozone 2 (2050–1520 cal. yrs b2k), in which selected biotic proxies report high level of diminishing (TOC ~0.12 %, TS < limit of detection, productivity ~2.63 × 10^4, in part richness ~19.2). This is supplemented by corresponding data trends within abiotic proxies. Specifically, MGS parameter decreases (~11.8→5.5 µm), which is in coincidence with higher clay content (~31.3 %), Al/Si values (~0.26), and on the other side decreased sand fraction (~0.03 %) together with Zr/Ti (~0.02). Re-dox proxy (O'Sullivan and Reynolds, 2008; Fe/Mn) potential is also relatively low (~59.31). χ_{FD} shows lowered intensity of chemical weathering (Chen et al., 1999; ~3.74 %), while χ suggests higher content (~13.07 × 10^{-9} $kg^{-1}.m^3$) of paramagnetic to ferromagnetic matter in the sediment (Evans and Heller, 2003). Decreased biogenic silica (BSi ~6.37) is also in agreement with biotic proxies' trend. In sum, all of these proxies disclose colder

climatic phase, most probably associated with limited meltwater, or precipitation input into the lake basin, which might have later resulted in lake level drop. Predominant (diatom) aerophilic species (*Brachysira minor*, *Nitzschia homburgiensis*) refer to water diminishing due to drier conditions. *Brachysira minor* (not found in the biozone 1) is connected mostly to these drier and colder conditions, whereas *Nitzschia homburgiensis* have been often found in muddy area or drying lakes of JRI (Bart van de Vijver, personal communication). It cannot be ruled out, that the lake has possibly dried out completely for some periods with almost no vegetational growth. Stable conditions are also supported by stability (uniformity) among diatoms species (higher Evenness ~0.87). Seasonal drying of shallow lakes appears on JRI also in present time, as has been shown by Váczi et al. (2012).

6.1.3 1520–220 cal. yrs b2k: Filling of the lake, high diatom variability

The next period corresponding with the biozone 3 limits is distinctive by its duration (~1300 years), however based on the abiotic proxies' outcomes, period was divided into three subzones (3a–c). Biozone 3a (1520–980 cal. yrs b2k) initiates on high peak (~32) of richness index at around 1500 cal. yrs b2k, which is followed with its falling course to ~900 cal. yrs b2k (biozone 3b: 980–460 cal. yrs b2k). Approximately 1100 cal. yrs b2k a small tinge of peak in the productivity occurs, which later credibly results as one of the factors increasing TOC content (maximum 1.85 %) in the biozone 3b.

In comparison to biozone 2, subzone 3a contains a slight decrease in Evenness (~0.76), which imply that diatom assemblages are less balanced, however still diverse. *Planothidium rostrolanceolatum* (~0.4) and *Sellaphora gracillima* (~0.1) forming ~50 % of the diatom assemblages in the biozone 3a suggest a significant influence of a flowing water in the lake basin. This observation might have indicated lake water re-filling (or formation of throughflow lake; Bart van de Vijver, personal communication) associated with high diatom species variability (high richness, but not necessarily low Evenness). Biozone 3a also begins with the highest peak of χ, which then starts to decrease (minimum ~500 cal. yrs b2k). Relatively high χ fits with reduction in sediment input (0.125 $mm.yr^{-1}$) lasting throughout all biozone 3 subzones. However, reduction in sedimentation rate, most probably associated with frozen water level (colder conditions), is not with a trend arrangement of some other biotic proxies (e.g. higher richness index in 3a – 26).

In comparison with 3a, diatom fauna in 3b is more balanced (Evenness 0.79), however less diverse (noticeable peak at ~530 cal. yrs b2k) and productive, which unexpectedly does not correspond with higher TOC content (~1.14 %). TOC variable then could be rather associated with increased abundance of other organisms (Leloup et al., 2013), such as green algae and cyanobacteria. The second half of the biozone 3b is also distinctive by increased presence of *Achnanthidium australexigum* (~0.1), a species typical for "allegedly warmer" biozone 1 (Kateřina Kopalová, personal communication), which could mean together with previous observations slow transition to warmer deflection in the climate, even though there is still no correspondence with productivity. Decrease of *Planothidium rostrolanceolatum*, followed by emergent increase in the biozone 3c (460–220 cal. yrs b2k), is in similarity with biozone 3a. Most of the remaining proxies (predominantly inorganic chemistry, together with grain-size distribution), except χ_{FD} (continual increase since 2000 cal. yrs b2k) are found to be oscillating around the same value in all three subzones (a–c), ensuing no significant course alters.

6.1.4 220 cal. yrs b2k–recent: Recent lake development

Lake development in the last ~220 years is affiliated with abiotic proxy changes, rather than with diatom assemblage alternations. Increasing χ_{FD}, MGS (~9.01 μm), and thus sand fraction (3.43 %) is probably originating in warmer phase connected with higher meltwater input and from thawing glaciers and permafrost active layer. This coincides with rapid advance of sedimentation rate towards the present times. In comparison to previous period, selected ratio proxies show a slightly higher variability, however no solid conclusion is possible to obtain due to reduced time resolution for this short time-interval.

6.1.5 Comparison of Lake Anonima proxy data with other palaeoclimatic reconstructions from wider area

Indication of warmer climatic phase, in Lake Anonima core recorded in the time interval 2440–2050 cal. yrs b2k, is in line with the findings published in several other papers from JRI region. Mulvaney et al. (2012) calculated temperature (°C; 10 or 100-yr average) anomalies (relative to 1961–1990 AD average) based on δD measurements, which were extracted from 363.9 m-long ice core from the top of Mt. Haddington (1630 m), JRI. The ice

core extends the longest among the other AP ice records (Thompson et al., 1994; Thomas et al., 2009), and covers almost 14,000 years of climatic history.

The Holocene temperature history from the JRI ice core is characterized by an early-Holocene climatic optimum (from now on a "hypsithermal" term is used) that was 1.3±0.3 °C warmer than present. This early-Holocene temperature shift on the eastern AP is distinctive by high magnitude and progression, which is in coincidence with trend observed in ice-core records from the Antarctic continent (Masson-Delmotte et al., 2011). Following this widespread early-Holocene hypsithermal, temperature trend shows a long interval of stable climate in the period 9250–2550 yrs b2k (mid-late Holocene hypsithermal). During this interval, the mean temperature anomaly (0.2±0.2 °C) indicates that conditions at JRI and around eastern AP were comparable to warm conditions observed at this site over recent decades. Within this interval of stability, the JRI isotope record indicates that from ~5050 to 3050 yrs b2k conditions may have been only marginally warmer than present. However, positive temperature anomalies at 10-yrs averages mostly persisted until 2000 yrs b2k and interchanged with negative temperature anomalies at 10-yrs averages starting from 2380 yrs b2k (Mulvaney et al., 2012). Therefore, the period 2550–2000 yrs b2k could be regarded as transition from mid-late Holocene hypsithermal to late Holocene Neoglacial phase.

Termination of the mid-late Holocene hypsithermal in Lake Anonima record is considered at 2050 cal. yrs b2k, which nearly correspond to 10-yrs average temperature anomalies from JRI ice-core record (Mulvaney et al., 2012), which significantly positive temperature anomalies terminates around 2000 yrs b2k. Lake Anonima transition is pre-dated by lake record from Beak Island (Sterken et al., 2012), situated ~20 km north of Lake Anonima, where mid-late Holocene hypsithermal is defined within the period 3219–2170 cal. yrs b2k. This phase is by Sterken et al. (2012) characterized by a prolonged peak in organic carbon content (eq. TOC), total pigment concentrations and an increase in sediment accumulation rates. According to authors, total diatom concentrations remained nearly stable, which suggest that this period of higher primary productivity was dominated (in studied lakes titled BK 1E and BK 1D) by other organisms including green algae, yellow-green algae and cyanobacteria representing an increase in the diversity of the phototrophic community. The reappearance of phaeophorbide *a* (product of chlorophyll breakdown → photosensitizer) is likely related with an increased grazing activity by zooplankton and the development of planktonic community; the latter being supported by the sub-dominance of

the tychoplanktonic diatom species *Staurosirella pinnata*. Higher TOC and diatom abundance at 2350 cal. yrs b2k in Herbert Sound is also presented by Minzoni et al. (2015). These observations are in a consistent agreement with biotic data from Lake Anonima core.

On the other side, Sterken et al. (2012) also proved a presence (although in small numbers) of some typical aerophilic diatoms, which are being in this case probably associated with the development of moss communities found on the north-western shores of the lakes, fed by small, braided melt-water streams. The presence of *Euglypha* genus within this interval could corroborate this interpretation, pointing to moss growth in the catchment or littoral area of the lake (Douglas and Smol, 1995; Vincke et al., 2006). Based on Sterken et al. (2012) and Lake Anonima data presented here, this period is in agreement with a warmer climate and longer ice-free periods.

The period of increased primary productivity coincides quite consistently (in advance) with a period of increased diatom abundance in southern Prince Gustav Channel from 4320 to 3580 cal. yrs b2k towards a peak between 2890 and 1390 cal. yrs b2k (Sterken et al., 2012). In general, it is likely an expression of the mid-late Holocene hypsithermal, a warm period found in several parts of the AP and elsewhere in Antarctica (Hodgson et al., 2004, Verleyen et al., 2011). The exact timing of this event is however still inadequately resolved around the continent (Hodgson et al., 2009), but at nearby JRI it is recorded in lake sediments between ~4730 and 3170 cal. yrs b2k (4050 and 3040 ^{14}C yrs b2k; Björck et al., 1996), although the dating resolution of this study is limited to two-three radiocarbon dates per core. Better-dated records (14 radiocarbon dates) from western AP, shows for the South Shetland Islands data the mid-late Holocene hypsithermal at ~4430–2580 cal. yrs b2k with an optimum slightly after 3170 cal. yrs b2k (4050–2580 and 3050 ^{14}C yrs b2k; Björck et al., 1993). More recent works from this region (Byers and Barton Peninsulas), based on dating of lake sediments and positions of frontal moraines, however revealed that no significant glacial advances have occurred during the last 2450 cal. yrs b2k (Oliva et al., 2016), which might be in correspondence with mid-late Holocene hypsithermal. Chun et al. (2017) proves that Fildes Peninsula (King George Island, South Shetlands) has experienced mid-late Holocene hypsithermal between 4450 and 2750 cal. yrs b2k. Similarly, to the north in the South Orkney Islands well-dated records (13–16 radiocarbon dates) place the mid-late Holocene hypsithermal between 3850–1450 cal. yrs (Jones et al., 2000; Hodgson and Convey, 2005). This suggests that the onset of warming at Beak, Vega and James Ross

islands might have been buffered by the cooler climate systems of the Weddell Sea Gyre to the east of the AP. Less precisely dated (due to marine reservoir effects) evidence for a warm period along the eastern margin of the AP suggests a previous collapse of the Prince Gustav Channel ending at ~1950 ^{14}C yrs b2k, when the ice shelf reformed (Pudsey and Evans, 2001). Also, Larsen-A ice shelf fluctuations within its stability/extent were recorded at ~3850, 2150 and 1450 cal. yrs b2k (Brachfeld et al., 2003). It is clear from previous text, that various proxy evidence exists for a mid-late Holocene hypsithermal on the AP (Bentley et al., 2009), although there is a significant lack of consensus on its spatiotemporal appearance not only in JRI region, but also for the whole AP area.

The following period, described by Sterken et al. (2012) as "climate deterioration" with an onset at 2170 cal. yrs b2k, is consistent with already mentioned significant shifts in most proxies from the Lake Anonima, however Beak Island records are slightly pre-dating this episode (circa 120 years) in comparison to our record. This might be affected by the scarcity of geochronological data around the shift in both studies and the onset of "climate deterioration" is thus based on the interpolation of underlying and overlying data in both age-depth models. During this phase, lakes BK1E and BK1D (Beak Island) reveal a rapid decrease of total pigment concentration and total organic content (in this case loss-on-ignition at 550 °C – LOI_{550}, which would correspond well to TOC presented in this study), which are in addition supplemented by detected presence of *Brachysira minor* and *Psammothidium abundans*. Existence of *Brachysira minor* on both localities during this phase enhances concurrent environmental signal consisting of low nutrients, low carbonate content and reduced productivity. According to Wetzel (2001) this diatom species might have been additionally associated with the acidic conditions originating in benthic mosses establishment onto the lake floor. Importance of *Brachysira minor* is evidenced by its use as a bioindicator for mentioned specifics also in other parts (lakes) of the AP region (Gibson and Zale, 2006), however other studies concerning this area set this "Neoglacial" period to a later start, justifying Weddell Sea Gyre as a main reason of cooling effect. Additionally, Pudsey and Evans (2001) conclude that around 1950 ^{14}C yrs b2k (2σ: 1730–1994 cal. yrs b2k) the Prince Gustav Channel has reformed its ice shelf, which is in slightly delayed correlation with Beak Island and Lake Anonima records. However, due to the usage of the radiocarbon age instead of calibrated one, comparison caution is on point. This observation is based on absence of ice-rafted debris (IRD) in the marine sedimentary cores after the mid-Holocene (time interval according to cited authors: 5000–2000 ^{14}C yrs b2k). Neoglacial

cooling might also be evidenced by ice shelf stability recorded in the Larsen-A region after 1450 ^{14}C yrs b2k (Brachfeld et al., 2003). Oppositely, Minzoni et al. (2015) shows counter trend consisting of high diatom abundance and TOC content at 1400 cal. yrs b2k.

Exception in "earlier beginning" holds JRI ice core record (Mulvaney et al., 2012), where the start of this pronounced cooling is registered at 2550 yrs b2k. However, the period 2550–2000 yrs b2k could be regarded as transitional from late Holocene hypsithermal to Neoglacial phase. Later on, temperatures between 850 and 450 yrs b2k were on average 0.7±0.3 °C and 1.8 ± 0.3 °C cooler than present on annual and decadal timescale, respectively. This coincides very fitly with higher values of PC1 ("climate") score of the Lake Anonima data (Fig. 17). The support of "earlier Neoglacial onset" is also presented by Minzoni et al. (2015), where 11-m long marine sedimentary record from Herbert Sound and Croft Bay, ~27 km to the south-west of Lake Anonima, evidences extended sea cover, decreased diatom productivity, cold-water diatoms presence (*Navicula* species, *Fursenkoina curta*), altogether with organic carbon content (eq. to TOC presented in this study) and sets onset of this trend at ~2550 cal. yrs b2k. Important to mention is, that increased IRD is considered as a result of a local glacier movement (colder period) delivering debris via iceberg calving on the continental shelf in the ice shelf absent environment. On the other side, since Pudsey and Evans (2001) operate in Prince Gustav Channel, the area of former ice shelf presence, they attribute a colder period rather to a decrease of IRD connected with ice shelf built up.

The previously published research show, that the Neoglacial period has been recognized in the AP region not as a period of far-reaching glacial advances, like those observed in the Northern Hemisphere (Badding et al., 2013) and Patagonia (Glasser et al., 2004), but rather as relatively cooler and drier conditions with suppressed biogenic productivity and increased sea-ice cover (Leventer et al., 1996; Yoon et al., 2003; Heroy et al., 2008). Spatiotemporal occurrence of Neoglacial period has been further described also in other studies concerning adjacent AP regions – e.g., South Shetland Islands (Björck et al., 1991a; 1993), Bransfield Strait (Fabrés et al., 2000) and East Antarctica (Verleyen et al., 2011).

Further development, corresponding with time interval 1520 cal. yrs b2k – till present, considered as less variable, reveals most proxies' changes as rather short-term (decadal, instead of centennial scale resolution). This period discloses some substantial changes, but in comparison to rapid shift at 2050 cal. yrs b2k, these changes are, rather short-term with

lower signposting ability. Therefore, interpretation and discussion are adapted to and the observations are thought out with different perspective.

Since 1300 to 430 cal. yrs b2k, Herbert Sound record (Minzoni et al., 2015) shows a long-term TOC increase together with IRD decrease, suggesting slow, but continual warming. In addition, subinterval 950–430 cal. yrs b2k in this area (DA1) reveals substantially more stable and warmer conditions, which might have corresponded with the hint of trend known as Medieval Climate Anomaly; despite the fact, it is not very prominent in AP region, as well as in other parts of Antarctica (Tavernier et al., 2014). On the other hand, the Lake Anonima record shows in the corresponding period (~670–490 cal. yrs b2k) rather colder conditions evidenced by a PC1 ("climate") increased values. However, since the Lake Anonima represents a more-detailed record (in comparison to Minzoni et al., 2015), colder phase more likely evidences short-term climate fluctuation, sort of which a long-term marine record cannot capture in a such detail. On the other side, Minzoni et al. (2015) shows an increase of IRD together with TOC decrease since 430 cal. yrs b2k, but it is not in chronological correlation with the Lake Anonima record. This is proved by the JRI ice-core δD record (Mulvaney et al., 2012), which reveals that the strongly negative temperature anomalies persisted here till 280 yrs b2k, however the coldest period was 650–420 yrs b2k with continuous temperature increase till present. This partly coincides with the Lake Anonima record, in which is this warming showed since 500 cal. yrs b2k by negative values of PC1 "climate" component.

As presented in 6.1.3 relatively high TOC at around 590 cal. yrs b2k does not suggest warmer conditions, but instead it could be indirectly linked with colder conditions (longer frozen lake). However, origin of TOC peak might have been explained by concurrent influence of cyanobacteria and green algae production. Together with decreased sedimentation rate it implies proportionally higher content of organic matter from planktonic organisms in seasonally melting lake, which died during the lake re-freezing.

In addition, lake sediments from Beak Island indicate warming with beginning at ~1510 cal. yrs b2k (Sterken et al., 2012), and together these records demonstrate collectively rather the absence of a wide-spread LIA signal around the AP, which is in general recorded in the peri-Atlantic sector of the Northern Hemisphere (Mann et al., 2008). Whether LIA in this region have existed or not, this "colder phase" signal (since 430 cal. yrs b2k) in Herbert Sound is equally supplemented by high variability in diatom abundance and TOC content

since 650 cal. yrs b2k, which might suggest enhanced seasonal variation in sea-ice and ice rafting.

Climate warming and associated recent ecological changes are marked also in Beak Island record since 593 cal. yrs b2k by peak of TOC, lower wet density, increase in diatom species richness and species favouring high nutrient concentrations (e.g. *Nitzschia frustulum, N. inconspicua*). From the recent climate perspective, the JRI ice core shows that the recent phase of warming on the northern AP began in the mid-1920s and that over the past 50 years the temperature has risen at a rate equivalent to 2.6 ± 1.2 °C per century. However, to address changes in lake archives for the most recent period, it is required to obtain a high-resolution data supplemented by firm ^{210}Pb and ^{137}Cs (or other type of) chronology.

Due to limited scope as well as time resolution per one sample (10–50 years), and also with respect to coherence extent of this thesis, discussion concerning linkage of forcing mechanisms (solar factors, ocean circulation, ENSO etc.) to AP climate change during the Holocene is not included into consideration. This topic is in more detail discussed by other authors, e.g. by Bentley et al. (2009). Nevertheless, the sediment core from Lake Anonima, Vega Island is amongst the first records (Zale and Karlén, 1989; Björck et al., 1991a; 1996; Ingólfsson et al., 1992; Hjort et al., 1997; Mulvaney et al., 2012; Sterken et al., 2012) to show a lacustrine response to the most recent period of Holocene environmental variability within a long-term historical context beyond instrumental records.

6.2 Lake Mathiesondalen 3 evolution in the Late Holocene

6.2.1 700–380 cal. yrs b2k: High sulphur and χ and low TOC

Age-depth model revealed that Lake Mathiesondalen 3 sedimentary record spans the last ~700 years of the environmental history, implying this record as rather short-aged with possible and thus advantageous low influence of the compaction effect. Not only more-detailed time resolution, but also age overlap with medieval and modern human times is considered as beneficial, meaning a possibility to synthesise environmental noesis with specifics of the human presence in the area. In contrast, short-aged information might represent different and misleading trend, not fitting into a medium- or long-term scale. Unchanging conditions, which have occurred during the sedimentation within the lake, lead to the fact that particular proxy data have enabled to estimate potential main events only. Notwithstanding data interpretations are also limited to only non-biotic results present here

(geochemistry and physical proxies), due to absence of diatom and *Cladocera* species, *Chironomidae*-based reconstruction will otherwise presumably reveal promising results. Notably in general, samples contain 50–150 chironomids per 1 g of dry sediment (Daniel Vondrák, personal communication) and result of *Chironomidae*-based reconstruction will be presented elsewhere. As a side note, unless stated otherwise, discussed are always both values (*d*+*w*) relating the same proxy.

Evident persistent TOC reduction/stagnation (oscillating around ~5 %) in this period might signify less progressive conditions, associated rather with slugging organic productivity (Maher and Thompson, 1999). Proxy for biogenic silica (BSi) estimation Si/Ti (Brown, 2015) demonstrates as well increasing trend towards the core's top, with apparent fluctuation at the bottom, which is in linkage (especially for dried samples) with TOC pattern suggesting association between organic matter and BSi (Boyle, 2001). Relatively low TC content (~8.5 %) is in line with comparatively increased χ values implying environment, that is comparatively low in inorganic carbon (carbonate, CO_2, carbonic acids, bicarbonate anions), but relatively rich on "magnetisable" matter. Although TOC is low, it still holds major proportion of TC, meaning TIC influence from carbonates within this period is less significant. Possible explanation of this trend might lie in a rather undeveloped melt-water streams supplying the lake and non-active permafrost and its active layer, which touts to increase the TC content in the lake as well (Hendy and Hall, 2006) due to likely low temperatures (resting in colder period?). Unlike TOC, the TIC steadily increases until the 380 cal. yrs b2k (followed by a rapid drop – 6.2.2) suggesting increasing TIC input from surrounding lake catchment area. In addition, due to the length of the drilled core, TIC is unlikeable to be sourced from carbonate bedrock in the lake floor. Instead, carbonates or evaporates were transported either dissolved, or in small particles by active layer thawing water from the catchment.

To interpret dominating patterns via PCA results of dried samples (Fig. 16), PC1 positively correlates with organic matter (TOC) as well as with carbonate material (TC, TIC). On the other side, PC1 shows tight negative relationship with the metal elements and χ. Therefore, PC1 might represent changes between of autochthonous (positive correlation – material native to its location) vs. allochthonous (negative correlation – sourced from catchment area) influence. This assumption would intent rather allochthonous input within this interval, meaning suppressed processes in a lake body and/or lake's closest area, and

oppositely more developed processes in more distant places influencing the lake. Allochthonous input is also supported by Al and Si "clustering" within a PCA suggesting a separate way of transport (origin) in the lake's composition, which is in agreement with the fact, that these two elements form (alumino-)silicates, as one of the most common mineral group in the Earth crust (Cuven et al., 2010). Some claim that Al/Si ratio might reflect weathering processes (Van Daele et al., 2014), however in the Mathiesondalen's case this proportion of dry material reveals rather stable values throughout the profile, indicating static supply of siliciclastic material to the lake during this time interval. Followingly, support of allochthonous input could be represented by χ measurements at different frequencies, which showed that $\chi_{15616Hz}$ (high-field) bears at some depths lower values than χ_{976Hz} (low-field). This implies negative, or extremely low χ_{FD} proposing sort of presence of stable single domain (SSD) magnetic grains instead of superparamagnetic (SP) ones (Dearing et al., 1996). All in all, these observations are likely in agreement with increased sedimentation rate in the time interval 700–600 cal. yrs b2k.

However, since an apparent form of bound between TS and Fe (*d* has tighter correlation) is appropriately reflected in the PCA's first components (Fig. 15, 16), interpretation gets more complicated. To explain, χ reflects Fe content very fitly, which consistently supports "allochthonous" interpretation from the previous paragraph, furthermore implying increased denudation and detrital input (Maher and Thompson, 1999). On the other side, as seen from PC1, the TS content reflects χ and Fe variability as well. This could mean, that TS content might have separate origin and thus its bound to PC1 is in this case probably very essential, since sulphur might be part of H_2S constituted by reducing bacteria (decomposition/oxygenation of organic matter; Wilkin and Barnes, 1997). Anoxic/anaerobic environment conditions (in amictic lakes) may force disulphide to react with Fe to create iron sulphide (FeS) and iron minerals, such as greigite (Fe_3S_4) and pyrite (FeS_2; Håkanson and Janson, 1983). However, and even though, magnetic minerals such as greigite are identified as a source of remanent magnetism in sediments, these deposits may be not only of inorganic origin, or biologically mediated by sulphate-reducing micro-organisms, but also of magnetotactic bacteria activity (Mann et al., 1990). Latter concerns mostly sulphid-rich environment, which implies this factor must be considered as the most likely. Nevertheless, TS in this period (almost) corresponds with decreasing trend of TOC supporting generally known correlation of these proxies in oligotrophic lakes (Cohen, 2003). Nutrient-poor

amictic and oligotrophic lake type might be supportive in this case when considering diatom absence causes.

However, sulphur might not be only a part of organic compounds nor H_2S, but also of sulphates and sulphides, such as gypsum ($CaSO_4 \cdot 2H_2O$) and anhydrite ($CaSO_4$), which are known from lake catchment (Dallmann et al., 2004) reflecting allochthonous interpretation. Another source of sulphur in the sediment within this study might have been associated with the sea spray process, emitting sulphur into the atmosphere in a form of marine aerosol and then falling through condensation into the lakes (O'Dowd et al., 1997). Via sea spray, the sulphur content can generally reach up to 8 % (Leng et al., 2012). However, there are also several other origins of sulphur in the freshwater lakes in general, such as volcanic eruptions (Pfeffer et al., 2006) or typhoon activity (Ding et al., 2016). Since these sulphur-enhancing phenomena have not been described from the studied area yet, they are not considered as influential.

Unlike in Lake Anonima, Rb/Sr correlation with other abiotic proxies, e.g. TS and χ (PC1) rather expresses changes in geochemistry (mineralogical or textural changes of mostly incoming material to the lake; Hošek et al., 2015) instead the climate changes, although even these conditions cannot be excluded, as they might play less important role. This prevailing assumption thus gives to the first component also secondary "physical-chemical" attribute, which induces most of the environment settings within the in-catchment conditions.

Assuming mentioned χ values measured in different frequencies, it cannot be excluded that presented data may be a result of instrument's error, or the detection limit. Supportive fact however is, that χ "wet" and dried samples are differentiated by nearly constant value (Fig. 12) intending diamagnetic H_2O influence as uniform throughout a profile. The H_2O proportion does not decrease towards the lowest section, as it is empirically described (Tjallingii et al., 2007). Notwithstanding, separate PCAs onto both sample groups (*d*+*w*) proved, that there is nearly no significance of H_2O influence onto main dominating patterns.

6.2.2 380 cal. yrs b2k–recent: Variable TOC and TC enhancement

Although it may seem that courses of particular proxies do not reply to environmental changes, nor these shifts are absent in general due to persistence of stability in the environment, some parameters' behaviour could be still attributed to different conditions' development. Since 380 cal. yrs b2k, the TOC content shows more developed variability

possibly supplemented by growing linear trend. TC is reaching its maximum with Ca content following the same (increasing) pattern (Fig. 11). Oppositely, TS and χ influence slowly vanishes, meaning probably the establishment of a carbonate-rich environment (possible $CaCO_3$ precipitation or water flow input of calcareous material; Koinig et al., 2003). Unlike the previous period (6.2.1), proglacial streams supplying the lake might have been more dynamic, bringing thus enlarged loads of glacial, i.e. siliciclastic, material (Cecil, 1990).

Apart from 700–380 cal. yrs b2k, this period shows several peaks and drops of certain proxies, which might be correlated between each other. Specifically, synchronous trend occurs at around ~380 cal. yrs b2k in Si (*d*; increase), Ca (*d*; decrease) and Al (*d*; decrease) suggesting potential enhancement of coarser particles or possible BSi increase. Another synchronic change occurs approximately at ~220 cal. yrs b2k, with TOC (*w*), Fe/Mn (*w*), Si/Ti (*w*), Zr/Ti (*w*) decrease and Al/Si (*w*), Si (*d*), Al (*d*+*w*), Ti (*d*) increase. Very similar shifts occur also at around ~50 cal. yrs b2k. Cause of such a change may arise from sudden material input, or also from in-lake processes. However, these assumptions need to be supported by better understanding of the environment based on further, especially biological data.

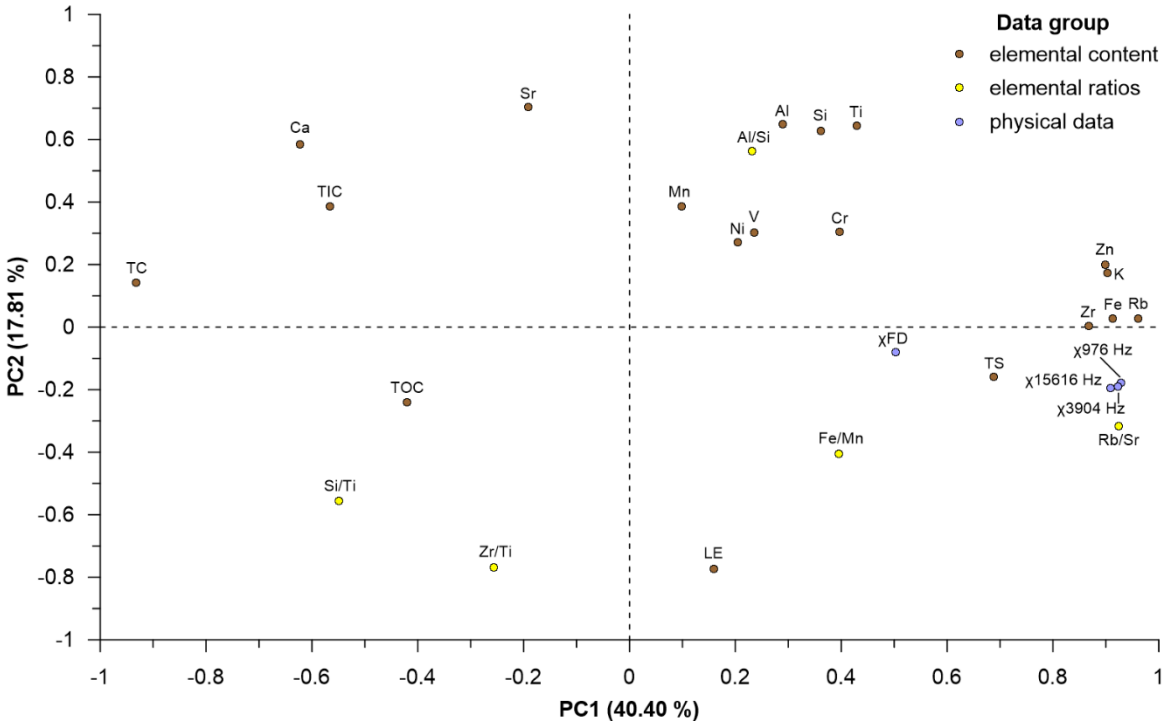

Figure 15 Lake Mathiesondalen 3: PCA 1 (two-dimensional) biplot plotting PC1 (40.40 %) against PC2 (17.81 %) along with all abiotic variables being extracted from "wet" (*w*) samples and colourised by data type.

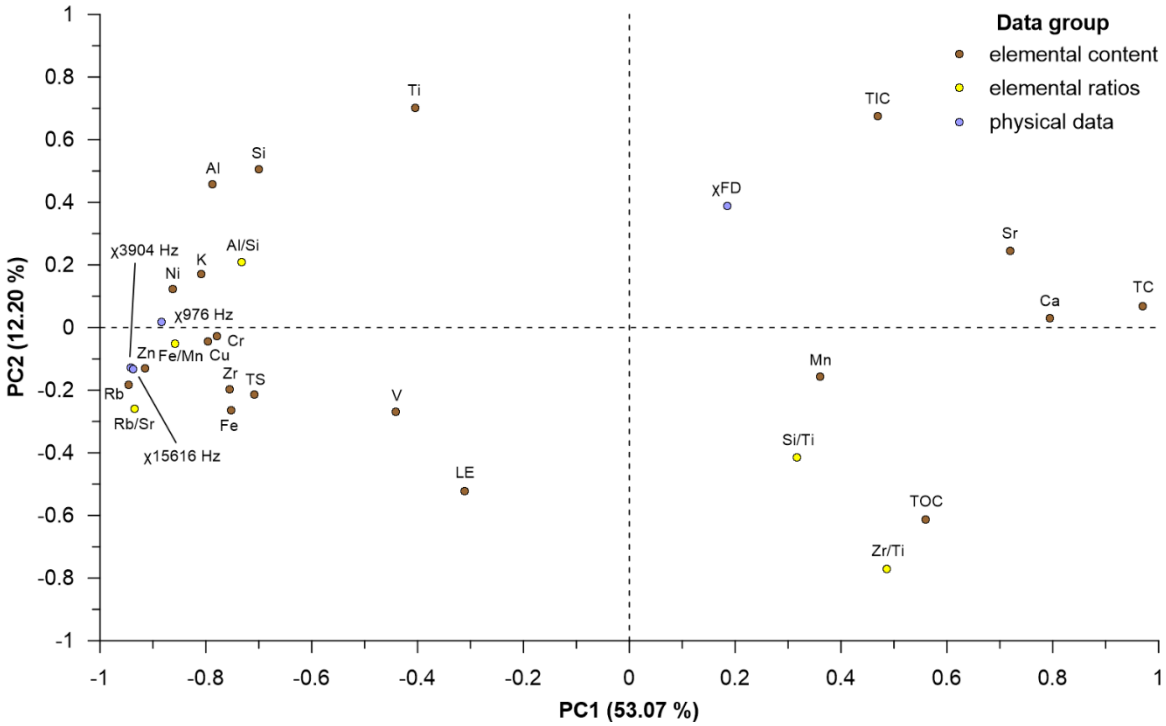

Figure 16 Lake Mathiesondalen 3: PCA 2 (two-dimensional) biplot plotting PC1 (53.07 %) against PC2 (12.20 %) along with all abiotic variables being extracted from dried (*d*) samples and colourised by data type.

6.2.3 Comparison of Lake Mathiesondalen 3 proxy data with other palaeoclimatic reconstructions from wider area

Palaeoenvironmental evolution in the area has been, from perspective of oceanic circulation patterns, influenced by enhanced water inflow from the Atlantic Ocean since ~1000 yrs b2k, which have later resulted in generally warming conditions, though the trend conditions differ in detail. This course was marked in numerous marine (Rasmussen et al., 2014; Werner et al., 2016) and lacustrine (D'Andrea et al., 2012; Balascio et al., 2018) records.

Specifically, D'Andrea et al. (2012), as one of the most suitable research to be compared with, show sub-decadal- to multidecadal-scale record of summer (June, July, August – JJA) temperatures for the past 1800 yrs b2k from lake sediments of Kongressvatnet on the West Spitsbergen. This study reveals, that JJA temperatures since ~700 yrs b2k till present were in this area more variable, but still with ongoing warming trend. Before this period, an interval ~1100–700 yrs b2k has confirmed rather colder conditions (supported by Humlum et al., 2005 in central Svalbard), which could have been sort of precursor to the possible LIA. Time (sub-)interval within the range ~750–700 yrs b2k has been typical by significantly colder summer temperatures, which corresponds to extensive alpine glaciation on Svalbard in some areas, already described by Baranowski and Karlén (1976) and Werner (1993). This

implies that reduced ablation (due to generally lower summer temperatures) contributed to glacier advances at this time, while oppositely following increased summer temperatures have become a limitation of these advances.

Authors claim that increased winter precipitation contributed to glacier advance more than generally low temperatures (Svendsen and Mangerud, 1997; Humlum et al., 2005) at the turn of the 18th and 19th century. This explanation is associated with North Atlantic Oscillation changes coming out from correlation between winter precipitation and North Atlantic Oscillation; Dickson et al., 2000). Nevertheless, overall warming trend has been recognized and attributed to the amount of Atlantic water transported towards the north by CDW, which in other words means that proximity of WSC plays an essential role despite a probable delay of warming distribution in west-east direction.

Another record from north-western part of Svalbard is analysed by Røthe et al. (2015) and its observations are in contrary to the D'Andrea et al. (2012). This research is focused on local glacier's equilibrium line altitude (ELA) reconstruction and reveals, that local climate conditions were in favour to a glacier advance at the time around ~1200 cal. yrs b2k. In the subsequent period 1200–900 cal. yrs b2k, ELA has oppositely risen, which resulted in glacier retreat, however unlike in D'Andrea et al. (2012) and according to other authors, LIA period lasted here since 500 cal. yrs b2k till the beginning of the 20th century (lowest position of ELA took place at: 450, 280, 180 cal. yrs b2k). On the other side warmer conditions, which were oppositely reported in interval 275–185 cal. yrs b2k (Røthe et al., 2015), are in correlation with enhanced warming during mid-18th century described by D'Andrea et al. (2012). Followingly, Røthe et al. (2015) claim the position of local glacier's ELA steadily rose since 100 cal. yrs b2k, which is in line with 20th century warming trend. Another record by van der Bilt et al. (2015) from north-western Svalbard supports glacier presence/advance (LIA decrease) after 750 cal. yrs b2k, which is in agreement with Røthe et al. (2015).

Despite the fact, that LIA has been described widely in the Arctic (Solomina et al., 2015), Lake Mathiesondalen 3 record does not seem to respond to such a phenomenon in a well-defined and full extent during the period after 700 cal. yrs b2k as well as at the turn of the 18th and 19th centuries. On the other side, proxy dataset does not seem to show an absence of these cold conditions, being probably expressed in this context as LIA. Specifically, interval 700–380 cal. yrs b2k shows TOC presence as comparatively low, which might have suggested mild phase within colder conditions associated with glacier advances due to

increased precipitation during a winter season, already described by D'Andrea et al. (2012) in the earlier interval. Assuming these colder conditions, allochthonous input might be supportive, when suggesting rather increased input from the upper part of the catchment triggered by glacier movement. Associated winter precipitations (inducing glacier advance) rather than reduced summer ablation (due to lower summer temperatures) might be positive when considering increase of magnetisable matter and TS. This could have been linked with lower summer temperatures creating frozen water lake level and thus rather oligotrophic (anaerobic) conditions in the lake supporting formation of sulphur compounds as described before (6.2.1). In addition, and also, increased precipitation inflow does not have to necessarily contradict with claimed "colder phase", which might have persisted until 380 cal. yrs b2k.

Increasing TOC, together with Ca increased share in the interval 380 cal. yrs b2k till recent can be correlated with higher productivity associated with ongoing warming and moistening, which is in line with higher influence of autochthonous productivity in the lake and surrounding catchment. As in the previous phase, these warmer conditions might correlate, although with certain time-lag with observed variable warming trend since 700 cal. yrs b2k presented by D'Andrea et al., 2012). Followingly, when considering dominant factor influencing climate-glacier behaviour, presented observations indicate, that WSC might play an important role as it brings warm and moist air from lower latitudes. This also suggests, that position of Lake Mathiesondalen 3 in central Svalbard could explain discussed and rather delayed onset of warming. This trend, although less clear and with earlier onset (~800 cal. yrs b2k), is supported also by diatom assemblages (*Amphora affinis*, *Citellus richardsonii*) in ~7 km distant (NW) Lake Garmaksla analysed by Roman (2014, 2017).

The record from Lake Garmaksla was supposed to be essential for synthesis/comparison, however after a stratigraphic correlation of three differences based on sequence slotting (Thompson et al., 2012) the lowermost section revealed to be distinctive by circa 5800 years (cal. yrs b2k), enabling thus potentially the comparison only with the topmost (mesotrophic) section. Nevertheless, biostratigraphy and cluster analyses of diatom communities defined five biozones (A–E) in total (Pinseel, 2014), with the upmost D (~870–450 cal. yrs b2k) and E (~450 cal. yrs b2k – present) zones nearly entirely overlapping Mathiesondalen's record. Assuming the correct age-depth modelling and presence of diatom biota in general, it is not excluded, that Mathiesondalen's biostratigraphy analysis would not have possibly reveal

similar results. After all, and as discussed previously, abiotic proxies slightly suggest minor (but substantial?) changes within the last ~380 years, which could have been associated with D to E biozones transition at around 450 cal. yrs b2k in Lake Garmaksla as well. However, these observations and assumptions need to be supplemented by further biostratigraphic data.

Presented research and observations suggest, that majority of available records present rather a widespread glacier growth evidence during the LIA, or glacier advances at the turn of the 18th and 19th century (Rachlewicz et al., 2007), although some studies have suggested just the opposite (D'Andrea et al., 2012; Spielhagen et al. 2011). Nevertheless, both Mathiesondalen 3 and Garmaksla records are shown to be very unique when studying a lake response to these widespread, but specific phenomena. This however implies that the climatic driver of glacier growth on Svalbard remains still elusive and thus deserves future investigation. We can only speculate about the effect of increasing precipitations, which would lead to positive mass balance of local glaciers even during phases of slow atmospheric warming. This might be the case of the turn of the 18th and 19th century. However, the continuous warming trend lead to subsequent glacier shrinkages, which started in the area from the end of the 19th century (Rachlewicz et al., 2007) and accelerates towards present (Małecki, 2016).

6.3 "Comparing the evolution of North and South since 700 cal. yrs b2k"

Previously presented outcomes based on a two-core palaeolimnological research have been used to set up a basis for a discussion, considered as the "state-of-the-art" component of this thesis. In comparison to the Lake Mathiesondalen 3 record, the Lake Anonima record shows more pronounced long-term changes, which could be attributed to a differently-parametrized and dominantly prevailing factors influencing the record. Also, as seen from proxy data synthesis (Fig. 17) the Lake Anonima record' resolution is less-detailed, implying more complicated capture of the short-term changes, which leads to a conclusion, that it is far more difficult to obtain solid and correct palaeoreconstruction. Followingly, due to the Lake Mathiesondalen 3 age, only the last 700 cal. yrs b2k are possible to be compared and also, due to a limited scope of this thesis, together with inability to compare all proxies in their best complexity and detail, author decided to describe only selected (most influential) variables, which explain behaviour throughout the major part of the overlapping time period.

Specifically, sedimentation rate, main PC's and TOC were chosen for comparison due to their most assuring ability in the context of comparison of environmental and climatic changes.

Sedimentation rate together with PCA's results were preferred in order to obtain complex image about the dynamics influencing the lake's catchment. To compare, average sedimentation rate for the last 700 cal. yrs b2k varies between cores within several orders. In Lake Anonima, a mean sedimentation rate is ~0.42 $mm.yr^{-1}$, while in the Lake Mathiesondalen 3 this parameter reaches up to 5.66 $mm.yr^{-1}$, meaning much faster material transport in the selected Arctic catchment. However, influence of *in situ* material together with compaction effect needs to be considered as well. Even though the sedimentation rate highly depends on many factors (i.e., glacier and hydrometeorological activity), the latter does not seem to correspond with generally known (Wolfe et al., 2004) extremely low sedimentation rates in Polar areas. Another variable, which reveals most of the core's behaviour is the "climate" component (explaining 61.73 % of variability) in the Lake Anonima and the first "allochthonous vs. autochthonous" component (explaining 53.07 % of variability) in the Lake Mathiesondalen 3. Both components' behaviour together with previously discussed sedimentation rate character explain main changes during the sedimentation since 700 cal. yrs b2k. This is properly supplemented by TOC proxy, which is considered as main indicator of primary productivity in the lake. Besides, the differences in principal component analysis explanation show that the Lake Anonima record is climatically affected and might bring regional interpretation of climatic and environmental changes. On the contrary, the Lake Mathiesondalen 3 record is affected principally by in-catchment and in-lake processes and explains predominantly changes of local environmental conditions.

Chronologically, development in the Lake Anonima is in this comparison initiated by small hint of "climate component" positive peak between ~670–490 cal. yrs b2k, suggesting indication of relatively colder period in the Lake Anonima area. This non-local (catchment), but rather regional climate pattern is also in agreement with low temperature (°C) anomalies vacillating between 0.20 and –1.79 °C (mean –0.71 °C), which were extracted from JRI deuterium-excess ice core record (Mulvaney et al., 2012). Subsequently, sedimentation rate in this interval is rather low, starting on ~0.1 $mm.yr^{-1}$ at 700 cal. yrs b2k and slowly rising up to 0.205 $mm.yr^{-1}$ at around 580 cal. yrs b2k. Even though low sedimentation rates are in

line with the previous observations, better time resolution of material input chronology would elucidate, whether the recorded "colder" peak is, or is not substantial and marked also by other proxies. In contrast, increased organic productivity expressed by TOC does not seem to correlate with the supposed colder peak. As described in 6.1.3 high TOC might not strictly link towards high (diatom) productivity, but rather to other organisms, such as green algae and/or cyanobacteria (Leloup et al., 2013) as well as to frozen lake level and proportionally less accumulated material due to lower sedimentation rate. On the contrary, the Lake Mathiesondalen 3 reveals, that the whole period since 700 till 380 cal. yrs b2k is typified by quite unique conditions. As presented before (6.2.3), proxies configuration might be probably associated with LIA lag, due to the delayed influence of WSC on Central Spitsbergen climate. Precipitation increase was essential, as it had dominant influence on glacier growth and input of allochthonous input into the lake, while generally lower (summer) temperatures were linked with TOC stagnation/decrease and TS together with χ enrichment via developed anoxic conditions. Increased sedimentation rate (~25 and decreasing to ~2 $mm.yr^{-1}$) at around 700 cal. b2k might be supportive when considering increased allochthonous (siliclastic) input during this period.

Subsequently, development in the Lake Anonima between ~490 and 340 cal. yrs b2k as well as since ~300 cal. yrs b2k till present, shows rather the negative scores of the "climate component", implying climate warming effect on the sedimentary record. The warming trend might have been interrupted by a short colder phase between ~340 and 300 cal. yrs b2k, as seen from Fig. 17. TOC parameter continuously decreases since ~590 cal. yrs b2k, and it does not probably respond to "climate component" variations since this time, neither. Also, sedimentation rate persists around 0.2 $mm.yr^{-1}$, meaning not well developed response to the "climate component". Nevertheless, during the last ~30 cal. yrs b2k this parameter steeply rises up to nearly 1 $mm.yr^{-1}$. The synchronous period (since 380 cal. yrs b2k) is in the Lake Mathiesondalen 3 marked by prevailing in-lake productivity, which might be properly supplemented by higher (but variable?) TOC content, as well as the TIC content affecting the general increase of total carbon towards the present. Sedimentation rate also rises up to 10 $mm.yr^{-1}$. This trend might reflect local climate amelioration.

To meet the aims of this chapter, and also to sum up and highlight the main patterns describing the proxy variability within studied cores, it is evident, that during the (at least) last 300 cal. yrs these particular localities have shown similar environmental (warming)

conditions. Additionally, and in comparison, to the Lake Anonima (Vega Island), the Lake Mathiesondalen 3 seems to reveal more dynamic and more rapidly changing environment, although this sentence needs to be taken into consideration with certain standoff, since enormous number of variables plays an essential role within a palaeoenvironmental "recording" in the lake sediments. However, generally it can be stated that the Lake Anonima record reflects principally the climate variability of Maritime Antarctica over the last two and half millennia. On the contrary, the Lake Mathiesondalen 3 record shows mainly variable environmental conditions within the lake and its catchment.

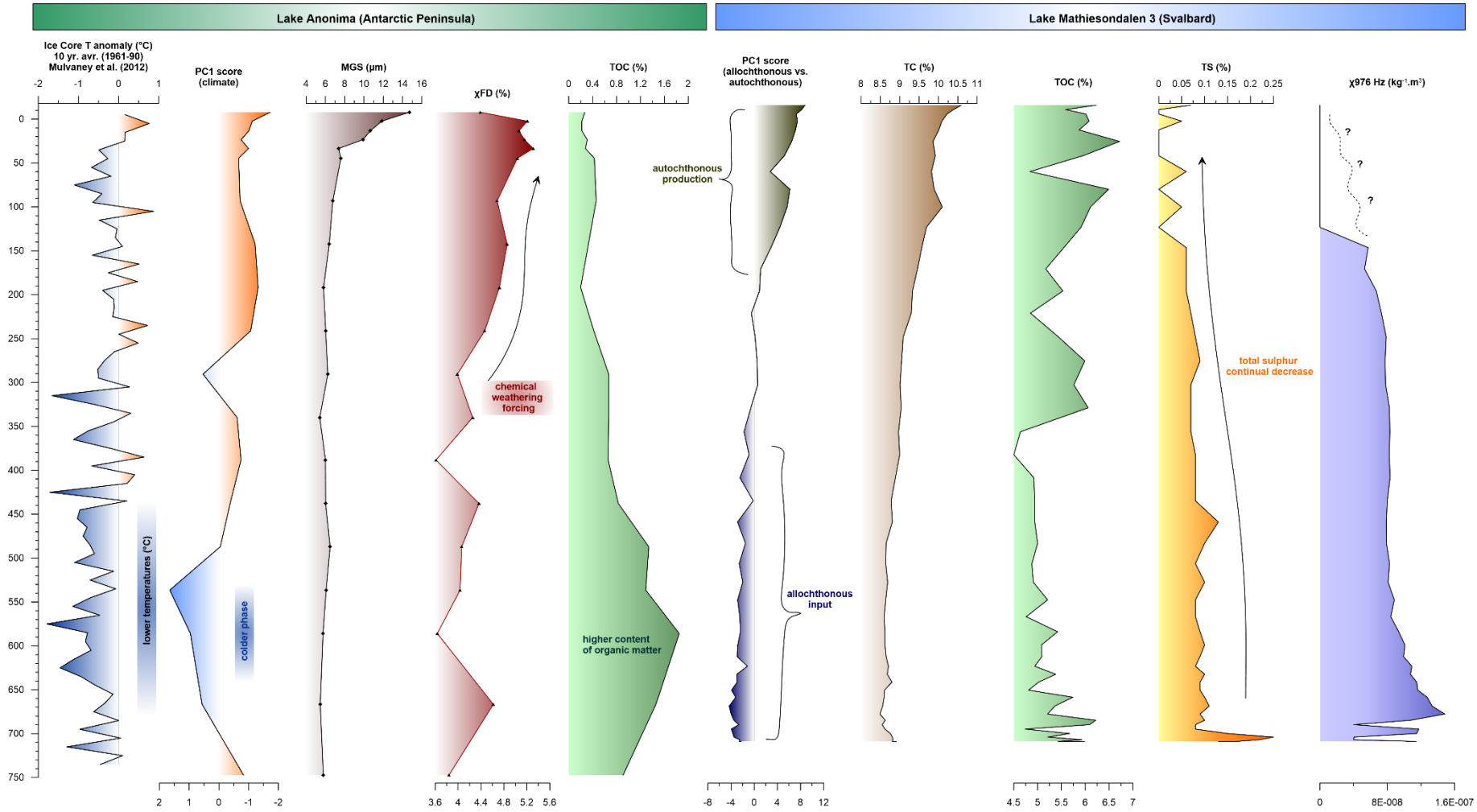

Figure 17 Proxy data synthesis (left to right): Mt. Haddington (JRI) Ice-core anomaly (°C) 10 yr. avg. (1961–1990; Mulvaney et al., 2012); Lake Anonima: PC1 (climate); MGS (µm); χ_{FD} (%) and TOC (%). Lake Mathiesondalen 3: PC1 (allochthonous input vs. autochthonous production); TC (%); TOC (%); TS (%) and χ_{976Hz}.

7 SUMMARY AND CONCLUSIONS

In this thesis, author has focused on a palaeolimnological research in the Polar areas, while selected regions (Vega Island, Antarctica; Mathiesondalen, Svalbard), have been subjected to a more-detailed view. In the literature review chapter, a comprehensive summary based on a physical-geographical description and published researches from these areas, was appropriately delivered. Presented palaeoenvironmental studies, which used multiple techniques and records (ice cores, marine and lacustrine sediments, geomorphology) for reconstruction, were mentioned and properly introduced.

Main part of the thesis was aimed to give information about the palaeolimnological evolution in two areas of Polar regions – Lake Anonima, Vega Island in Antarctica and Lake Mathiesondalen 3, Spitsbergen in Svalbard (Arctic). Using a multi-proxy approach (petrophysical and in/organic geochemistry) and robust chronostratigraphic framework based on radiocarbon (^{14}C) and short-lived isotope (^{210}Pb, ^{137}Cs) absolute dating, which was supplemented by adequate statistical methods (PCA), author was able to extract information about the dominating patterns driving the environmental changes in selected polar areas.

The presented palaeoenvironmental record of Lake Anonima covers the last 2400 cal. yrs b2k and captures the termination of the Late Holocene Hypsithermal, together with its following shifts towards Neoglacial period and recent warming. These phases have been evidenced by diatom community changes as well as other abiotic proxies. Younger sedimentary record from the Lake Mathiesondalen 3 includes the last 700 cal. yrs b2k and based on abiotic proxies it provides unique decadal archive of the local catchment evolution in the Mathiesondalen, Central Spitsbergen.

In the final chapter, the main differences based on the most valuable proxy data (PC1, TOC, sedimentation rate), were established. Specifically, it has been concluded that the Lake Anonima record reflects principally the climate variability of Maritime Antarctica over the last two and half millennia, but on the other hand, the Lake Mathiesondalen 3 record shows mainly variable environmental conditions within the lake and its catchment.

REFERENCES

Monographies, papers from scientific journals and theses

Aagaard, K., Foldvik, A., Hillman, S. R. (1987): The West Spitsbergen Current: Disposition and water mass transformation. Journal of Geophysical Research, 92, č. C4, s. 3778–3784.

Ambrožová, K., Láska, K. (2016): Změny teploty vzduchu na ostrově Jamese Rosse v kontextu Antarktického poloostrova. In: Nováček, A. [eds.]: Sborník příspěvků Výroční konference České geografické společnosti. Jihočeská univerzita v Českých Budějovicích, České Budějovice, s. 20–25.

Allen, J. R. L., Thornley, D. M. (2004): Laser granulometry of Holocene estuarine silts: effects of hydrogen peroxide treatment. The Holocene, 14, č. 2, s. 290–295.

Appleby, P. G., Oldfield, F., Thompson, R., Huttenen, P., Tolonen, K. (1979): ^{210}Pb dating of annually laminated lake sediments from Finland. Nature, 280, č. 5717, s. 53–55.

Aristarain, A. J., Jouzel, J. Pourchet, M. (1986): Past Antarctic Peninsula climate (1850–1980) deduced from an ice core isotope record. Climatic Change, 8, č. 1, s. 69–89.

Badding, M. E., Briner, J. P., Kaufman, D. S. (2013): ^{10}Be ages of late Pleistocene deglaciation and Neoglaciation in the north-central Brooks Range, Arctic Alaska. Journal of Quaternary Science, 28, č. 1, s. 95–102.

Balascio, N. L., D'Andrea, W. J., Gjerde, M., Bakke, J. (2018): Hydroclimate variability of High Arctic Svalbard during the Holocene inferred from hydrogen isotopes of leaf waxes. Quaternary Science Reviews, 183, č. 5, s. 177–187.

Baranowski, S., Karlén, W. (1976): Remnants of Viking Age tundra in Spitsbergen and northern Scandinavia. Geografiska Annaler, 58, č. 1–2, s. 35–39.

Bennett, K. D. (1996): Determination of the number of zones in a biostratigraphical sequence. New Phytologist, 132, č. 1, s. 155–170.

Bentley, M. J., Fogwill, C. J., Kubik, P. W., Sugden, D. E. (2006): Geomorphological evidence and cosmogenic Be/Al exposure ages for the Last Glacial Maximum and deglaciation of the Antarctic Peninsula Ice Sheet. Geological Society of America Bulletin, 118, č. 9–10, 1149–1159.

Bentley, M. J., Hodgson, D. A., Smith, J. A., Cox, N. J. (2005a): Relative sea level curves for the South Shetland Islands and Marguerite Bay, Antarctic Peninsula. Quaternary Science Reviews, 24, č. 10–11, s. 1203–1216.

Bentley, M. J., Hodgson, D.A., Smith, J.A., Ó Cofaigh, C., Domack, E.W., Larter, R.D., Roberts, S.J., Brachfeld, S., Leventer, A., Hjort, C., Hillenbrand, C-D., Evans, J. (2009): Mechanisms of Holocene palaeoenvironmental change in the Antarctic Peninsula region. The Holocene, 19, č. 1, s. 51–69.

Björck, S., Håkansson, H, Olssen, S., Banekow, L., Janssens, J. (1993): Paleoclimatic studies in south Shetland islands, Antarctica, based on numerous stratigraphic variables in lake sediments. Journal of Paleolimnology, 8, č. 3, s. 233–272.

Björck, S., Håkansson, H., Zale, R., Karlén, W., Jönssen, B. L. (1991a): A late Holocene lake sediment sequence from Livingston Island, south Shetland islands, with palaeoclimatic implications. Antarctic Science, 3, č. 1, s. 61–72.

Björck, S., Olsson, S., Ellis-Evans, C., Håkansson, H., Humlum, O., de Lirio, J.M. (1996): Late Holocene palaeoclimatic records from lake sediments on James Ross island, Antarctica. Palaeogeography, Palaeoclimatology, Palaeoecology, 121, č. 3–4, s. 195–220.

Bjornsson, H., Gjessing, Y., Hamran, S. E., Hagen, J. O., Liestol, O., Palsson, F., Erlingsson, B. (1996): The Thermal regime of sub-polar glaciers mapped by multi-frequency radio-echo sounding. Journal of Glaciology, 42, č. 140, s. 23–32.

Blauww, M. (2010): Methods and code for 'classical' age-depth modeling of radiocarbon sequences. Quaternary Geochronology, 5, č. 5, s. 512–518.

Blaszczyk, M., Jania, J. A., Hagen, J. O. (2009): Tidewater glaciers of Svalbard: recent changes and estimates of calving fluxes. Polish Polar Research, 30, č. 2, 85–142.

Blott, S. J., Pye, K. (2001): GRADISTAT: a grain size distribution and statistics package for the analysis of unconsolidated sediments. Earth Surface Processes and Landforms, 26, č. 11, s. 1237–1248.

Böning, P., Bard, E., Rose, J. (2007): Toward direct, micron-scale XRF elemental maps and quantitative profiles of wet marine sediments. Geochemistry, Geophysics, Geosystems, 8, č. 5, s. 1–14.

Boyle, J. F. (2001): Inorganic geochemical methods in paleolimnology. In: Last, W. M., Smol, J. P. [eds.]: Tracking Environmental Change Using Lake Sediments. Volume 2: Physical and Geochemical Methods. Developments in Paleoenvironmental Research, Kluwer, Dordrecht, s. 83–142.

Bradley, R. S. (2015): Paleoclimatology: Reconstructing Climates of the Quaternary. 3rd edition. Academic Press, Amsterdam, 675 s.

Brachfeld, S., Domack, E., Kissel, C., Laj, C., Leventer, A., Ishman, S., Gilbert, R., Camerlenghi, A., Eglinton, L. B. (2003): Holocene history of the Larsen-A ice shelf constrained by geomagnetic paleointensity dating. Geology, 31, č. 9, s. 749–752.

Brown, E. T. (2015): Estimation of Biogenic Silica Concentrations Using Scanning XRF: Insights from Studies of Lake Malawi Sediments. In: Croudace, I. W., Rothwell, R. G. [eds.]: Micro-XRF Studies of Sediment Cores: Applications of a Non-Destructive Tool for the Environmental Sciences, Developments in Paleoenvironmental Research. Springer, Dordrecht, s 267–278.

Cecil, C. B. (1990): Paleoclimate controls on stratigraphic repetition of chemical and siliciclastic rocks. Geology, 18, č. 6, s. 533–536.

Chaparro, M. A. E., Chaparro, M. A. E., Córdoba, F. E., LeComte, K. L., Gargiulo, J. D., Barrios, A. M., Urán, G. M., Manograsso Czalbowski, N. T., Lavat, A., Böhnel, H. N. (2017): Sedimentary analysis and magnetic properties of Lake Anonima, Vega Island. Antarctic Science, 29, č. 5, s. 429–444.

Chen, J., Zhisheng, A., Head, J. (1999): Variation of Rb/Sr ratios in the loess-paleosol sequences of central China during the last 130,000 years and their implications for monsoon paleoclimatology. Quaternary Research, 51, č. 3, s. 215–219.

Chun, Z., Sun, L., Wang, Y., Huang, T., Zhou, X. (2017): Depositional environment and climate changes during the Holocene in Grande Valley, Fildes Peninsula, King George Island, Antarctica. Antarctic Science, 29, č. 6, s. 545–554.

Clapperton, C. M., Sugden, D. E. (1982): Late Quaternary glacial history of George VI Sound area, West Antarctica. Quaternary Research, 18, č. 3, s. 243–267.

Cohen, A. S. (2003): Paleolimnology: the history and evolution of lake systems. Oxford University Press, New York, 500 s.

Cook, A. J., Vaughan, D. G. (2010): Overview of areal changes of the ice shelves on the Antarctic Peninsula over the past 50 years. The Cryosphere, 4, č. 1, s. 77–98.

Cuven, S., Francus, P., Lamoureux, S. F. (2010): Estimation of grain size variability with micro X-ray fluorescence in laminated lacustrine sediments, Cape Bounty, Canadian High Arctic. Journal of Paleolimnology, 44, č. 3, s. 803–817.

D'Andrea, W. J., Vaillencourt, D. A., Balascio, N. L., Werner, A., Roof, S. R., Retelle, M., Bradley, R. S. (2012): Mild Little Ice Age and unprecedented recent warmth in an 1800 year lake sediment record from Svalbard. Geology, 40, č. 11, s. 1007–1010.

De Wet, G. A., Balascio, N. L., D'Andrea, W. J., Bakke, J., Bradley, R. S., Perren, B. (2018): Holocene glacier activity reconstructed from proglacial lake Gjøavatnet on Amsterdamøya, NW Svalbard. Quaternary Science Rewievs, 183, č. 5, s. 188–203.

Dearing, J. A., Dann, R. J. L., Hay, K., Lees, J. A., Loveland, P. J., Maher, B. A., O'Grady, K. (1996): Frequency-dependent susceptibility measurements of environmental materials. Geophysical Journal International, 124, č. 1, s. 228–240.

Dickson, R. R., Osborn, T. J., Hurrell, J. W., Meincke, J., Blindheim, J., Ådlandsvik, B., Vinje, T., Alekseev, G., Maslowski, W. (2000): The Arctic Ocean response to the North Atlantic Oscillation: Journal of Climate, 13, č. 15, s. 2671–2696.

Ding, X., Li, D., Zheng, L., Bao, H., Chen, H. F., Kao, S. J. (2016): Sulfur Geochemistry of a Lacustrine Record from Taiwan Reveals Enhanced Marine Aerosol Input during the Early Holocene. Scientific Reports, 6, č. 38989, s. 1–9.

Domack, E. W., Foss, D. J. P., Syvitski, J. P. M., McMclennen, C. E. (1994): Transport of suspended particulate matter in an Antarctic Fjord. Marine Geology, 121, č. 3–4, s. 161–170.

Domack, E. W., Leventer, A., Root, S., Ring, J., Williams, E., Carlson, D., Hirshorn, E., Wright, W., Gilbert, R., Burr, G. (2003b): Marine sedimentary record of natural environmental variability and recent warming in the Antarctic Peninsula. In: Domack, E. W., Leventer, A., Burnett, A., Bindschadler, R., Convey, P., Kirby, M. [eds.]: Antarctic Peninsula Climate Variability: Historical and Paleoenvironmental Perspectives. American Geophysical Union, Washington, D.C., s. 205–222.

Douglas, M. S. V., Smol, J. P. (1995): Paleolimnological significance of observed distribution patterns of chrysophyte cysts in arctic pond environments. Journal of Paleolimnology, 13, č. 1, 1–5.

Dylmer, C. V., Giraudeau, J., Eynaud, F., Husum, K., De Vernal, A. (2013): Northward advection of Atlantic water in the eastern Nordic Seas over the last 3000 yr. Climate of the Past, 9, č. 4, s. 1505–1518.

Engel, Z., Nývlt, D., Láska, K. (2012): Ice thickness, areal and volumetric changes of Davies Dome and Whisky Glacier in 1979–2006 (James Ross Island, Antarctic Peninsula). Journal of Glaciology, 58, č. 211, s. 904–914.

Ermolin, E., De Angelis, H., Skvarca, P. (2002): Mapping of permafrost on Vega Island, Antarctic Peninsula, using aerial photography and satellite image. Annals of Glaciology, 34, č. 1, s. 184–188.

Evans, M., Heller, F. (2003): Environmental Magnetism: Principles and applications of enviromagnetics. Vol. 86. Academic press, New York, 417 s.

Evans, J. A., Pudsey, C. J., Ó Cofaigh, C., Morris, P., Domack, E. (2005): Late Quaternary glacial history, flow dynamics and sedimentation along the eastern margin of the Antarctic Peninsula Ice Sheet. Quaternary Science Reviews, 24, č. 5–6, s. 741–774.

Fabrés, J., Calafat, A. M., Canals, M., Bárcena, M. A., Flores, J. A. (2000): Bransfield basin fine grained sediments: Late Holocene sedimentary processes and oceanographic and climatic conditions. The Holocene, 10, č. 9, s. 703–718.

Feyling-Hanssen, R. W. (1955): Stratigraphy of the marine Late-Pleistocene of Billefjorden, Vestspitsbergen. Norsk Polarinstitutt, Oslo, 186 s.

Folk, R. L., Ward, W. C. (1957): Brazos River bar [Texas]; a study in the significance of grain size parameters. Journal of Sedimentary Research, 27, č. 1, s. 3–26.

Førland, E. J., Benestad, R., Hanssen-Bauer, I., Haugen, J. E., Skaugen, T. E. (2011): Temperature and precipitation development at Svalbard 1900–2100. Advances in Meteorology, 2011, č. 1, s. 15.

Gersonde, R., Abelmann, A., Brathaeur, U., Becquey, S., Bianchi, C., Cortese, G., Grobe, H., Kuhn, G., Niebler, H. S., Segl, M., Sieger, R., Zielinski, U., Futterer, D. K. (2003): Last glacial sea surface temperatures and sea-ice extent in the Southern Ocean (Atlantic-Indian sector): a multiproxy approach. Paleoceanography and Paleoclimatology, 18, č. 3, s. 1–18.

Gibas, J., Rachlewicz, G., Szczuciński, W. (2005): Application of DC resistivity soundings and geomorphological surveys in studies of modern Arctic glacier marginal zones, Petuniabukta, Spitsbergen. Polish Polar Research, 26, č. 4, s. 239–258.

Gibson, J. A. E., Zale, R. (2006): Holocene development of the fauna of Lake Boeckella, northern Antarctic Peninsula. The Holocene, 16, č. 5, s. 625–634.

Gjerde, M., Bakke, J., D'Andrea, W. J., Balascio, N. L., Bradley, R. S., Vasskog, K., Ólafsdottir, S., Røthe, T. O., Perren, B. B., Hormes, A. (2018): Holocene multi-proxy environmental reconstruction from lake Hakluytvatnet, Amsterdamøya Island, Svalbard (79.5°N). Quaternary Science Reviews, 183, č. 5, s. 164–176.

Glasser, N. F., Harrison, S., Winchester, V., Aniya, M. (2004): Late Pleistocene and Holocene palaeoclimate and glacier fluctuations in Patagonia. Global and Planetary Change, 43, č. 1–2, s. 79–101.

Hagen, J. O., Kohler, J., Melvold, K., Winther, J. G. (2003a): Glaciers in Svalbard: mass balance, runoff and freshwater flux. Polar Research, 22, č. 2, s. 145–159.

Håkanson, L., Jansson, M. (1983): Principles of Lake Sedimentology. Springer, Berlin, 316 s.

Hamilton, G. S., Dowdeswell, J. A. (1996): Controls on glacier surging in Svalbard. Journal of Glaciology, 42, č. 140, s. 157–168.

Harland, W. B. (1997): The Geology of Svalbard. The Geological Society, London, 539 s.

Haus, N. W., Wilhelm, K. R., Bockheim, J. G., Fournelle, J., Miller, M. (2016): A case for chemical weathering in soils of Hurd Peninsula, Livingston Island, South Shetland Islands, Antarctica. Geoderma, 263, č. 3, s. 185–194.

Hendey, N. I. (1964): An introductory account of the smaller algae of British coastal waters. Fishery Investigation Series. Part 5: Bacillariophyceae (Diatoms). Her Majesty's Stationery Office, London, 317 s.

Hendy, C. H., Hall, B. L. (2006): The radiocarbon reservoir effect in proglacial lakes: Examples from Antarctica. Earth and Planetary Science Letters, 241, č. 3–4, s. 413–421.

Hennekam, R., Lange, G. (2012): X-ray fluorescence core scanning of wet marine sediments: methods to improve quality and reproducibility of high-resolution paleoenvironmental records. Limnology and Oceanography: Methods, 10, č. 12, s. 991–1003.

Hernández-Molina, F. J., Larter, R. D., Rebesco, M., Maldonado, A. (2006): Miocene reversal of bottom water flow along the Pacific Margin of the Antarctic Peninsula: stratigraphic evidence from a contourite sedimentary tail. Marine Geology, 228, č. 1–4, s. 93–116.

Heroy, D. C., Anderson, J. B. (2005): Ice-sheet extent of the Antarctic Peninsula region during the Last Glacial Maximum (LGM) – insights from glacial geomorphology. Geological Society of America Bulletin, 117, č. 11–12, s. 1492–1512.

Heroy, D. C., Sjunneskog, C., Anderson, J. B. (2008): Holocene climate change in the Bransfield Basin, Antarctic Peninsula: evidence from sediment and diatom analysis. Antarctic Science, 20, č. 1, s. 69–87.

Hjort, Ch., Ingólfsson, O., Möller, P., Lirio, J. M. (1997): Holocene glacial history and sea-level changes on James Ross Island, Antarctic Peninsula. Journal of Quaternary Science, 12, č. 4, 259–273.

Hodgson, D.A., Abram, N., Anderson, J., Bargelloni, L., Barrett, P., Bentley, M.J., Bertler, N.A.N., Chown, S., Clarke, A., Convey, P., Crame, A., Crosta, X., Curran, M., di Prisco, G., Francis, J.E., Goodwin, I., Gutt, J., Massé, G., Masson-Delmotte, V., Mayewski, P.A., Mulvaney, R., Peck, L., Pörtner, H.-O., Röthlisberger, R., Stevens, M.I., Summerhayes, C.P., van Ommen, T., Verde, C., Verleyen, E., Vyverman, W., Wiencke, C., Zane, L. (2009): Antarctic climate and environment history in the pre-instrumental period. In: Turner, J., Convey, P., di Prisco, G., Mayewski, P.A., Hodgson, D.A., Fahrbach, E., Bindschadler, R., Gutt, J. [eds.]: Antarctic Climate Change and the Environment. Scientific Committee for Antarctic Research, Cambridge, s. 115–182.

Hodgson, D. A., Convey, P. (2005): A 7000-Year record of Oribatid Mite communities on a Maritime-Antarctic island: responses to climate change. Arctic Antarctic and Alpine Research, 37, č. 2, s. 239–245.

Hodgson, D. A., Doran, P., Roberts, D., McMinn, A. (2004): Paleolimnological studies from the Antarctic and subantarctic islands. In: Pienitz, R., Douglas, S. V., Smol, J. P. [eds.]: Long-term Environmental Change in Arctic and Antarctic Lakes. Springer, Dordrecht, s. 419–474.

Hodgson, D. A., Smol, J. P. (2008): High latitude paleolimnology. In: Vincent, W. F., Laybourn-Parry, J. [eds.]: Polar lakes and rivers – limnology of Arctic and Antarctic aquatic ecosystems. Oxford University Press, Oxford, s. 43–64.

Hogg, A. G., Hua, Q., Blackwell, P. G., Niu, M., Buck, C. E., Guilderson, T. P., Heaton, T. J., Palmer, J. G., Reimer, P. J., Reimer, R. W., Turney, C. S. M., Zimmerman, S. R. J. (2013): SHCal13 southern hemisphere calibration, 0–50,000 cal BP. Radiocarbon, 55, č. 4, s. 1889–1903.

Hošek, J., Hambach, U., Lisá, L., Grygar, T. M., Horáček, I., Meszner, S., Knésl, I. (2015): An integrated rock-magnetic and geochemical approach to loess/paleosol sequences from

Bohemia and Moravia (Czech Republic): Implications for the Upper Pleistocene paleoenvironment in central Europe. Palaeogeography, Palaeoclimatology, Palaeoecology, 418, č. 2, s. 344–358.

Howe, J. A., Pudsey, C. J. (1999): Antarctic circumpolar deep water: a Quaternary paleoflow record from the northern Scotia Sea, South Atlantic ocean. Journal of Sedimentary Research, 69, č. 4, s. 847–861.

Hrbáček, F., Nývlt, D., Láska, K. (2017): Active layer thermal dynamics at two lithologically different sites on James Ross Island, Eastern Antarctic Peninsula. Catena, 149, č. 4, s. 592–602.

Hua, Q., Barbetii, M., Rakowski, A. Z. (2013): Atmospheric radiocarbon for the period 1950–2010. Radiocarbon, 55, č. 4, s. 2059–2072.

Humlum, O., Elberling, B., Hormes, A., Fjordheim, K., Hansen, O. H., Heinemeier, J. (2005): Late-Holocene glacier growth in Svalbard, documented by subglacial relict vegetation and living soil microbes. The Holocene, 15, č. 3, s. 396–407.

Ingólfsson, O., Hjort, Ch., Björck, S., Smith, L. R. I. (1992): Late Pleistocene and Holocene glacial history of James Ross Island, Antarctic Peninsula. Boreas, 21, č. 3, s. 209–222.

Isaksson, E., Kohler, J., Pohjola, V., Moore, J., Igarashi, M., Karlöf, L., Martma, T., Meijer, H., Motoyama, H., Vaikmäe, R., van de Wal, R. S. W. (2005): Two ice-core $\delta^{18}O$ records from Svalbard illustrating climate and sea-ice variability over the last 400 years. The Holocene, 15, č. 4, s. 501–509.

Isaksson, E., Pohjola, V., Jauhiainen, T., Moore, J., Pinglot, J. F., Vaikmäe, R., van de Wal, R. S. W., Hagen, J. O., Ivask, J., Karlöf, L., Martma, T., Meijer, H. A. J., Mulvaney, R., Thomassen, M., van den Broeke, M. (2001): A new ice-core record from Lomonosovfonna, Svalbard: viewing the 1920 – 97 data in relation to present climate and environmental conditions. Journal of Glaciology, 47, č. 157, s. 335– 345.

Jones, V. J., Hodgson, D. A., Chepstow-Lusty, A. (2000): Palaeolimnological evidence for marked Holocene environmental changes on Signy Island, Antarctica. The Holocene 10, č. 1, s. 43–60.

Juggins, S. (2017): rioja: Analysis of Quaternary Science Data, R package version (0.9-15.1)

Kadey, F. L. (1983): Diatomite. In: LeFond, S. J. [eds.]: Industrial Rocks and Minerals. American Institute of Mining, Metallurgical, and Petroleum Engineers, New York, s. 677–708.

Kaufman, D. S., Schneider, D. P., McKay, N. P., Ammann, C. M., Bradley, R. S., Briffa, K. R., Miller, G. H., Otto-Bliesner, B. L., Overpeck, J. T., Vinther, B. M., Arctic Lakes 2k Project Members (2009): Recent Warming Reverses Long-Term Arctic Cooling. Science, 325, č. 5945, s. 1236–1239.

King, J. C. (1994): Recent climate variability in the vicinity of the Antarctic Peninsula. International Journal of Climatology, 14, č. 4, s. 357–369.

Klinck, J. M., Hofmann, E. E., Beardsley, R. C., Salihoglu, B., Howard, S. (2004): Water-mass properties and circulation on the west Antarctic Peninsula Continental Shelf in Austral Fall and Winter 2001. Deep-Sea Research Part II – Topical Studies in Oceanography, 51, č. 17–19, s. 1925–1946.

Koinig, K. A., Shotyk, W., Lotter, A. F., Ohlendorf, Ch., Sturm, M. (2003): 9000 years of geochemical evolution of lithogenic major and trace elements in the sediment of an alpine lake – the role of climate, vegetation, and land-use history. Journal of Paleolimnology, 30, č. 3, s. 307–320.

Kylander, M. E., Klaminder, J., Wohlfarth, B., Löwemark, L. (2013): Geochemical responses to paleoclimatic changes in southern Sweden since the late glacial: the Hässeldata Port lake sediment record. Journal of Paleolimnology, 50, č. 1, s. 57–70.

Larsen, D. J., Miller, G. H., Geirsdóttir, Á. (2013): Asynchronous little ice age glacier fluctuations in Iceland and European alps linked to shifts in subpolar North Atlantic circulation. Earth and Planetary Science Letters, 380, č. 20, s. 52–59.

Láska, K., Witoszová, D., Prošek, P. (2012): Weather patterns of the coastal zone of Petuniabukta, central Spitsbergen in the period 2008–2010. Polish Polar Research, 33, č. 4, s. 309–326.

Last, W. M., Smol, J. P. (2001): Tracking Environmental Change Using Lake Sediments. Volume 1: Basin Analysis, Coring, and Chronological Techniques. Kluwer Academic Publishers, Dordrecht, The Netherlands, 573 s.

Leloup, M., Nicolau, R., Pallier, V., Yéprémian, C., Feuillade-Cathalifaud, G. (2013): Organic matter produced by algae and cyanobacteria: Quantitative and qualitative characterization. Journal of Environmental Sciences, 25, č. 6, 1089–1097.

Leng, M. J., Wagner, B., Anderson, N. J., Bennike, O., Woodley, E., Kemp, S. J. (2012): Deglaciation and catchment ontogeny in coastal south-west Greenland: implications for terrestrial and aquatic carbon cycling. Journal of Quaternary Science, 27, č. 6, s. 575–584.

Leventer, A., Domack, E. W., Ishman, S. E., Brachfeld, S., McClennen, C. E., Manley, P. (1996): Productivity cycles of 200–300 years in the Antarctic Peninsula region: understanding linkages among the sun, atmosphere, oceans, sea ice, and biota. Geological Society of America Bulletin, 108, č. 12, s. 1626–1644.

Lopez, P., Navarro, E., Marce, R., Ordoñez, J., Caputo, L., Armengol, J. (2006): Elemental ratios in sediments as indicators of ecological processes in Spanish reservoirs. Limnetica, 25, č. 1–2, s. 499–512.

Maher, B. A., Thompson, R. (1999): Quaternary climates, environments and magnetism. Cambridge University Press, Cambridge, 403 s.

Małecki, J. (2016): Accelerating retreat and high-elevation thinning of glaciers in central Spitsbergen. The Cryosphere, 10, č. 3, s. 1317–1329.

Mann, M., Zhang, Z., Hughes, M. K., Bradley, R. S., Miller, S. K., Rutherford, S., Ni, F. (2008): Proxy-based reconstructions of hemispheric and global surface temperature variations over the past two millennia. Proceedings of the National Academy of Sciences, 105, č. 36, s. 13252–13257.

Mann, S., Sparks, N. H. C., Frankel, R. B., Bazylinski, D. A., Jannasch, H. W. (1990): Biomineralization of ferrimagnetic greigite (Fe_3S_4) and iron pyrite (FeS_2) in a magnetotactic bacterium. Nature, 343, č. 6255, s. 258–261.

Marinsek, S., Ermolin, E. (2015): 10-year mass balance by glaciological and geodetic methods of Glaciar Bahía del Diablo, Vega Island, Antarctic Peninsula. Annals of Glaciology, 56, č. 70, s. 141–146.

Masson-Delmotte, V., Buiron, D., Ekaykin, A., Frezzotti, M., Gallée, H., Jouzel, J., Krinner, G., Landais, A., Motoyama, H., Oerter, H., Pol, K., Pollard, D., Ritz, C., Schlosser, E., Sime, L.C., Sodemann, H., Stenni, B., Uemura, R., Vimeux, F. (2011): A comparison of the present and last interglacial periods in six Antarctic ice cores. Climate of the Past, 7, č. 2, s. 397–423.

Matsuoka, K. H., Narita, K., Sugiyama, S., Matoba, S., Motoyama, Watanabe, O. (1997): Characteristics of AC-ECM signals obtained by use of the Vestfonna ice core, Svalbard. Proceedings NIPR Symp. Polar Meteorolog. Glaciol. 11, č. 1, s. 67–76.

Minzoni, R. T., Anderson, J. B., Fernandez, R., Wellner, J. S. (2015): Marine record of Holocene climate, ocean, and cryosphere interactions: Herber Sound, James Ross Island, Antarctica. Quaternary Science Reviews, 129, č. 23, s. 239–259.

Moholdt, G., Nuth, C., Hagen, J. O., Kohler, J. (2010): Recent elevation changes of Svalbard glaciers derived from ICESat laser altimetry. Remote Sensing of Environment, 114, č. 11, s. 2756–2767.

Morris, E. M., Vaughan, D. G. (2003): Spatial and temporal variations of surface temperature on the Antarctic Peninsula and the limit of variability of ice shelves. In: Domack, E. W., Leventer, A., Burnett, A., Bindschadler, R., Convey, P., Kirby, M. [eds.]: Antarctic Peninsula Climate Variability: Historical and Paleoenvironmental Perspectives. American Geophysical Union, Washington, D.C., s. 61–68.

Müller, J., Werner, K., Stein, R., Fahl, K., Moros, M., Jansen, E. (2012): Holocene cooling culminates in sea ice oscillations in Fram Strait. Quaternary Science Reviews, 47, č. 12, s. 1–14.

Mulvaney, R., Abram, N.J., Hindmarsh, R.C.A., Arrowsmith, C., Fleet, L., Triest, J., Sime, L. C., Alemany, O., Foord, S. (2012): Recent Antarctic Peninsula warming relative to Holocene climate and ice-shelf history. Nature, 489, č. 7414, s. 141–144.

Navas, A., López-Martínez, J., Casas, J., Machín, J., Durán, J.J., Serrano, E., Cuchi, J.-A., Mink, S. (2008): Soil characteristics on varying lithological substrates in the South Shetland Islands, maritime Antarctica. Geoderma, 144, č. 1–2, s. 123–139.

Naveira Garabota, A. C., Heywood, K. J., Stevens, D. P. (2002): Modification and pathways of Southern Ocean Deep Waters in the Scotia Sea. Deep-Sea Research I, 49, č. 4, s. 681–705.

Nedbalová, L., Nývlt, D., Lirio, J. M., Kavan, J., Elster, J. (2017): Current distribution of *Branchinecta gaini* on James Ross Island and Vega Island. Antarctic Science 29, č. 4, s. 341–342.

Nydal, R., Löwseth, K. (1983): Tracing bomb ^{14}C in the atmosphere 1962–1980. Journal of Geophysical Research: Ocean, 88, č. C6, s. 3621–3642.

O'Dowd, C. D., Smith, M. H., Consterdine, I. E., Lowr, J. A. (1997): Marine aerosol, sea-salt, and the marine sulphur cycle: A short review. Atmospheric Environment, 31, č. 1, 73–80.

O'Sullivan, P. et al. (2008): The lakes handbook: limnology and limnetic ecology (Vol. 1). John Wiley & Sons, USA, 709 s.

Oliva, M., Antonieades, D., Giralt, S., Granados, I., Pla Rabes, S., Toro, M., Sanjurjo, J. (2016): La deglaciación de las áreas libres de hielo de las islas Shetland del Sur (Antártida). Ejemplos de Byers (Livingston) y Barton (King George). Cuaternario y Geomorfología, 30, č. 1–2, s. 105–118.

Orsi, A. H., Whitworth, T., III, Nowlin, W. D. Jr (1995): On the meridional extent and fronts of the Antarctic Circumpolar Current. Deep-Sea Research I, 42, č. 5, s. 641–673.

Peel, D. A., Mulvaney, R. (1992): Time trends in the pattern of Ocean–atmosphere exchange in an ice core from the Weddell Sea sector of Antarctica. Tellus Series B – Chemical and Physical Meteorology, 4, č. 4, s. 430–442.

Pfeffer, M., Langmann, B., Graf, H.-F. (2006): Atmospheric transport and deposition of Indonesian volcanic emissions. Atmospheric Chemistry and Physics, 6, č. 9, s. 2525–2537.

Phillips, W., Briner, J. P., Gislefoss, L., Linge, H., Koffman, T., Fabel, D., Xu, S., Hormes, A. (2017): Late Holocene glacier activity at inner Hornsund and Scottbreen, southern Svalbard. Journal of Quaternary Science, 32, č. 4, 501–515.

Pielou, E. (1966): The measurement of diversity in different types of biological collections. Journal of Theoretical Biology, 13, č. 10, s. 31–144.

Pinsel, E. (2014): Environmental Changes in a High Arctic Ecosystem. Diplomová práce. Antwerpen, 160 s.

Pudsey, C. J., Evans, J. (2001): First survey of Antarctic sub-ice shelf sediments reveals Mid-Holocene ice shelf retreat. Geology, 29, č. 9, s. 787–790.

Rabassa, J. (1983): Stratigraphy of the glacigenic deposits in northern James Ross Island, Antarctic Peninsula. In: Evenson, E., Schlüchter, C., Rabassa, J. [eds.]: Tills and related deposits. A. A. Balkema, Rotterdam, s. 329–40.

Rachlewicz, G., Szczucínski, W., Ewertowski, M. (2007): Post-"Little Ice Age" retreat rates of glaciers around Billefjorden in central Spitsbergen, Svalbard. Polish Polar Research, 28, č. 3, s. 159–186.

Rasmussen, T. L., Thomsen, E., Skirbekk, K., Ślubowska-Woldengen, M., Klitgaard Kristensen, D., Koç, N. (2014): Spatial and temporal distribution of Holocene temperature maxima in the northern Nordic seas: interplay of Atlantic-, Arctic- and polar water masses. Quaternary Science Reviews, 92, č. 9, s. 280–291.

Reimer, P. J., Bard, E., Bayliss, A., Beck, J. W., Blackwell, P. G., Bronk Ramsey, C., Buck, C. E., Edwards, R. L., Friedrich, M., Grootes, P. M., Guilderson, T. P., Haflidason, H., Hajdas, I., Hatté, C., Heaton, T. J., Hoffmann, D. L., Hogg, A. G., Hughen, K. A., Kaiser, K. F., Kromer, B., Manning, S. W., Niu, M., Reimer, R. W., Richards, D. A., Scott, E. M., Southon, J. R., Turney, C. S. M., Van Der Plicht, J. (2013): IntCal13 and Marine13 radiocarbon age calibration curves, 0–50,000 years cal BP. Radiocarbon, 55, č. 4, s. 1869–1887.

Reimer, P. J., Brown, T. A., Reimer, R. W. (2004): Discussion: reporting and calibration of post-bomb ^{14}C data. Radiocarbon, 46, č. 3, s. 1299–1304.

Reynolds, J. M. (1981): The distribution of mean annual temperatures in the Antarctic Peninsula. British Antarctic Survey Bulletin, 54, č. 1, s. 123–133.

Roberts, S. J., Hodgson, D. A., Bentley, M. J., Smith, J. A., Millar, I., Olive, V., Sugden, D. E. (2008): The Holocene history of George VI Ice Shelf, Antarctic Peninsula from clast-provenance analysis of epishelf lake sediments. Palaeogeography, Palaeoclimatology, Palaeoecology, 259, č. 2–3, s. 258–283.

Roberts, E. M., Lamanna, M. C., Clarke, J. A., Meng, J., Gorscak, E., Sertich, J. J. W., O'Connor, P. M., Claeson, K. M., MacPhee, R. D. E. (2014): Stratigraphy and vertebrate paleoecology of Upper Cretaceous – lowest Paleogene strata on Vega Island, Antarctica. Palaeogeography, Palaeoclimatology, Palaeoecology, 402, č. 10, s. 55–72.

Robinson, S. A., Wasley, J., Tobin, A. K. (2003): Living on the edge–plants and global change in continental and maritime Antarctica. Global Change Biology, 9, č. 12, s. 1681–1717.

Roman, M. (2014): Holocenní vývoj arktických jezer. Bakalářská práce, Praha, 66 s.

Roman, M. (2017): Correlation of abiotic proxies in Holocene lacustrine sediments of Peri-Atlantic Arctic. Diplomová práce. Praha, 119 s.

Ross, R., Cox, E. J., Karayeva, N. I., Mann, D. G., Paddock, T. B. B., Simonsen, R., Sims, P. A. (1979): An amended terminology for the siliceous components of the diatom cell. Nova Hedwigia, 30, č. 1–4, s. 513–533.

Rothwell, R. G., Rack, F. R. (2006): New techniques in sediment core analysis: an introduction. In: Rothwell, R. G. [eds.]: New Techniques in Sediment Core Analysis. Geological Society, London, s. 1–29.

Røthe, T. O., Bakke, J., Vasskog, K., Gjerde, M., D'Andrea, W. J., Bradley, R. S. (2015): Arctic Holocene glacier fluctuations reconstructed from lake sediments at Mitrahalvøya, Spitsbergen. Quaternary Science Reviews, 109, č. 3, s. 111–125.

Round, F. E., Crawford, R. M., Mann, D. G. (1990): The Diatoms: biology and morphology of the genera. Cambridge University Press, Cambridge, 760 s.

Salvigsen, O., Lauritzen, Ø., Mangerud, J. (1983): Karst and karstification in gypsiferous beds in Mathiesondalen, Central Spitsbergen, Svalbard. Polar Research, 1, č. 1, s. 83–88.

Sarnthein, M., van Kreveld, S., Erlenkeuser, H., Grootes, P. M., Kucera, M., Pflaumann, U., Schulz, M. (2003): Centennial-to-millennial scale periodicities of Holocene climate and sediment injections off the western Barents shelf, 75°N. Boreas, 32, č. 3, s. 447–461.

Shannon, C. E., Weaver W. (1949): The mathematical theory of communication. Urbana University Press, Illinois, 125 s.

Schumacher, B. A. (2002): Methods for the Determination of Total Organic Carbon (TOC) in Soils and Sediments. Ecological Risk Assessment Support Center, Office of Research and Development, US Environmental Protection Agency, Las Vegas, 1, č. 1, s. 1–23.

Schwerdtfeger, W. (1975): The effect of the Antarctic Peninsula on the temperature regime of the Weddell Sea. Monthly Weather Review, 103, č. 1, s. 45–51.

Simmonds, I. (2003): Modes of atmospheric variability over the Southern Ocean. Journal of Geophysical Research – Oceans, 108, č. C4, s. 78–80.

Sjunneskog, C., Taylor, F. (2002): Postglacial marine diatom record of the Palmer Deep, Antarctic Peninsula (ODPL Leg 178, Site 1098) 1. Total diatom abundance. Paleoceanography and Paleoclimatology, 17, č. 3, s. 1–8.

Smellie, J. L., Johnson, J. S., McIntosh, W. C., Esser, R., Gudmundsson, M. T., Hambrey, M. J., De Vries, B. V. W. (2008): Six million years of glacial history recorded in volcanic lithofacies of the James Ross Island Volcanic Group, Antarctic Peninsula. Palaeogeography, Palaeoclimatology, Palaeoecology, 260, č. 1–2, s. 122–148.

Smith, D. A., Hofmann, E. E., Klinck, J. M., Lascara, C. M. (1999): Hydrography and circulation of the west Antarctic Peninsula continental shelf. Deep-Sea Research Part I – Oceanographic Research Papers, 46, č. 6., s. 925–949.

Smith, D. A., Klinck, J. M. (2002): Water properties on the west Antarctic Peninsula continental shelf: a model study of surface fluxes and sea-ice. Deep-Sea Research Part II – Topical Studies in Oceanography, 49, č. 21, s. 4863–4886.

Solomina, O. N., Bradley, R. S., Hodgson, D. A., Ivy-Ochs, S., Jomelli, V., Mackintosh, A. N., Nesje, A., Owen, L. A., Wanner, H., Wiles, G. C., Young, N. E. (2015): Holocene glacier fluctuations. Quaternary Science Reviews, 111, č. 5, s. 9–34.

Spielhagen, R. F., Werner, K., Sørensen, S. A., Zamelczyk, K., Kandiano, E., Budeus, G., Husum, K., Marchitto, T. M., Hald, M. (2011): Enhanced modern heat transfer to the Arctic by warm Atlantic water. Science, 331, č. 6016, s. 450–453.

Stensrud, D. J. (1996): Importance of low-level jets to climate: a review. Journal of Climate, 9, č. 8, s. 1698–1711.

Sterken, M., Roberts, S. J., Hodgson, D. A., Vyverman, W., Balbo, A. L., Sabbe, K., Moreton, S. G., Verleyen, E. (2012): Holocene glacial and climate history of Prince Gustav Channel, northeastern Antarctic Peninsula. Quaternary Science Reviews, 31, č. 1, s. 93–111.

Suess, H. E. (1955): Radiocarbon concentration in modern wood. Science, 122, č. 3166, s. 415–417.

Sugden, D. E., Bentley, M. J., Ó Cofaigh, O. (2006): Geological and geomorphological insights into Antarctic ice sheet evolution. Philosophical Transactions of the Royal Society A, 364, č. 1605–1625.

Sund, M., Eiken, T., Hagen, J. O., Kääb, A. (2009): Svalbard surge dynamics derived from geometric changes. Annals of Glaciology, 50, č. 52, s. 50–60.

Svendsen, J. I., Mangerud, J. (1997): Holocene glacial and climatic variations on Spitsbergen, Svalbard. The Holocene, 7, č. 1, s. 45–57.

Taboada, T., Cortizas, A. M., García, C., García-Rodeja, E. (2006): Particle-size fractionation of titanium and zirconium during weathering and pedogenesis of granitic rocks in NW Spain. Geoderma, 131, č. 1–2, s. 218–236.

Tavernier, I., Verleyen, E., Hodgson, D. A., Heirman, K., Roberts, S. J., Imura, S., Kudoh, S., Sabbe, K., De Batist, M., Vyverman, W. (2014): Absence of Medieval Climate Anomaly, Little Ice Age and twentieth century warming in Skarvsnes, Lutzow Holm Bay, East Antarctica. Antarctic Science, 26, č. 5, s. 585–598.

Thomas, E. R., Dennis, P. F., Bracegirdle, T. J., Franzke, C. (2009): Ice core evidence for significant 100-year regional warming on the Antarctic Peninsula. Geophysical Research Letters, 36, č. 20, s. 1–5.

Thompson, L. G., Peel, D. A., Mosley-Thompson, E., Mulvaney, R., Dai, J., Lin, P. N., Davis, M. E., Raymond, C. F. (1994): Climate since 1510 AD on Dyer Plateau, Antarctic Peninsula: Evidence for recent climate change. Annals of Glaciology, 20, č. 2, s. 420–426.

Thompson, R., Clark, R. M., Boulton, G. S. (2012): Core Correlation. In: Birks, H. J. B. [eds.]: Tracking Environmental Change Using Lake Sediments. Vol 5: Data Handling and Numerical Techniques. Springer, Dordrecht. s. 415–430.

Thompson, R., Oldfield, F. (1986): Environmental Magnetism. George Allen and Unwin, London, 227 s.

Tjallingii, R., Röhl, U., Kölling, M., Bickert, T. (2007): Influence of the water content on X-ray fluorescence core-scanning measurements in soft marine sediments. Geochemistry, Geophysics, Geosystems, 8, č. 2, s. 1–12.

Vaasma, T. (2008): Grain-size analysis of lacustrine sediments: a comparison of pre-treatment methods. Estonian Journal of Ecology, 57, č. 4, s. 231–243.

Váczi, P., Barták, M., Nedbalová, L., Elster, J. (2011): Comparative analysis of temperature courses in Antarctic lakes of different morphology: Study from James Ross Island, Antarctica. Czech Polar Reports, 1, č. 2, s. 78–87.

Van Daele, M., Moernaut, J., Silversmit, G., Schmidt, S., Fontijn, K., Heirman, K., Vandoorne, W., De Clercq, M., Van Acker, J., Wolff, C., Pino, M., Urrutia, R., Roberts, S.J., Vincze, L., De Batist, M. (2014): The 600 yr eruptive history of Villarrica Volcano (Chile) revealed by annually laminated lake sediments. Bulletin of the Geological Society of America 126, č. 3–4, s. 481–498.

Van der Bilt, W. G. M., Bakke, J., D'Andrea, W. J., Vasskog, K., Bradley, R. S., Ólafsdóttir, S. (2015): Reconstruction of glacier variability from lake sediments reveals dynamic Holocene climate in Svalbard. Quaternary Science Reviews, 126, č. 9, s. 201–218.

Van der Bilt, W. G. M., D'Andrea, W. J., Bakke, J., Balascio, N. L., Werner, J. P., Gjerde, M., Bradley, R. S. (2018): Alkelone-based reconstructions reveal four-phase Holocene temperature evolution for High Arctic Svalbard. Quaternary Science Reviews 183, č. 5, s. 204–213.

Van der Werff, A. (1955): A new method of concentrating and cleaning diatoms and other organisms. Verhandlungen Internationalen Vereinigung für Theoretische und Angewandte Limnologie 2, 13, č. 1, s. 276–277.

Vaughan, D. G., Marshall, G., Connolley, W. M., Parkinson, C., Mulvaney, R., Hodgson, D. A., King, J. C., Pudsey, C. J., Turner, J., Wolff, E. (2003): Recent rapid regional climate warming on the Antarctic Peninsula. Climatic Change, 60, č. 3, s. 243–274.

Verleyen, E., Hodgson, D. A., Sabbe, K., Cremer, H., Emslie, S. D., Gibson, J., Hall, B., Satoshi, I., Kudoh, S., Marshall, G. J., McMinn, A., Melles, M., Newman, L., Roberts,

D., Roberts, S., Singh, S. M., Sterken, M., Tavernier, I., Verkulich, S., Van de Vyver, E., Van Nieuwenhuyze, W., Wagner, B., Vyverman, W. (2011): Postglacial climate variability along the east Antarctic coastal margin evidence from shallow marine and coastal terrestrial records. Earth-Science Reviews, 104, č. 4, s. 199–212.

Vincke, S., Van de Vijver, B., Gremmen, N., Beyens, L. (2006): The moss dwelling testacean fauna of the Stromness Bay (South Georgia). Acta Protozoologica, 45, č. 1–4, 65–75.

Walkley, A., Black, I. A. (1934): An examination of the Degtjareff method for determining soil organic matter, and a proposed modification of the chromic acid titration method. Soil Science, 37, č. 1, s. 29–38.

Wellner, J. S., Heroy, D. C., Anderson, J. B. (2006): The death mask of the Antarctic Ice Sheet: comparison of glacial geomorphic features across the continental shelf. Geomorphology, vol. 75, č. 1–2, s. 157–171.

Weltje, G. J., Tjallingii, R. (2008): Calibration of XRF core scanners for quantitative geochemical logging of sediment cores: theory and application. Earth and Planetary Science Letters, 274, č. 3–4, s. 423–438.

Werner, A. (1993): Holocene moraine chronology, Spitsbergen, Svalbard: Lichenometric evidence for multiple Neoglacial advances in the Arctic. The Holocene, 3, č. 2, s. 128–137.

Werner, K., Müller, J., Husum, K., Spielhagen, R. F., Kandiano, E. S., Polyak, L. (2016): Holocene sea subsurface and surface water masses in the Fram Strait – Comparisons of temperature and sea-ice reconstructions. Quaternary Science Reviews, 147, č. 17, s. 194–209.

Wetzel, R. G. (2001): Limnology: Lake and River ecosystems. Academic Press, San Diego, 1006 s.

Wilkin, R. T., Barnes, H. L. (1997): Formation processes of framboidal pyrite. Geochimica et Cosmochimica Acta, 61, č. 2, s. 323–339.

Winkelmann, D., Knies, J. (2005): Recent distribution and accumulation of organic carbon on the continental margin west off Spitsbergen. Geochemistry, Geophysics, Geosystems, 6, č. 9, s. 1–22.

Wolfe, A. P., Miller, G. H., Olsen, C. A., Forman, S. L., Doran, P. T., Holmgren, S. U. (2004): Geochronology of High Latitude lake sediments. In: Pienitz, R., Douglas, S. V., Smol, J. P. [eds.]: Long-term Environmental Change in Arctic and Antarctic Lakes. Springer, Dordrecht, s. 419–474.

Worm, H. U. (1998): On the superparamagnetic – stable single domain transition for magnetite, and frequency dependence of susceptibility. Geophysical Journal International, 133, č. 1, s. 201–206.

Xu, H., Liu, B., Wu, F. (2010): Spatial and temporal variations of Rb/Sr ratios of the bulk surface sediments in Lake Qinghai. Geochemical Transactions, 11, č. 1, s. 1–8.

Yoon, H. I., Park, P. K., Kim, Y., Kang, Yun, Cheon, Kang, S. H. (2003): Origins and paleoceanographic significance of the layered diatom ooze interval from the Bransfield Straight in the northern Antarctic Peninsula around 2500 years BP. In: Domack, E. W., Leventer, A., Burnett, A., Bindschadler, R., Convey, P., Kirby, M. [eds.]: Antarctic Peninsula Climate Variability: Historical and Paleoenvironmental Perspectives. American Geophysical Union, Washington, D.C., s. 225–238.

Zale, R., Karlén, W. (1989): Lake sediment cores from the Antarctic Peninsula and surrounding island. Geografiska Annaler: Series A, Physical Geography, 71, č. 3–4, s. 211–220.

Zhang, Y., Renssen, H., Seppä, H. (2016): Effects of melting ice sheets and orbital forcing on the early Holocene warming in the extratropical Northern Hemisphere. Climate of the Past, 12, č. 5, s. 1119–1135.

Zidarova, R., Kopalová, K., Van de Vijver, B. (2016): Diatoms from the Antarctic Region. I: Maritime Antarctica. Iconographia Diatomologica, vol. 24. Hardcover, Königstein, 509 s.

Maps and atlases

Dallmann, W. K., Piepjohn, K., Blomeier, D. (2004): Geological Map of Billfjorden, Central Spitsbergen, Svalbard: With Geological Excursion Guide. 1:50 000. Norsk polarinstitutt, Oslo.

Smellie, J. L., Johnson, J. S., Nelson, A. E. (2013): Geological map of James Ross Island. 1. James Ross Island Volcanic Group. BAS GEOMAP 2 Series, Sheet 5. 1:125 000. British Antarctic Survey, Cambridge, UK

APPENDIX

APPENDIX

Table 1 Clam's (R) modelled b2k ages in the Lake Anonima. (*Appendix 1*)

depth (cm)	min 95 %	best-age	max 95 %
0.0	–15	–13	–11
0.5	–10	–8	–6
1.0	–4	–3	–1
1.5	1	2	4
2.0	6	8	9
2.5	12	13	14
3.0	17	18	19
3.5	22	23	24
4.0	27	28	29
4.5	32	33	34
5.0	38	38	39
5.5	43	44	44
6.0	67	68	69
6.5	90	92	95
7.0	113	117	120
7.5	137	141	146
8.0	160	166	171
8.5	183	190	197
9.0	207	214	222
9.5	230	239	248
10.0	253	263	273
10.5	277	288	299
11.0	300	312	324
11.5	323	337	350
12.0	346	361	375
12.5	370	385	401
13.0	393	410	427
13.5	416	434	452
14.0	440	459	478
14.5	463	483	503
15.0	486	507	529
15.5	510	532	554
16.0	533	556	580
16.5	556	581	605
17.0	597	621	645
17.5	637	661	685
18.0	677	701	726
18.5	716	741	767
19.0	755	781	809
19.5	793	821	851
20.0	831	861	893
20.5	870	901	935
21.0	908	941	976

depth (cm)	min 95 %	best-age	max 95 %
21.5	945	981	1018
22.0	983	1021	1060
22.5	1021	1061	1102
23.0	1058	1101	1144
23.5	1095	1142	1187
24.0	1134	1182	1229
24.5	1171	1222	1272
25.0	1209	1262	1314
25.5	1246	1302	1357
26.0	1284	1342	1400
26.5	1322	1382	1443
27.0	1359	1422	1486
27.5	1396	1462	1529
28.0	1433	1502	1572
28.5	1470	1542	1614
29.0	1482	1553	1625
29.5	1494	1564	1634
30.0	1506	1575	1644
30.5	1519	1586	1654
31.0	1531	1598	1664
31.5	1543	1609	1674
32.0	1555	1620	1685
32.5	1567	1631	1695
33.0	1579	1642	1706
33.5	1590	1653	1716
34.0	1602	1664	1726
34.5	1614	1675	1737
35.0	1625	1686	1747
35.5	1637	1697	1758
36.0	1648	1708	1769
36.5	1659	1719	1780
37.0	1671	1731	1792
37.5	1682	1742	1803
38.0	1694	1753	1814
38.5	1705	1764	1826
39.0	1717	1775	1837
39.5	1728	1786	1850
40.0	1739	1797	1861
40.5	1751	1808	1874
41.0	1762	1819	1886
41.5	1773	1830	1898
42.0	1784	1841	1910
42.5	1795	1852	1921
43.0	1806	1864	1932
43.5	1817	1875	1943
44.0	1828	1886	1955

depth (cm)	min 95 %	best-age	max 95 %
44.5	1839	1897	1966
45.0	1850	1908	1977
45.5	1861	1919	1988
46.0	1871	1930	2000
46.5	1882	1941	2011
47.0	1893	1952	2022
47.5	1904	1963	2033
48.0	1915	1974	2045
48.5	1926	1985	2056
49.0	1936	1996	2068
49.5	1947	2008	2080
50.0	1958	2019	2092
50.5	1968	2030	2104
51.0	1979	2041	2115
51.5	1990	2052	2127
52.0	2000	2063	2139
52.5	2011	2074	2151
53.0	2021	2085	2164
53.5	2031	2096	2176
54.0	2041	2107	2188
54.5	2051	2118	2200
55.0	2061	2129	2213
55.5	2070	2141	2225
56.0	2080	2152	2238
56.5	2089	2163	2251
57.0	2099	2174	2265
57.5	2109	2185	2278
58.0	2118	2196	2292
58.5	2127	2207	2305
59.0	2136	2218	2319
59.5	2145	2229	2333
60.0	2154	2240	2346
60.5	2164	2251	2360
61.0	2173	2262	2373
61.5	2183	2274	2387
62.0	2191	2285	2401
62.5	2200	2296	2415
63.0	2209	2307	2429
63.5	2218	2318	2443
64.0	2227	2329	2456
64.5	2237	2340	2469
65.0	2246	2351	2483
65.5	2255	2362	2497
66.0	2264	2373	2511
66.5	2272	2384	2525
67.0	2281	2395	2538

depth (cm)	min 95 %	best-age	max 95 %
67.5	2290	2407	2552
68.0	2299	2418	2566
68.5	2308	2429	2580
69.0	2317	2440	2593

Table 2 Clam's (R) modelled b2k ages in the Lake Mathiesondalen 3. (*Appendix 1*)

depth (cm)	min 99 %	best-age	max 99 %
0.00	–21	–18	–14
0.25	–19	–16	–13
0.50	–16	–13	–11
0.75	–14	–11	–8
1.00	–11	–8	–6
1.25	–9	–6	–3
1.50	–5	–2	1
1.75	–1	2	5
2.00	3	6	10
2.25	8	12	15
2.50	14	18	22
2.75	20	25	29
3.00	28	33	37
3.25	35	41	47
3.50	43	50	57
3.75	51	59	67
4.00	59	69	78
4.25	67	79	90
4.50	75	89	103
4.75	83	99	115
5.00	92	110	129
5.25	101	122	143
5.50	109	133	157
5.75	118	145	172
6.00	126	157	187
6.25	136	169	202
6.50	145	181	218
6.75	154	194	234
7.00	163	207	250
7.25	172	219	267
7.50	182	233	283
7.75	192	246	300
8.00	202	259	317
8.25	212	273	334
8.50	221	286	351
8.75	231	300	368
9.00	240	313	386
9.25	249	326	403

depth (cm)	min 99 %	best-age	max 99 %
9.50	259	340	420
9.75	269	353	437
10.00	278	366	454
10.25	288	379	471
10.50	297	392	488
10.75	306	405	504
11.00	316	418	520
11.25	325	431	536
11.50	334	443	552
11.75	343	455	567
12.00	352	467	582
12.25	361	479	597
12.50	370	490	611
12.75	379	502	624
13.00	387	512	638
13.25	395	523	650
13.50	403	533	663
13.75	412	543	674
14.00	420	553	685
14.25	428	562	696
14.50	436	571	705
14.75	443	579	714
15.00	451	587	723
15.25	457	594	730
15.50	464	601	737
15.75	471	607	743
16.00	477	613	748
16.25	483	618	753
16.5	489	623	756
16.75	495	627	760
17.00	500	632	763
17.25	506	636	767
17.50	511	640	769
17.75	516	645	773
18.00	521	649	777
18.25	526	653	781
18.50	530	658	786
18.75	535	663	791
19.00	539	667	796
19.25	543	672	801
19.50	546	676	805
19.75	550	679	809
20.00	552	682	812
20.25	554	684	815
20.50	556	687	819
20.75	558	689	820

depth (cm)	min 99 %	best-age	max 99 %
21.00	560	692	823
21.25	563	694	825
21.50	565	696	827
21.75	567	698	829
22.00	568	699	831
22.25	569	701	833
22.50	569	702	835
22.75	569	703	837
23.00	570	704	839
23.25	566	703	841
23.50	557	700	842

Table 3 Correlation (*r*) matrix of geochemical data in the Lake Anonima. (*Appendix 2*)

	TOC	LE	Si	Fe	Ca	Al	Ti	Mn	Sr	Rb	Zr	Ni
Ni	-0.79	-0.84	0.39	0.88	0.83	0.68	0.80	0.86	0.87	-0.62	0.65	
Zr	-0.60	-0.65	0.40	0.67	0.59	0.53	0.54	0.69	0.69	-0.20		
Rb	0.70	0.76	-0.29	-0.77	-0.82	-0.61	-0.71	-0.71	-0.77			
Sr	-0.93	-0.97	0.46	0.99	0.97	0.78	0.86	0.95				
Mn	-0.89	-0.93	0.47	0.95	0.93	0.75	0.82					
Ti	-0.84	-0.79	0.10	0.87	0.87	0.50						
Al	-0.70	-0.87	0.87	0.78	0.78							
Ca	-0.92	-0.97	0.46	0.97								
Fe	-0.92	-0.97	0.46									
Si	-0.34	-0.61										
LE	0.90											
TOC												

Table 4 Correlation (*r*) matrix of geochemical data (dried samples) in the Lake Mathiesondalen 3. (*Appendix 2*)

	TOC	LE	Si	Fe	Ca	Al	Ti	Mn	Sr	Rb	Zr	Ni
Ni	-0.56	0.09	0.70	0.50	-0.60	0.77	0.31	-0.50	-0.62	0.75	0.59	
Zr	-0.32	0.32	0.34	0.77	-0.55	0.45	0.30	-0.12	-0.49	0.78		
Rb	-0.46	0.36	0.51	0.86	-0.72	0.60	0.29	-0.17	-0.64			
Sr	0.09	-0.22	-0.41	-0.36	0.47	-0.54	-0.13	0.60				
Mn	0.13	0.11	-0.38	0.24	0.16	-0.42	-0.17					
Ti	-0.51	-0.16	0.52	0.20	-0.31	0.53						
Al	-0.70	-0.08	0.94	0.38	-0.63							
Ca	0.51	-0.69	-0.69	-0.63								
Fe	-0.37	0.44	0.28									
Si	-0.69	-0.03										
LE	0.03											
TOC												